Innovation, Business Cycles, and the Climate Transition*

Diego R. Känzig   Maximilian Konradt

Lixing Wang   Donghai Zhang

September, 2026

Abstract

We study how business cycle fluctuations shape the pace and direction of innovation. Non-green innovation is procyclical, while green innovation is countercyclical, both over the cycle and in response to economic shocks. We explain this divergence in a dynamic general equilibrium model with endogenous green and non-green innovation. Green patents derive more value from distant profits, making green innovation less sensitive to short-run fluctuations. Endogenous innovation costs reinforce this mechanism, making green and non-green innovation effective substitutes. Evidence from market-implied patent valuations and scientist earnings supports the mechanism. The model implies larger and greener effects of innovation subsidies during downturns.

JEL classification: E32, O31, Q55, Q58

Keywords: Green innovation, patenting, business cycles, medium-run impacts

*Känzig: Northwestern University, CEPR and NBER (email: dkaenzig@northwestern.edu); Konradt: University of Bonn (email: konradt@uni-bonn.de); Wang: University of Bonn (email: wang.lixing@uni-bonn.de); Zhang: National University of Singapore (email: donghai.d.zhang@gmail.com). We thank Adrien Auclert, Marios Angeletos, Esther Bøler, Patrick Bolton, Gadi Barlevy, Gideon Bornstein, Andrea Caggese, Nida Çakır Melek, Maarten De Ridder, Luca Fornaro, Bard Harstad, David Hémous, Ben Jones, Marcin Kacperczyk, Pete Klenow, Yueran Ma, Marti Mestieri, Mirabelle Muûls, Conny Olovsson, Dimitris Papanikolaou, Evi Pappa, Marcel Peruffo, Monika Piazzesi, Giorgio Primiceri, Felipe Saffie, Martin Schneider and Jaume Ventura as well as participants at the Chicago Fed, the KC Fed, Kellogg, Stanford, HKUST, Tinbergen, NUS, Cornell University, the University of Pittsburgh, York University, the University of Cambridge, Imperial College London, University of Bonn, University of Amsterdam, CREi, Barcelona Summer Forum, SED, UC3M, Bank of England, Banco de Espana, Banque de France, Riksbank, CityUHK, UCD, Tor Vergata, HKMA, ifo Institute, University of Hamburg and IWH for helpful comments and suggestions. This paper previously circulated under the title "Green Business Cycles". Konradt acknowledges financial support from the Swiss National Science Foundation (grant 222367). Wang acknowledges financial support from the Bonn Graduate School of Economics. Zhang thanks the Singapore Ministry of Education for financial support under the SSRTG grant SSRC2023-SSRTG-026.

1. Introduction

Climate change is the defining challenge of our time, posing severe threats to lives, livelihoods, ecosystems, and the global economy. Carbon pricing remains a central tool for mitigation, but its distributional impacts have sparked public resistance, as higher energy costs weigh disproportionately on low-income households and carbon-intensive industries. Against this backdrop, green innovation is key for a successful transition, enabling emissions reductions while sustaining economic growth. Yet recent global shocks, such as the COVID-19 pandemic and subsequent recession, have raised concerns that economic downturns may stall the green transition by tightening financial constraints or shifting firms' innovation priorities. Understanding how green innovation responds to the business cycle is therefore critical.

This paper provides an anatomy of the cyclicality of innovation, with a focus on green and non-green technologies. We define green innovation as the development of clean technologies that replace or reduce the reliance on existing carbon-intensive ones. Based on the universe of patents filed in the United States, we document a striking pattern: while overall patenting activity is procyclical, green and non-green innovation exhibit markedly different cyclical behavior. Non-green patenting moves with the business cycle, declining during downturns, whereas green patenting is *countercyclical*, increasing during contractions. As a result, the share of green patents rises during recessions—but notably, we also find evidence that the absolute number of green patents increases.

To establish these patterns, we examine the dynamics of patent applications—both unconditionally over the business cycle and conditional on macroeconomic shocks. For the former, we analyze the dynamic correlations of the number of patent applications with business cycle shocks, measured as innovations to output that cannot be forecasted using past macroeconomic variables. For the latter, we estimate the dynamic causal effects of monetary policy shocks on patenting. We think of monetary policy shocks as a stand-in for a well-identified demand shock. Moreover, these shocks have the appealing feature that they induce a negative co-movement between real interest rates and output, allowing us to shed light on underlying transmission channels.

The patenting responses to business cycle and monetary policy shocks are remarkably similar: the green patent share increases after a contractionary shock, driven by a rise in the number of green patents and a decline in non-green patenting. The procyclicality of non-green innovation aligns with the common notion that tighter credit conditions, lower revenues, and reduced profits during economic downturns result in cuts to R&D budgets and a decrease in patenting intensity. This raises the question of what can explain the different cyclicality of green innovation.

A key difference between green and non-green patents lies in their duration. As the economy transitions away from carbon-intensive technologies, green patents generate profits that are heavily backloaded. This payoff structure makes the value of green patents and thus green patenting less sensitive to business cycle shocks, which operate at much shorter frequencies. There are two channels that could be driving this result. The first works through cash flows: as profits are backloaded, they are less affected by transitory shocks. The second works through discounting: economic contractions are typically associated with a fall in discount rates. Thus, future profits are discounted by less, which helps stabilize patent values. The fact that we find comparable results for general business cycle and monetary policy shocks suggests that the cash flow channel dominates—since monetary policy shocks imply a negative co-movement between output and discount rates, the discount rate channel would predict more cyclical green innovation.

The contrasting cyclical patterns of green and non-green patenting are robust across multiple dimensions. First, we show that these cyclical patterns extend beyond national borders. While our primary focus is on the United States, we document similar divergent cyclicality between green and non-green patenting in OECD countries and globally. Second, we show that the cyclicality is comparable for patenting among listed and private firms. Third, the result holds true not only in the aggregate but also at the firm level. By linking patent data with balance sheet information for U.S. public firms, we find comparable firm-level patenting responses to monetary policy shocks, even when controlling for firm characteristics such as leverage, size, or firm age. Importantly, we also document a reallocation from non-green to green patenting *within* firms. Finally, we show that firms with longer duration, as proxied by a low book-to-market value, display a more pronounced green patenting increase following a contractionary shock.

To explain the different cyclicality of green and non-green innovation, we develop a dynamic stochastic general equilibrium model with directed technical change. The model features endogenous innovation in green and non-green technologies. We first study a simple production economy, taking the aggregate level of innovation and labor as given. The production block consists of a final good producer that assembles the final good using materials and energy. The energy input is a composite of fossil fuels and green energy. Intermediate input producers supply non-green materials and green energy varieties.

We show that in this economy, the equilibrium market share of the green energy composite increases along the green transition, and green patents generate higher profits in the future. We label this phenomenon "*green is in the future*". The intuition for this result goes as follows. In our model, the number of green varieties reflects the productivity of green inputs. As the green share increases along the transition, the productivity of green inputs rises, leading to lower prices and higher demand for green inputs. Consequently, the profits from producing green inputs are higher in the future. This implies that the value of a green patent, which is proportional to the discounted sum of future profits, is more heavily influenced by future profits than that of a non-green patent.

The backloaded profit structure of green patents, combined with the transitory nature of business cycle shocks, gives rise to a *green duration channel*: the value of green patents responds less to such shocks than the value of non-green patents. This, in turn, creates an incentive to adjust green patenting intensity by less in response to macroeconomic shocks. We keep discount rates fixed in this partial equilibrium setting, but provide a decomposition between the cash flow and discount rate channel in general equilibrium.

We close the model by introducing innovators that use skilled labor as an innovation input to create new green and non-green varieties, and a standard household block. The model features a positive externality from the aggregate technological level, assuming that each successful innovation creates new varieties of green energy and materials.

The green duration channel—as distilled in partial equilibrium—is able to generate the countercyclicality of the share of green varieties, also in general equilibrium. Even though we allow for the discount rate channel which could work against the countercyclicality, we find that the cash flow channel generally dominates.

While this channel can account for the relative cyclicality, it cannot generate the countercyclicality of the number of green patents. In general equilibrium, however, there is an additional force operating through the inelastic supply of skilled labor. When the labor supply curve is positively sloped, a recessionary shock reduces non-green innovation, which in turn lowers aggregate demand for skilled labor and thus wages. The lower wage then decreases the cost of green R&D, incentivizing firms to undertake more green innovation and offsetting the partial equilibrium effect. When this effect is sufficiently strong, the model is able to generate the differential cyclicality of the number of green and non-green patents observed in the data.

We provide empirical evidence supporting the key mechanisms of the model. To test the green duration channel, we use the market-implied values of U.S. patents from Kogan et al. (2017). Consistent with the model, green patent values fluctuate less over the business cycle and respond less to identified macroeconomic shocks, including monetary policy shocks. This pattern holds in both patent-level estimates and firm-level indices of green and non-green patent values.

To shed light on the general equilibrium effects operating through innovation costs, we examine adjustments in the skilled labor market. Following a contractionary monetary policy shock, scientist earnings fall significantly, while the number of green inventors at firms increases. These patterns are consistent with the model's predicted general equilibrium adjustment through the skilled labor market.

Finally, we use the model for two additional analyses. First, we study the long-run effects of business cycle shocks, which we cannot directly estimate from the data. By reallocating innovation between green and non-green technologies, transitory business cycle shocks permanently alter the composition of technology and, hence, the green patent share. Second, we conduct counterfactual policy exercises showing that the effects of R&D subsidies are state dependent. Because downturns lower skilled R&D wages, neutral subsidies generate more innovation per dollar in recessions than in booms. The patents they generate also have a greener composition during downturns, reflecting the higher baseline green share. Green-targeted subsidies, by contrast, directly shift the composition of innovation toward green technologies, and also do so more strongly during downturns.

Related literature. This paper contributes to several strands of literature. First, it relates to the extensive body of research on the cyclicality of innovation. A large literature documents that aggregate innovation, as measured by R&D expenditures and patent filings, is procyclical (e.g. Aghion et al., 2010; Aghion et al., 2012; Barlevy, 2007). Related research shows that business cycle shocks can have long-lasting effects on economic activity through their impact on investment, innovation and productivity (Antolin-Diaz and Surico, 2022; Jordà, Singh, and Taylor, 2024; Ilzetzki, 2024; Furlanetto et al., 2025). In recent work, Ma and Zimmermann (2023) focus on monetary policy and show that contractionary monetary shocks decrease aggregate innovation. The procyclicality of innovation is typically explained by the fact that economic contractions reduce firms' cash flows and tighten financial constraints, leading to lower R&D investment and innovation output. Our findings confirm this broad pattern for overall patenting but reveal an important distinction between green and non-green innovation.

Second, our paper relates to the literature on green innovation and its determinants. Given recent estimates of the social cost of carbon (Burke et al., 2023; Bilal and Känzig, 2024), understanding the drivers of green innovation is of utmost importance. Prior studies have examined how environmental policies, such as carbon pricing and subsidies, influence green technological development (Calel and Dechezleprêtre, 2016; Colmer et al., 2024; Aghion et al., 2016; Känzig, 2023). Popp (2002) provides early evidence that higher energy prices induce clean innovation by directing inventive activity. Acemoglu et al. (2012) emphasize the central role played by market size and price effects on the direction of technical change. Acemoglu et al. (2023) examine the shale gas revolution, showing that the natural gas boom discourages green innovation.

Two closely related papers study how financial conditions and constraints affect green innovation. Aghion et al. (2026) and Fornaro et al. (2026) show that young firms and firms with a high share of green patents reduce their innovative activity more sharply when financial conditions tighten. Our analysis complements theirs by studying business cycle shocks more broadly rather than financial shocks per se. Moreover, our firm-level results focus on large, more mature firms, for which financial constraints are less likely to bind. Yet these firms account for the bulk of green patenting in the United States, even though green patents represent only a moderate share of their patent portfolios.

Our paper contributes to this literature by documenting the cyclicality of green patenting and providing a theoretical explanation for its countercyclicality. Unlike Fornaro, Guerrieri, and Reichlin (2025), we document reallocative effects between green and non-green innovation both across and *within* firms. This reallocation is consistent with the Schumpeterian view (Aghion and Saint-Paul, 1998): economic downturns and the associated fall in wages reduce the opportunity cost of innovative activity and induce more green innovation at the expense of non-green innovation.

Our general equilibrium model with green and non-green innovation also contributes to the literature on medium-run fluctuations, which emphasizes the interplay between technological progress, capital accumulation, and business cycle dynamics (Comin and Gertler, 2006; Anzoategui et al., 2019, among others). A number of influential studies focus on understanding the historically slow recoveries from recessions (Benigno and Fornaro, 2018; Bianchi, Kung, and Morales, 2019; Queralto, 2020). Other research examines the implications for asset prices and exchange rates (Kung and Schmid, 2015; Gornemann, Guerrón-Quintana, and Saffie, 2021). Recent work emphasizes how innovator heterogeneity shapes business-cycle propagation, with Wang and Zhang (2025) focusing on the distribution of firms' readiness to launch innovation projects and Benedetti-Fasil et al. (2025) on changes in the composition of innovating firms through selection, entry, and exit. While existing models typically focus on aggregate technical change, our framework incorporates the dynamics of directed green and non-green innovation during the climate transition.

Outline. The paper proceeds as follows. Section 2 presents stylized facts on the cyclicality of green and non-green innovation: in the aggregate and at the firm-level, as well as unconditionally and conditional on macroeconomic shocks. Section 3 introduces our business cycle model with green and non-green innovation. In Section 4, we confront key model predictions with the data. Section 5 explores what these results imply for the effectiveness and design of innovation subsidies. Section 6 concludes.

2. Green Innovation Over the Business Cycle

How does innovation activity vary with the business cycle? Does green innovation display a different sensitivity to economic downturns and upswings than other types of innovation? Answering these questions presents two key challenges. First, how to accurately measure different types of innovation. Second, how to best represent the business cycle. For the former, we will rely on patent data—a widely used proxy for innovation (see e.g. Nagaoka, Motohashi, and Goto, 2010). For the latter, we start by documenting the unconditional dynamic co-movements of patenting with the business cycle before studying the relationship conditional on structural economic shocks.

2.1. Measuring Green Innovation

Measuring innovation presents a fundamental challenge in understanding how technological change responds to economic fluctuations. Patent data offer a well-established proxy for innovation, providing a consistent and detailed record of inventive activity across industries and time. Importantly, patents capture both the scale and nature of innovation: a detailed classification system enables researchers to distinguish between green and non-green technological advances.

The ability to classify patents is a key advantage over R&D expenditure data, another widely used measure of innovation. Unlike patents, R&D expenditure data are typically reported at the aggregate level and lack detailed breakdowns by type of research activity. This poses a challenge because firms engage in many types of research simultaneously. These activities do not necessarily correlate with observable characteristics, making it difficult to disentangle targeted investments in specific technologies from broader innovation efforts. For instance, many firms in carbon-intensive industries display substantial engagement in green R&D. Patents, by contrast, provide a direct and observable measure of directed innovation, which is why we focus on patent data in our analysis.

We rely on the Worldwide Patent Statistical Database (PATSTAT), which encompasses bibliographic information for close to the universe of patents globally. The data allow us to identify patent families—patents representing the same innovation filed at different patent offices. To avoid double counting, we treat all patents in a family as a single innovation (Hémous et al., 2025). For each patent family, we use the first application date to capture the time of innovation and assign nationality based on the respective filing office.

Our key goal is to measure green innovation. To that end, we use the International Patent Classification (IPC) and Cooperative Patent Classification (CPC) codes associated with patent filings. The European Patent Office (EPO) has developed specific categories for climate change mitigation technologies (Y02) and smart grids (Y04S), allowing us to

Figure 1: Green patenting across the globe, 1986–2019

(a) Green patent share (b) Cyclical component of patenting

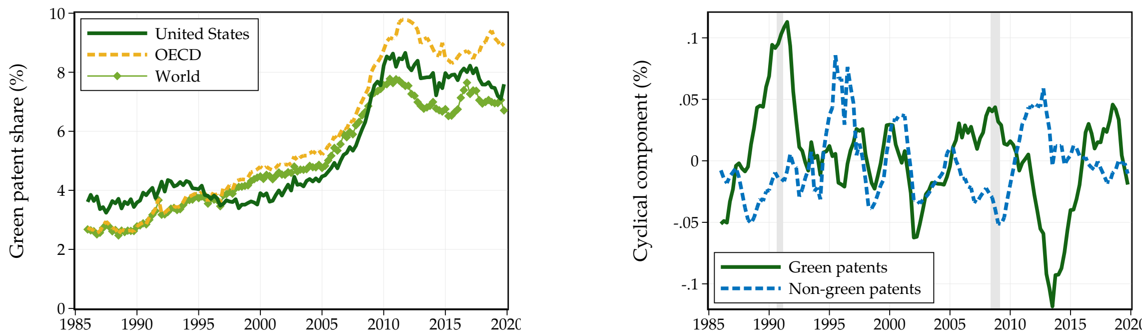

Notes: Trends and cycles in green and non-green patenting. Left panel: Share of green patents for the world, OECD countries and the United States, based on our selection of Y02 subclasses. Right panel: The cyclical components of green and non-green patent counts in OECD countries after applying a centered 3-quarter moving average, extracted using the Hodrick-Prescott filter with $\lambda = 1,600$. Gray bars denote global recessions following Kose, Sugawara, and Terrones (2020).

systematically identify and track relevant technological advancements (see Veefkind et al., 2012; Angelucci, Hurtado-Albir, and Volpe, 2018). Our definition of green patents includes all Y02 subclasses (see, e.g., Aghion et al., 2026). Removing adaptation technologies (Y02A), narrowing the definition to energy technologies (Y02E), or adding smart grid technologies (Y04S) as in Calel and Dechezleprêtre (2016) produces very similar results, see Appendix B.1.2.

Since a patent family is typically associated with many classification codes, we consider it green when any of the codes meet our criteria. We treat the remaining patents as non-green (or gray). Table A.2 in the Appendix includes some examples of green patents.

Aggregate trends and fluctuations. Based on our patent database, we compute aggregate patent application counts and report statistics for the world, OECD countries, and the United States.[1] Figure 1a shows the evolution of green patents as a share of total patents across these geographies from the mid-1980s through 2019. The series exhibit both a pronounced upward trend and considerable fluctuations around it. Starting from relatively low levels—around 3% in the United States and 2% in both the OECD and the world—the green patent share rises gradually at first and then surges between 2005 and 2010, reaching a peak of 7-8% around 2011. It subsequently declines somewhat and continues to fluctuate below its peak. The patterns are very similar across geographies and are consistent with findings in the existing literature (see, e.g., Aghion et al., 2026).

We next zoom in on the cyclical behavior of inventive activity. Figure 1b shows the cyclical components of green and non-green patent filings in OECD countries, extracted

[1] Among patent applications filed in OECD countries, those filed with the USPTO account for 21% of all patents and 22% of green patents.

using the Hodrick–Prescott filter. Both types of patents vary meaningfully over the business cycle. Strikingly, however, green and non-green patents do not co-move strongly: while non-green patents tend to be procyclical—declining during the early 1990s recession and the 2008 global financial crisis—green patent filings appear countercyclical, increasing during those same downturns.

Firm-level statistics. Which firms account for the bulk of green and non-green patenting? To better understand the key innovators, we merge the PATSTAT dataset with corporate balance sheet data. For firm-level financials, we use Compustat North America, covering the universe of publicly listed companies in the United States. To link the patent data, we rely on two datasets that connect patents to firms. The first is Orbis Intellectual Property, which provides global patent portfolios linked to Orbis companies (see Hémous et al., 2025); we match these to Compustat using ISIN identifiers. The second is the dataset by Arora, Belenzon, and Sheer (2021), which extends the NBER patent database (Hall, Jaffe, and Trajtenberg, 2001) and directly links USPTO patents to Compustat firms.

We use the unique patent application number common to both datasets to merge them with information from PATSTAT. In total, we successfully match 1.7 million distinct patent families—including approximately 103,000 distinct green patents—to over 2,600 Compustat firms. Reassuringly, the overlap in matched patents across the two sources is high (see Appendix A for details).

Table 1: Green patenting and firm size

	Firm size quartiles			
	First	Second	Third	Fourth
Number of green patents	2,419	5,178	9,836	91,384
Green patent share (%)	26.03	13.19	10.20	10.99
Size	46.66	273.23	1,261.51	17,061.79
Age	14.91	18.41	22.05	31.47
Book to market ratio	0.19	0.45	0.37	0.32
GHG emission intensity	34.82	33.47	92.02	320.89

Notes: The table reports the total number of green patents and the average share of green patents across four quartiles of the firm size distribution. Firm size is measured by average total assets (in millions of 2017 USD) as reported in Compustat from 1986 to 2019. Average firm age is based on incorporation dates from Worldscope. Average GHG emissions intensity is calculated as Scope 1 emissions relative to revenue, using data from Trucost. As a result of co-inventions, the total number of green patents exceeds the number of distinct patents.

We find that a substantial share of green patents—on average, 35% of quarterly green patent filings—are filed by listed firms. Among these, Table 1 presents descriptive statistics on green patenting by firm size. The bulk of green patenting in the U.S. is concentrated in the largest companies (top size quartile), accounting for more than four out of five green patents filed between 1986 and 2019. While smaller and younger firms patent relatively more in green technology classes, the bottom half of the size distribution accounts for less than 7% of the green patents in our sample. By contrast, the 20 largest green innovators account for close to 50% of green patent filings (see Table B.1 in the Appendix).

Thus, large firms appear to be important drivers behind green innovation in the United States.[2] Interestingly, these firms are not particularly green according to conventional metrics. As shown in Table 1, larger firms exhibit a substantially higher GHG emissions intensity than smaller ones. Their patent portfolios are also less weighted toward green technology classes (see also Fornaro, Guerrieri, and Reichlin, 2024). This pattern is consistent with recent evidence in Cohen, Gurun, and Nguyen (2020) showing that utilities and energy companies are important drivers of green innovation. As expected, firm size is positively correlated with firm age. When examining the book-to-market ratio, growth firms are primarily concentrated in both the smallest and largest size quartiles, while value firms are more evenly distributed across the middle of the size distribution.

Due to data limitations, our focus is on listed firms. However, an important question is how patenting activity in listed firms compares to that in unlisted firms. To explore this, we construct a green patent share based on the sample of patents that cannot be linked to listed firms, which we attribute to unlisted firms.[3] As shown in Figure A.1 in the Appendix, unlisted firms display patterns of green patenting very similar to those of listed firms.

2.2. The Cyclicality of Green Innovation at the Macro Level

How do green and non-green innovation vary with the business cycle? Theoretically, the cyclicality of innovation is ambiguous. According to the Schumpeterian view, economic downturns and the associated fall in wages reduce the opportunity cost of innova-

[2]Importantly, this relationship may differ across countries. For instance, Aghion et al. (2026) document that smaller firms account for a large share of green patenting in German data. However, firms in our sample tend to be substantially larger—a firm at the 90th percentile of their fixed asset distribution (97 million EUR) would fall into the bottom quartile of our total asset distribution—complicating a direct comparison.

[3]The residual category may, in principle, include unmatched patents of listed firms as well as patents filed by non-firm applicants, such as universities or government agencies. We expect such cases to be limited. Compustat covers 97–99% of the market capitalization of all listed U.S. firms between 1975–2015 (Kahle and Stulz, 2017), and because we assign patent nationality based on the original patent office, we also expect filings by foreign corporations to be modest. Moreover, only about 1% of U.S. patents are publicly owned (Gazzani et al., 2026).

tive activity and induce higher long-term productivity growth (Aghion and Saint-Paul, 1998). However, the effect can be overturned in the presence of financial constraints (Aghion et al., 2010). Thus, whether innovation is procyclical or countercyclical—and how strongly—is ultimately an empirical question.

To shed light on this, we perform two complementary exercises. First, we study how patenting changes after "business cycle shocks" by analyzing the dynamic correlation between patenting measures and unexpected changes in GDP and other business cycle indicators. Second, we estimate the dynamic causal effects of monetary policy shocks—used here as a stand-in for well-identified demand shocks—on patenting. These shocks also have the desirable property of moving output and interest rates in opposite directions, which will be informative of the underlying mechanisms at play.

Unconditional cyclicality. To assess how patenting varies with the cycle, we estimate simple local projections (LPs) à la Jordà (2005) on business cycle shocks in the spirit of Angeletos, Collard, and Dellas (2020). Specifically, we estimate

$$y_{t+h} = \alpha^h + \psi^h bc_t + \boldsymbol{\beta}_x^h \mathbf{x}_{t-1} + \varepsilon_{t+h}, \tag{1}$$

where y_{t+h} is the innovation measure of interest h-quarters ahead, bc_t is a business cycle indicator, $\mathbf{x}_{t-1}$ is a vector of controls and ε_{t+h} is a potentially serially correlated error term. As the relevant innovation measures, we consider the number of overall patents filed, the number of green and non-green patents (all expressed in logs), and the green patent share.[4] In our baseline, we use real GDP growth as the business cycle indicator. However, our results are robust to using alternative indicators (see Appendix Figure B.2).

Our controls include 4 lags of the business cycle indicator and the patenting measure. Moreover, we include quarterly dummy variables and a linear time trend to account for seasonality and trending behavior.[5] By controlling for lags of GDP growth and the patenting measure, we isolate an innovation in GDP that is not forecastable by past economic and innovative activity.[6] The coefficients ψ^h are the dynamic effects of interest: they capture how an unexpected change in GDP affects patenting both contemporaneously and over future periods. It is important to note that these estimates are dynamic correlations and do not have a causal interpretation. Standard errors are computed using the lag-augmentation approach (Montiel Olea and Plagborg-Møller, 2021).

[4] We apply a one-quarter backward-looking moving average to the patent counts to address volatility in patent filings. However, the results are robust to using raw patent counts.

[5] The U.S. patent data exhibits spikes in patent filings in 1995Q2 and 2013Q1, driven by changes in U.S. patent law associated with the Uruguay Round Agreements Act and the America Invents Act, which we account for using two additional dummy variables. The results are robust to omitting these controls.

[6] In this way, we recover a "shock" that maximizes variations in GDP on impact—a special case of the approach in Angeletos, Collard, and Dellas (2020) who target variations over a finite short-run horizon.

Figure 2: Green and non-green patenting responses to business cycle shock

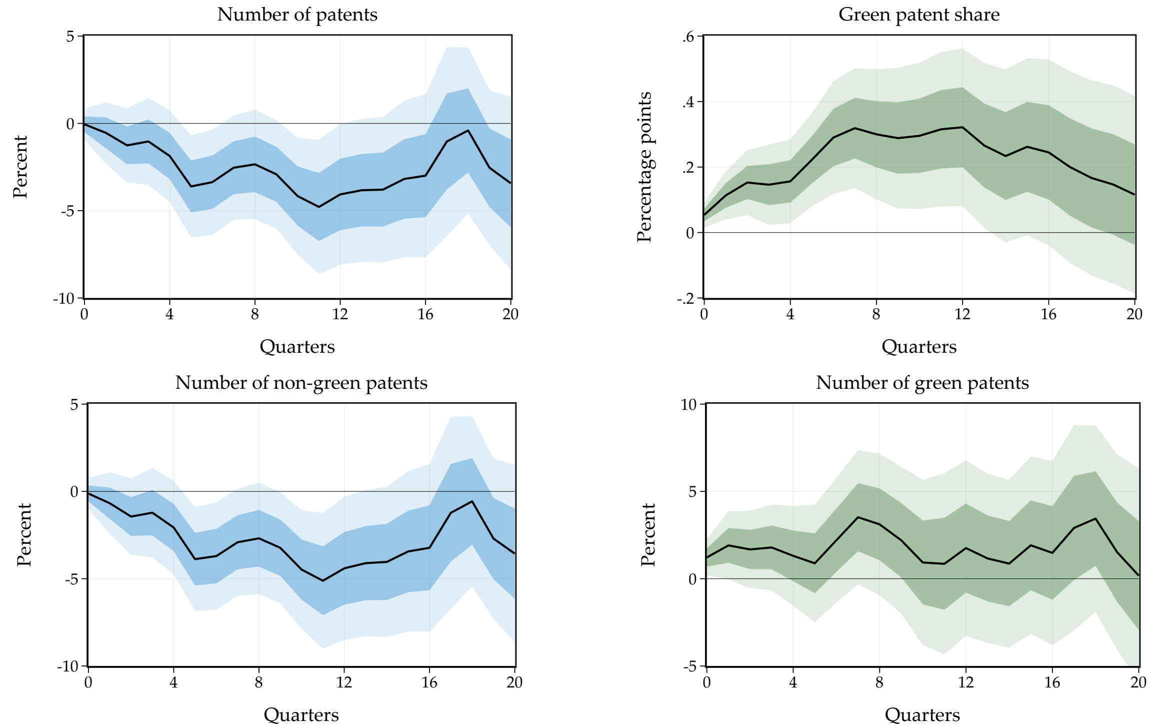

Notes: Responses of green and non-green patenting in the U.S. to a recessionary GDP shock, estimated based on (1). Shock is normalized to decrease GDP growth by 1% on impact. Solid line: point estimate. Dark and light shaded areas: 68 and 95% confidence bands based on lag-augmented standard errors.

We estimate equation (1) based on U.S. data. Our estimation sample spans the period from 1986Q1, when consistent reporting in the Compustat data begins, and ends in 2019Q4, before the onset of the Covid pandemic. Due to substantial reporting lags in the PATSTAT data, extending the sample to more recent periods is challenging.

Figure 2 presents the results. Looking first at overall innovative activity, we find that patenting is procyclical—patent filings tend to increase during economic expansions and decrease during downturns. This pattern is consistent with the view that tighter credit conditions, lower revenues, and reduced profits in recessions lead firms to cut R&D spending, resulting in fewer patent filings (Aghion et al., 2010; Aghion et al., 2012).

Comparing the cyclicality of green and non-green patenting reveals a striking result: the green patent share increases significantly following an economic downturn. This increase is not only statistically but also economically significant. A fall in GDP growth by 1% leads to an increase in the green patent share by close to 0.3 percentage points. What is driving the relative increase in green patenting? A comparison of the responses in the bottom panels reveals that non-green patent applications decline more strongly than the total, whereas green patenting even tends to rise. This suggests that green patenting is not only less cyclical than non-green patenting, but may even be *countercyclical*—though

Figure 3: Green patenting responses to business cycle shock over different sample periods

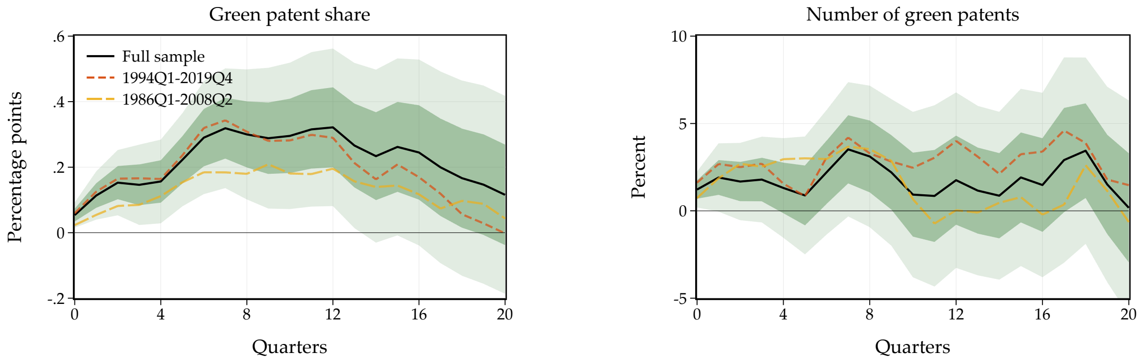

Notes: Responses of green and non-green patenting in the U.S. to a recessionary GDP shock, estimated based on (1) for different sub-samples: 1994Q1–2019Q4 and 1986Q1–2008Q2. Shock is normalized to decrease GDP growth by 1% on impact. Lines: point estimates. Dark and light shaded areas: baseline 68 and 95% confidence bands based on lag-augmented standard errors.

the increase is not very precisely estimated.

How robust is the relationship between green patenting and the business cycle? To address this question, we estimate local projections for two subsamples: 1994Q1–2019Q4 and 1986Q1–2008Q2. The former omits the early-1990s period, which featured energy price shocks related to the Gulf crisis and changes in U.S. clean energy legislation, while the latter excludes the global financial crisis, which coincided with a sharp increase in green patenting. As Figure 3 shows, the estimated responses are very similar across subsamples. Appendix B.1.3 presents additional evidence showing the results are not driven by outliers or pre-trends.

Cyclicality conditional on monetary policy shocks. While the unconditional time-series evidence is informative, it may confound the impacts of different underlying shocks driving the business cycle. Therefore, it is important to establish the cyclicality of green patenting *conditional* on structural economic shocks.

Over our sample period of interest, business cycles are thought to be mainly demand driven. Credibly identifying demand shocks is challenging. We focus on monetary policy shocks, as a well-identified instance of a demand shock. Another appealing feature is that they imply an opposing effect on interest rates and output, which will help to shed light on underlying transmission channels. In Appendix B.1.1, we study the robustness of the results when conditioning on other shocks such as oil price shocks.

To identify monetary policy shocks, we rely on high-frequency identification techniques (Gertler and Karadi, 2015; Nakamura and Steinsson, 2018). We employ the monetary surprises constructed by Bauer and Swanson (2023), purged from macroeconomic and financial data.[7] Using these surprises as an instrument, we estimate the dynamic causal effects of a monetary policy shock on green patenting. Specifically, we run a series of instrumental variable-local projections (LP-IVs):

$$y_{t+h} = \alpha^h + \theta^h r_t + \boldsymbol{\beta}_x^h \mathbf{x}_{t-1} + \varepsilon_{t+h}, \tag{2}$$

where y_{t+h} again corresponds to the innovation measure of interest h-quarters ahead, r_t is the policy rate, which we instrument using monetary surprises, and $\mathbf{x}_{t-1}$ is a vector of controls to account for macroeconomic and financial conditions. We use the federal funds rate as the relevant monetary policy indicator, but account for the zero lower bound using a dummy variable. Using the one-year rate instead produces very similar results. The controls include 4 lags of the policy rate, log real GDP, the unemployment rate, log GDP deflator, and the excess bond premium from Gilchrist and Zakrajšek (2012). We keep including quarterly dummy variables and a linear time trend to account for seasonality and trending behavior. The key object of interest is θ^h, the dynamic causal effect of a monetary policy shock on the innovation measure.

Reassuringly, the effective F-statistic in the first stage is 12.3, suggesting that there is no weak instrument problem at hand. We thus proceed by conducting standard inference. Before looking at the patenting responses, we also confirm that the responses of U.S. macroeconomic variables to our identified monetary policy shocks are consistent with existing empirical evidence, see Appendix Figure B.1. Throughout, we normalize the monetary policy shock to increase the Fed funds rate by 25 basis points.

Figure 4 shows the results. In line with the unconditional evidence, we find that overall patenting is procyclical: a contractionary monetary policy shock leads to a significant fall in aggregate patenting. This finding is consistent with the evidence in Ma and Zimmermann (2023).

Next, we turn to the responses of green and non-green patenting. We confirm that green patenting is countercyclical, even conditional on monetary policy shocks. A contractionary monetary policy shock leads to a significant and persistent increase in the green patent share, with a peak effect of 0.3 percentage points after 15 quarters. The number of non-green patents declines substantially—slightly more than the decline in overall patenting—while the number of green patents rises. This increase is more pronounced and statistically significant compared to the unconditional evidence.

These findings differ from Aghion et al. (2026), who show that young, financially constrained firms in Germany cut green innovation more sharply when credit conditions tighten. Our sample is tilted towards larger, more mature U.S. firms, which are less likely

[7] Our results are robust to using the monetary surprises from Jarociński and Karadi (2020), see Appendix B.1.1.

Figure 4: Green and non-green patenting responses to a monetary policy shock

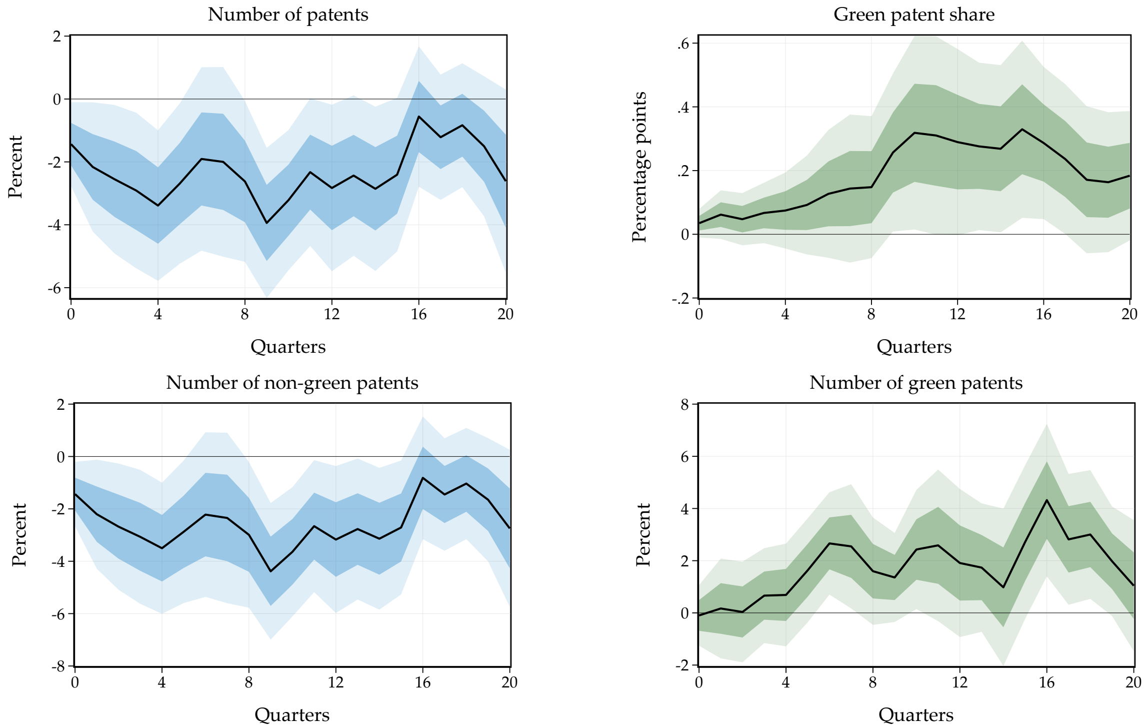

Notes: Responses of green and non-green patenting in the U.S. to a contractionary monetary policy shock, estimated based on LP-IV model (2). Shock is normalized to increase federal funds rate by 25 basis points on impact. Solid line: point estimate. Dark and light shaded areas: 68 and 95% confidence bands based on lag-augmented standard errors.

to be financially constrained. Differences in firm composition and geography may therefore help explain the contrasting results.[8]

Mechanism. Why is green patenting less cyclical than non-green—and even tends to be countercyclical? A key difference lies in the timing of expected profits. Green patents tend to generate returns further in the future, whereas non-green patents have a more frontloaded profit structure. Indeed, as we show in Appendix B.2.1, green patents are significantly more likely to be renewed, consistent with the notion of more backloaded returns. Since business cycle shocks primarily affect short-term economic conditions, this makes the value of green patents—and thus the intensity of green patenting—less sensitive to cyclical fluctuations.

This mechanism can operate through two distinct channels: a *cash flow* channel and a *discount rate* channel. The first channel captures that, at fixed discount rates, the cash flows of green patents are less affected by short-term business cycle fluctuations because of their backloaded profile. The second channel captures the notion that discount rates tend to fall in recessions, and thus the more distant cash flows of green patents are discounted by less,

[8]For a more detailed comparison with Aghion et al. (2026), see Appendix B.1.4.

making green patent values less cyclical.

Our evidence conditional on monetary policy shocks helps shed light on the relative importance of these channels. Monetary policy shocks imply a negative co-movement between discount rates and output: discount rates increase after a contractionary monetary policy shock. Thus, in this case the discount rate channel would predict more cyclical and not less cyclical green innovation. Our finding that both business cycle and monetary policy shocks generate similar cyclical patterns in green and non-green patenting suggests that the cash flow channel dominates the discount rate channel.

Sensitivity. We perform a number of sensitivity and robustness checks. First, we show that the estimated effects extend beyond the sample of U.S. patents. In light of the well-documented global propagation of U.S. monetary policy shocks (Miranda-Agrippino and Rey, 2020), we use U.S. monetary policy shocks as a stand-in for global demand shocks. Figure 5a presents the response of the green patent share in OECD countries and worldwide to a contractionary U.S. monetary policy shock. We find an increase in green patenting similar to that observed in the U.S. sample.

Second, we analyze whether the cyclicality of green patenting differs between listed and unlisted U.S. firms. To this end, we construct the green patent share separately for two samples: patents linked to listed firms and the remaining patents, which we attribute to unlisted firms. Figure 5b shows that green patenting increases in both groups. Interestingly, the green patent share rises more quickly among listed firms, while the increase among unlisted firms takes longer to materialize—consistent with the idea that listed firms, with larger R&D departments, can respond more rapidly to economic conditions.

Third, we examine whether the responses are similar across sectors, again restricting the analysis to patents attributable to listed firms. Focusing on patents within sectors ensures that our comparison of green and non-green innovation is based on more comparable technologies. Figure 5c shows an increase in the green patent share across energy, utilities and transportation, and manufacturing sectors. Figure 5d further suggests the estimated responses are comparable within narrower manufacturing subsectors.

Fourth, we consider several alternative channels that could account for the countercyclicality of green innovation. One possibility is that countercyclical fiscal support disproportionately benefits the green sector. For example, the American Recovery and Reinvestment Act of 2009 included substantial green components—such as investments in renewable energy, energy efficiency, and clean technology—aimed at both stimulating the economy and advancing the low-carbon transition (Chen et al., 2021). Such policies may sustain green innovation during downturns, potentially contributing to its observed countercyclicality. To assess this channel, we control for research, development,

Figure 5: Sensitivity with respect to geography, firm types and sectors

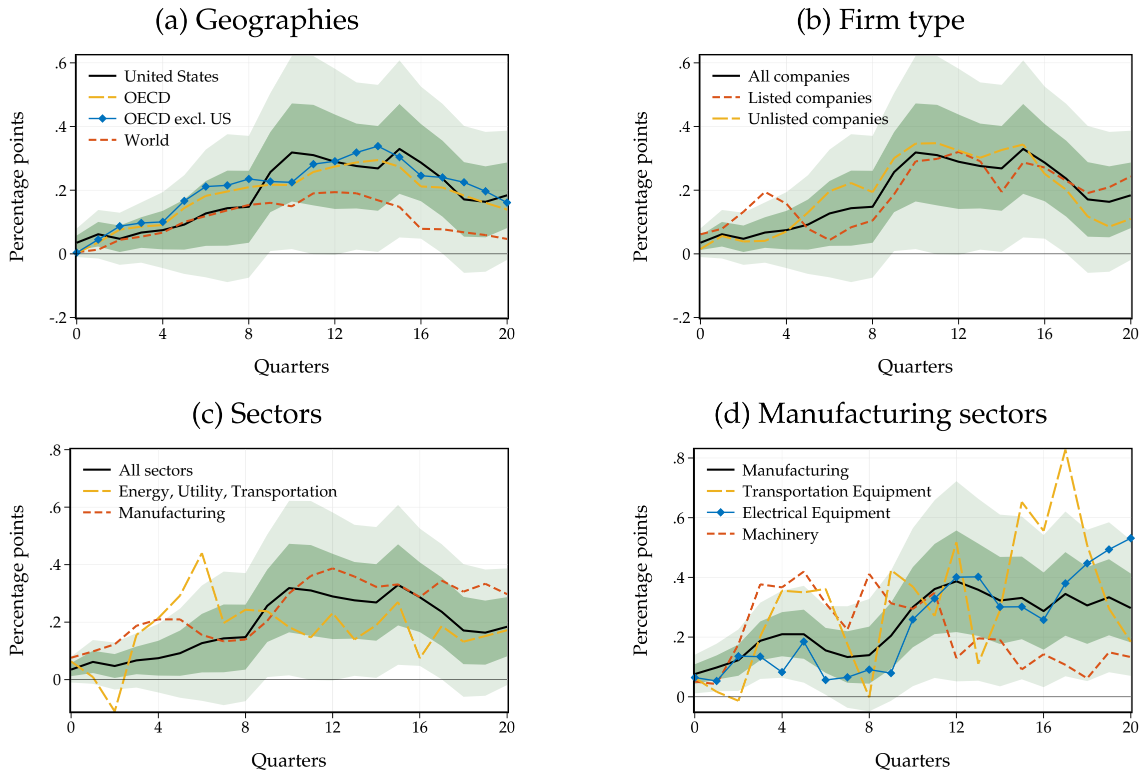

Notes: Responses of the green patent share to a U.S. monetary policy shock across different geographies (Panel a), firm types (Panel b) and sectors (Panels c and d) estimated based on (2). Sectoral patent counts are smoothed using a three-quarter backward-looking moving average. Shock is normalized to increase the federal funds rate by 25 basis points on impact. Lines: point estimates. Dark and light shaded areas: baseline 68 and 95% confidence bands based on lag-augmented standard errors.

and demonstration (RD&D) expenditures on renewable energy by the U.S. Department of Energy (see Appendix A.5 for details on the construction of this series). As shown in Figure 6, our results remain virtually unchanged.

A second possibility relates to physical climate risks. Natural disasters could both depress economic activity and increase demand for climate-mitigation technologies. We address this possibility by controlling for the climate news index of Engle et al. (2020), a text-based measure of climate-change-related news coverage. The results are robust.

A third possibility is that green patenting responds to commodity prices, particularly oil prices. If a recession is triggered by an adverse oil supply shock, the resulting increase in oil prices may induce directed technical change (Popp, 2002; Hassler, Krusell, and Olovsson, 2021). Because our analysis focuses on demand-driven business cycle and monetary policy shocks, however, this channel is unlikely to drive our baseline results. Figure 6a shows that our results are robust to controlling for oil prices. We also find that adverse oil supply shocks—which raise oil prices and reduce activity—do not generate a materially stronger green patenting response than our baseline demand shocks, suggest-

Figure 6: Sensitivity of green patenting responses to a monetary policy shock

(a) Sensitivity with respect to controls

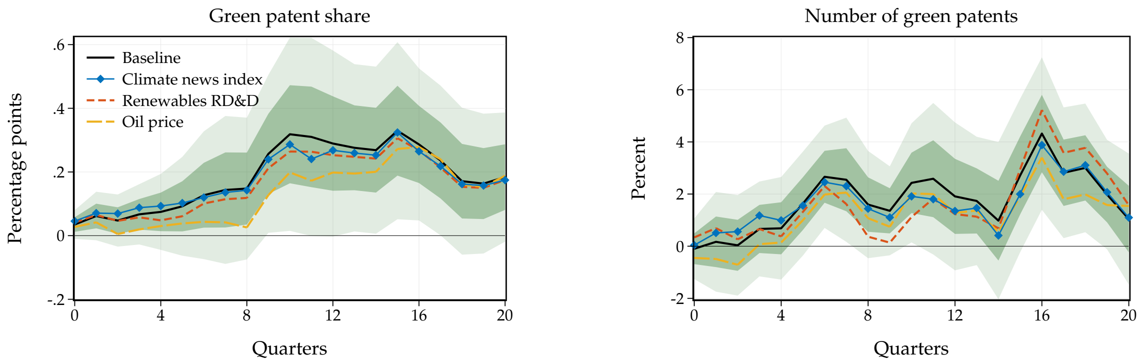

(b) Pre-trends

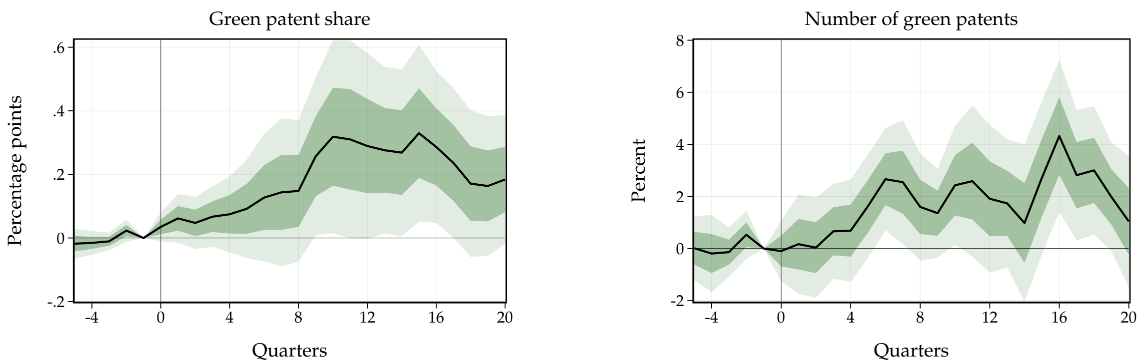

(c) Scatter plot at $h = 12$

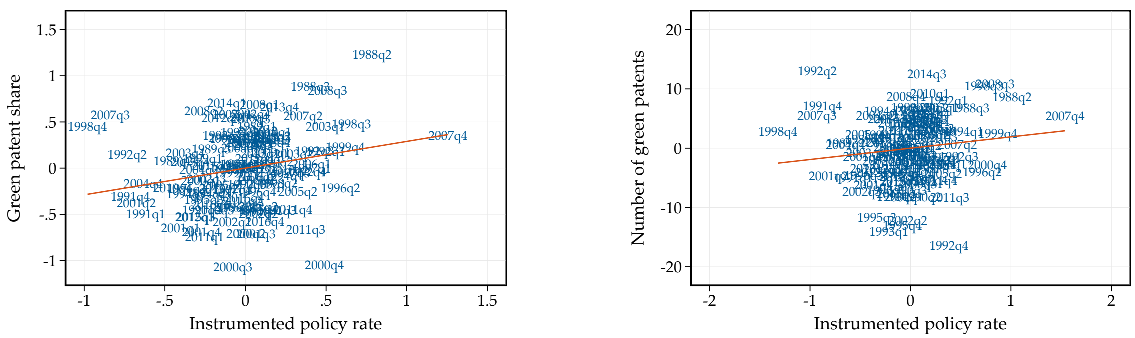

Notes: Sensitivity of green patenting responses to a monetary policy shock, estimated based on (2). Top panels: responses controlling for the Engle et al. (2020) climate news index, renewables RD&D expenditure by the U.S. DOE, and oil prices. Middle panels: baseline responses with pre-trends. Estimate for $h{=}-1$ is zero by construction; for $h{=}-4,\ldots,-2$ the lag corresponding to the horizon is excluded from the specification. Shock is normalized to increase the federal funds rate by 25 basis points on impact. Lines: point estimates. Dark and light shaded areas: baseline 68 and 95% confidence bands based on lag-augmented standard errors. Bottom panels: Scatter plot of monetary shocks against the cumulative change in the outcomes after 12 quarters, conditional on our set of controls.

ing a limited role for oil-price-induced directed technical change in explaining our results (see Appendix B.1.1).

Fifth, we examine the evolution of patenting prior to the shock to assess the presence of pre-trends. In particular, the concern is that the estimated effects may capture pre-existing trends in green patenting rather than a causal response to the shock. Reassuringly, we find no evidence of such pre-trends, see Figure 6b.

Sixth, we assess whether the estimated countercyclicality of green patenting is driven by a small number of extreme observations. Figure 6c shows the 12-quarter changes in the green patent share and the number of green patents against the instrumented policy rate at time t, after residualizing with respect to our controls. Both panels reveal a robust positive relationship that is not driven by particular outliers. A complementary jackknife exercise confirms this finding (see Appendix B.1.3).

Finally, we examine the sensitivity of our results to the measurement of green innovation. The results remain robust when we use alternative green patent classifications or account for patent quality (see Appendix B.1.2).

2.3. The Cyclicality of Green Innovation at the Firm Level

The macro evidence suggests that green patenting is countercyclical. Is this pattern driven by a subset of firms that specialize in green technologies, or is there some reallocation from non-green to green patenting even within firms?

To examine this, we study firm-level patenting responses in a large panel of listed U.S. companies. Formally, we estimate a panel version of the LP-IV specification (2):

$$y_{i,t+h} = \alpha_i^h + \theta^h r_t + \boldsymbol{\beta}_{xi}^h \mathbf{x}_{i,t-1} + \boldsymbol{\beta}_x^h \mathbf{x}_{t-1} + \varepsilon_{i,t+h}, \tag{3}$$

where $y_{i,t+h}$ now corresponds to the outcome variable of firm i, h-quarters ahead. As outcome variables, we consider firms' overall number of patents filed, the green patent share, and the number of green or non-green patents. In this specification, we also control for firm fixed effects, α_i^h, to absorb any time-invariant firm characteristics. To allow for general forms of cross-sectional and temporal dependence in the panel data, we compute standard errors using the Driscoll and Kraay (1998) approach.

We restrict our sample to companies that are consistently observed for 20 quarters and, following Hémous et al. (2025), have at least one green patent over our sample period. We exclude firms in the finance, insurance, real estate or public administration sectors. The results are robust to these sample restrictions.[9] Our final sample consists of 166,000 firm-quarter observations, covering more than 2,100 companies and about 93,000 green patents from 1986Q1–2019Q4.

A challenge for the firm-level estimation is the sparsity of the patent data. Many firm-quarter observations contain zero patent filings, particularly for green patents, making logarithmic transformations infeasible. We address this issue in two ways. First, we

[9] In particular, the results are robust to including firms that never filed a green patent.

Figure 7: Green and non-green patenting responses of U.S. firms

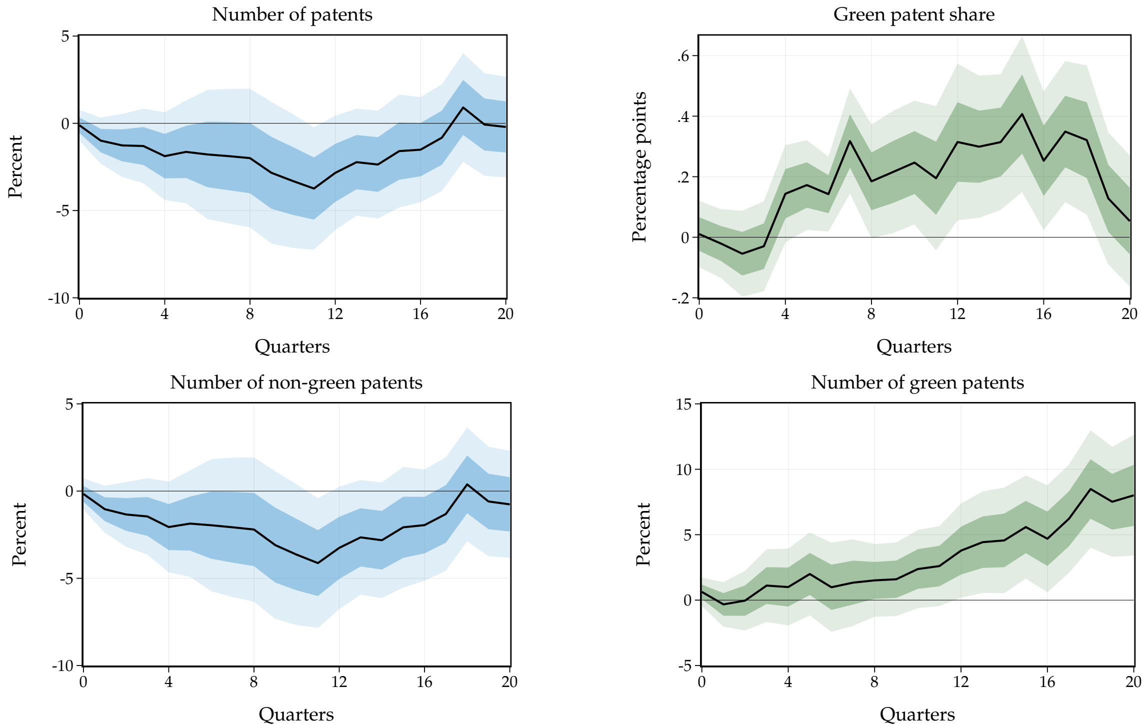

Notes: Responses of firm-level patenting measures in the U.S. to a monetary policy shock, estimated based on (3). Shock is normalized to increase the federal funds rate by 25 basis points on impact. Solid line: point estimate. Dark and light shaded areas: 68 and 95% confidence bands based on Driscoll and Kraay (1998) standard errors.

smooth the firm-level patenting measures using a backward-looking three-quarter moving average. Second, we estimate the responses of patent counts in levels rather than logs and scale the impulse responses by the corresponding average patent count.

Figure 7 shows the firm-level patenting responses to a contractionary monetary policy shock. The estimated responses align well with the aggregate evidence, both qualitatively and quantitatively. We find a significant fall in overall and non-green patents and an increase in the number of green patents. We also document an increase in the firm-level green patent share, which peaks at around 0.4 percentage points. This is striking, because it suggests a shift from non-green to green patenting even *within* a given firm.

An alternative approach to deal with the sparseness in the patent data is to employ a Poisson Pseudo Maximum Likelihood (PPML) estimator (see e.g. Aghion et al., 2026):

$$\mathrm{E}\left[\sum_{h=1}^{20} y_{i,t+h} \,\middle|\, r_t, \mathbf{x}_{i,t-1}, \mathbf{x}_{t-1}, i\right] = \exp\left(\alpha_i + \theta r_t + \boldsymbol{\beta}'_{xi}\mathbf{x}_{i,t-1} + \boldsymbol{\beta}'_{x}\mathbf{x}_{t-1}\right), \qquad (4)$$

where $\sum_{h=1}^{20} y_{i,t+h}$ captures firm i's cumulative number of green and non-green patents, 20 quarters ahead. By focusing on cumulative patents, we allow for a sufficiently long lag between R&D expenditures and patent applications, in line with Hémous et al. (2025). As

Table 2: Heterogeneity by firms' profit structures

Dep. var.:	Green patents$_{it+h}$			Non-green patents$_{it+h}$		
	(1)	(2)	(3)	(4)	(5)	(6)
r_t	0.013**	0.013**		-0.034**	-0.034**	
	(0.006)	(0.006)		(0.015)	(0.015)	
$\text{r}_t \times \overline{\text{btm}}_i$		-0.004***	-0.004***		0.004***	0.004***
		(0.001)	(0.001)		(0.001)	(0.001)
Observations	84,505	84,505	84,505	84,136	84,136	84,136
Firms	1,523	1,523	1,523	1,523	1,523	1,523
Time FE	No	No	Yes	No	No	Yes

Notes: Patenting semi-elasticities to monetary policy shock, estimated from PPML-IV model (4). Dependent variables: firm's cumulative, 20-quarter ahead number of green and non-green patents. Shock is normalized to increase the federal funds rate by 25 basis points. We include interaction terms with the average, standardized book-to-market ratio. Driscoll and Kraay (1998) standard errors in parentheses. Significance levels denoted by *** $p < 0.01$, ** $p < 0.05$, * $p < 0.10$.

before, we instrument the Fed funds rate using monetary surprises and include a set of (lagged) controls and firm fixed effects.

Firm-level heterogeneity. How does the patenting response vary with firm-level characteristics? Do firms with a more backloaded profit structure display a stronger green patenting response? Based on the more parsimonious PPML specification, we study how monetary policy shocks interact with firm-level characteristics, $\overline{d}_i$:

$$\mathrm{E}\left[\sum_{h=1}^{20} y_{i,t+h} \,\middle|\, r_t\overline{d}_i, \mathbf{x}_{i,t-1}, i, t\right] = \exp\left(\alpha_i + \delta_t + \gamma\, r_t\overline{d}_i + \boldsymbol{\beta}'_{xi}\mathbf{x}_{i,t-1}\right). \tag{5}$$

We instrument the interaction $r_t\overline{d}_i$ with the corresponding interaction between $\overline{d}_i$ and the high-frequency monetary policy surprise.

To proxy for firms' profit structures we focus on the book-to-market ratio. The idea is that growth firms—i.e. firms with low book-to-market—have a more backloaded profit structure. We rely on the firm-level average over the first half of the sample, $\overline{\text{btm}}_i$, to assess this margin. The results are robust to using the full-sample average instead.

This specification allows us to control for time fixed effects, δ_t, which helps to further sharpen the identification of the (relative) effects of monetary policy shocks. We also report the base effect from a specification without time fixed effects, controlling instead for the aggregate macro controls introduced above. For inference, we rely on Driscoll and Kraay (1998) standard errors, but find comparable estimates using a bootstrap approach.

Table 2 presents the results. The baseline estimates for green and non-green patenting are shown in columns (1) and (4). We find that a 25-basis-point monetary policy shock is associated with a significant 1.3% increase in cumulative green patenting and a 3.4%

decline in cumulative non-green patenting over 20 quarters. The signs and magnitudes of these estimates are broadly consistent with the local projection evidence.

In columns (2)-(3) and (5)-(6), we report the interaction effects with the book-to-market value. To facilitate interpretation, we standardize the interaction terms. Consistent with our purported mechanism, we find a significantly stronger green patenting response for growth firms. These effects are also economically meaningful: firms one standard deviation below the mean book-to-market increase green patenting about 30% more than the average firm (0.017 vs. 0.013). The interaction effect is robust to including time fixed effects. Similarly, the base effects are largely unchanged when introducing the interactions.

Do the patenting responses also vary with other firm-level characteristics? In Appendix B.2.3, we consider several additional firm-level characteristics, including proxies for financial constraints and firms' R&D intensity. While some of these interactions are significant, we find no systematic evidence that they can account for the differential green and non-green patenting responses. Importantly, the interaction with book-to-market remains robust when we jointly control for these additional interactions and, if anything, becomes slightly larger.

3. A Model of Directed Technical Change Over the Cycle

The empirical evidence points to the backloaded profit structure of green innovations as an important driver of their countercyclicality. We now assess whether a model centered on this mechanism can account for the empirical responses, both qualitatively and quantitatively. To this end, we develop a dynamic stochastic general equilibrium (GE) model with endogenous green and non-green innovation. The model comprises three building blocks: a production block, an innovation block, and a household block governing consumption and labor supply.

We begin by describing the problem of the firm in Section 3.1, taking overall innovation and labor outcomes as given. This partial equilibrium setting allows us to isolate key mechanisms. In Section 3.4, we embed the production block into a full general equilibrium model and discuss the potential role of general equilibrium effects.

3.1. Firms

The production economy features a final good that uses both material and energy composites as inputs. The energy input itself is a composite of fossil fuels and green energy.

Final good producer. There is a representative firm that produces the final good by employing unskilled labor L_t, a material composite M_t, and an energy composite E_t:

$$Y_t = (Z_t L_t)^{\alpha_L} M_t^{\alpha_M} E_t^{1-\alpha_L-\alpha_M}, \tag{6}$$

where Z_t is an aggregate labor productivity, evolving as $\log Z_t = \rho_z \log Z_{t-1} + \sigma_z \varepsilon_t^z$.

We think of the material composite as the gray, or non-green, input. The energy composite E_t consists of fossil fuel f_t and a green energy composite G_t, which are combined by the final goods producer using a CES technology:

$$E_t = \left(f_t^{\frac{\rho-1}{\rho}} + G_t^{\frac{\rho-1}{\rho}} \right)^{\frac{\rho}{\rho-1}}. \tag{7}$$

The parameter ρ is crucial: it governs the elasticity of substitution between fossil fuel and the green energy composite. We assume $\rho > 1$, indicating that f_t and G_t are substitutes.

The green energy composite G_t and the materials composite M_t each aggregate a continuum of differentiated inputs:

$$M_t = \Big(\int_0^{A_t^M} m_{ht}^{\frac{1}{\mu_M}} \, dh \Big)^{\mu_M}, \qquad G_t = \Big(\int_0^{A_t^G} g_{jt}^{\frac{1}{\mu_G}} \, dj \Big)^{\mu_G}, \tag{8}$$

where, as in Romer (1990), A_t^G and A_t^M denote the number of available green energy and materials varieties, respectively.

The final good producer's optimization problem is:

$$\max_{L_t, \{m_{ht}\}, f_t, \{g_{jt}\}} P_t \left[(Z_t L_t)^{\alpha_L} M_t^{\alpha_M} E_t^{1-\alpha_L-\alpha_M} \right] - \int_0^{A_t^M} p_{ht}^m \, m_{ht} \, dh - \int_0^{A_t^G} p_{jt}^g \, g_{jt} \, dj - P_t^f \, f_t - W_t L_t. \tag{9}$$

Solving this problem yields the following demand equations:

$$m_{ht} = \left(\frac{p_{ht}^m}{P_t^M} \right)^{\frac{\mu_M}{1-\mu_M}} M_t, \qquad g_{jt} = \left(\frac{p_{jt}^g}{P_t^G} \right)^{\frac{\mu_G}{1-\mu_G}} G_t, \tag{10}$$

where $P_t^M = \left(\int_0^{A_t^M} (p_{ht}^m)^{\frac{1}{1-\mu_M}} \, dh \right)^{1-\mu_M}$ and $P_t^G = \left(\int_0^{A_t^G} (p_{jt}^g)^{\frac{1}{1-\mu_G}} \, dj \right)^{1-\mu_G}$ are the corresponding price indices of M_t and G_t.

Intermediate input producers. Intermediate input producers—firms that produce non-green and green varieties, m_{ht} and g_{jt}—maximize profits subject to the demand equations in (10).

Green energy varieties. The green energy varieties are produced by a continuum of firms operating under monopolistic competition. Each green variety g_{jt} is indexed by $j \in [0, A_t^G]$. Consider a generic variety j. Its production uses a linear production technology: each unit of green energy variety j requires one unit of final good

$$g_{jt} = Y_t^j, \tag{11}$$

where Y_t^j represents the final good used as an input by variety j.

The profit maximization problem for producing this green energy variety is:

$$\Pi_{jt}^{G} = \max_{p_{jt}^{g}} \left(p_{jt}^{g} g_{jt} - g_{jt} \right) \quad \text{s.t. the demand equation in (10).} \tag{12}$$

We assume that each period, there is a fixed probability $1-\phi$ that the variety becomes obsolete. This is a reduced-form way to capture the notion that some varieties will be replaced by better varieties over time. In Appendix C.11, we endogenize this to allow for creative destruction in the spirit of Aghion and Howitt (1992).[10]

The value of owning the intellectual property (IP) right to produce the green variety j, V_{jt}^{G}, is thus given by:

$$V_{jt}^{G} = \sum_{s=0}^{\infty} \phi^{s}\, \mathbb{E}_t \left[\Lambda_{t,t+s}\, \Pi_{j,t+s}^{G} \right], \tag{13}$$

where Π_{jt}^{G} is the period profit, as defined in (12). Given this setup, the value of owning a green patent today is the expected sum of future profits Π_{jt+s}^{G}, discounted using the discount factor $\Lambda_{t,t+s}$ and adjusted by the survival probability ϕ^{s}.

IP values determine innovators' incentives to innovate. We postpone the discussion of innovators' optimization problems to Section 3.3.

Non-green material varieties. Non-green material varieties are produced and sold similarly to green energy varieties. Each variety m_{ht} is indexed by $h \in [0, A_t^M]$ and produced via a linear technology:

$$m_{ht} = Y_t^h, \tag{14}$$

where Y_t^h represents the final good used as an input by non-green variety h.

The profit maximization problem for producing the non-green variety h is:

$$\Pi_{ht}^{m} = \max_{p_{ht}^{m}} \left(p_{ht}^{m} m_{ht} - m_{ht} \right) \quad \text{s.t. the demand equation in (10).} \tag{15}$$

Similar to green varieties, each non-green variety becomes obsolete with probability $1-\phi$.

The value of holding the IP rights to a non-green variety h satisfies:

$$V_{ht}^{M} = \sum_{s=0}^{\infty} \phi^{s}\, \mathbb{E}_t \left[\Lambda_{t,t+s}\, \Pi_{h,t+s}^{m} \right]. \tag{16}$$

Fossil fuel. We follow Acemoglu et al. (2016) to model the oil market as follows. Fossil fuel is extracted by a set of competitive firms using final goods as the sole input. Extraction

[10] All our results go through in the quality ladder model, but the tractability of the expanding varieties model allows us to derive some propositions in closed form. Specifically, when we endogenize the obsolescence rate, we are no longer able to obtain closed-form solutions for the allocation of skilled labor across green and non-green innovation activities. See Appendix C.11 for more details.

follows a linear technology:

$$f_t = \xi_f \cdot Y_t^f, \tag{17}$$

where f_t denotes the quantity of fossil fuel extracted in period t, $\xi_f > 0$ governs the productivity, and Y_t^f is the amount of final good allocated to extraction.

Let R_t denote the oil reserves at time t. Oil reserves evolve as:

$$R_{t+1} = R_t - f_t, \tag{18}$$

which indicates that reserves decrease over time as a result of extraction. The resource constraint requires that the oil reserves be non-negative in the long run: $\lim_{t\to\infty} R_t \geq 0$.

This is a simple, reduced-form way of modeling the oil market. We assume fixed marginal extraction costs, resulting in a constant fossil fuel price. Thus, any change in the relative price of green energy arises from changes in the price of green energy itself.

As robustness checks, we consider two alternative specifications of the oil market. In Appendix C.9, we consider an extension that allows for technological progress in fossil fuel extraction, following Aghion et al. (2016). This introduces some dynamic pricing considerations, similar in spirit to Bornstein, Krusell, and Rebelo (2023). In Appendix C.10, we implement an alternative formulation of extraction costs following Bornstein, Krusell, and Rebelo (2023), where costs are convex in the extraction rate. These extensions illustrate that our results generalize to more realistic fossil market structures.

For now, we consider a real economy in which the final good serves as the numeraire, so that $P_t = 1$. In Section 3.5, we introduce nominal rigidities to study the effects of monetary policy shocks, as in our empirical analysis.

3.2. Green Is in the Future

The partial equilibrium setting allows us to distill some of the key mechanisms driving the cyclicality of green and non-green patenting. We assume that final and intermediate goods firms maximize their profits, taking the evolution of A_t^M and A_t^G as given. We restrict our analysis to an economy on a balanced growth path (BGP) where A_t^M and A_t^G share the same long-run growth rate, with A_t^M / A_t^G nondecreasing along the transition.[11] For now, we assume that such a path exists. We discuss the existence of a BGP when we move to the general equilibrium setting.

We consider an economy undergoing a green transition. Along this transition path, A_t^G rises, leading to an increase in the green share of energy, $\frac{G_t}{E_t}$—despite the fact that fossil reserves are not exhausted.

[11]Section 3.4 makes the technology path endogenous; Lemma D.1 shows that the no-shock equilibrium satisfies this restriction.

Lemma 3.1 (Condition for the Green Transition). *Define the green transition as the process in which the green share of energy, $\frac{G_t}{E_t}$, increases during the transition period. The economy undergoes the green transition if and only if $\frac{P_t^f}{P_t^G}$ increases over time, where $P_t^G = \mu_G (A_t^G)^{1-\mu_G}$.*

Proof. See Appendix D. ■

The intuition for the above lemma is straightforward: the green share of energy increases over time if and only if the price of green energy, relative to the price of fossil fuel, declines over time. In a Romer (1990)-type growth model, the total number of varieties reflects productivity in the economy. Analogously, in our framework, A_t^G captures the productivity of green inputs. As a result, green innovations that increase A_t^G raise the productivity of green energy, lower its relative price, and induce final goods producers to substitute toward green energy inputs.

Under our assumptions, this condition is trivially satisfied as the price of fossil energy is fixed while the price of green decreases as A_t^G increases.

Given the symmetry, all green varieties charge the same price, produce the same quantity, and earn the same profit; the same holds within the materials sector. We henceforth drop variety indices and write Π_t^G, Π_t^M, V_t^G, V_t^M for per-variety profit and IP value. We obtain the following proposition:

Proposition 3.1 (Green Is in the Future). *During the green transition:*

(1) The equilibrium market share of green energy, given by $\frac{P_t^G G_t}{P_t Y_t}$, increases over time.

(2) The relative profits of green varieties compared to non-green varieties, measured by $\frac{\Pi_t^G}{\Pi_t^M}$, increase over time.

Proof. See Appendix D. ■

Proposition 3.1 shows that, during the green transition, the equilibrium market share of G_t, denoted by $\frac{P_t^G G_t}{P_t Y_t}$, increases over time, and profits per green variety rise relative to those per non-green variety. We label this phenomenon as *green is in the future*. The intuition for this result is as follows. As the share of green energy in total energy use rises, the overall market share of green energy in the economy increases. This shift leads final good producers to substitute away from fossil fuel toward green energy inputs.

The resulting increase in relative profits shifts the weight of green cash flows toward the future. This implies that the value of a green patent, V_t^G, reflecting the discounted sum of future profits, is more backloaded relative to that of non-green patents.

The backloaded profit structure of green patents suggests that V_t^G is less affected by an exogenous, transitory disturbance to Y_t than V_t^M—holding discount rates and other prices fixed. The key intuition is that business-cycle shocks operate at much shorter horizons and thus do not affect cash flows further out in the future. Proposition 3.2 formalizes this insight: the relative value of producing g_{jt}, defined as $\frac{V_t^G}{V_t^M}$, exhibits countercyclicality.

Proposition 3.2 (Cyclicality during the Green Transition). *During the green transition, and holding the discount factor constant, the relative value of producing g_{jt}, defined as $\frac{V_t^G}{V_t^M}$, exhibits countercyclicality. Formally, $\frac{d\log V_t^G}{d\log Y_t} < \frac{d\log V_t^M}{d\log Y_t}$, or equivalently $\frac{d\log\left(V_t^G/V_t^M\right)}{d\log Y_t} < 0$. We coin this the "green duration channel".*

Proof. See Appendix D. ■

So far, we have kept discount rates fixed. How do changes in discount rates affect the cyclicality of innovation? To shed light on this, we employ the following decomposition:

$$\frac{d\log V_t^K}{d\log Y_t} = \underbrace{\sum_{s=0}^{\infty}\phi^s \frac{\Lambda_{t,t+s,ss}\Pi^K_{t+s,ss}}{V^K_{t,ss}} \frac{d\log \Pi^K_{t+s}}{d\log Y_t}}_{\text{Cash flow channel}} + \underbrace{\sum_{s=0}^{\infty}\phi^s \frac{\Lambda_{t,t+s,ss}\Pi^K_{t+s,ss}}{V^K_{t,ss}} \frac{d\log \Lambda_{t,t+s}}{d\log Y_t}}_{\text{Discount rate channel}}, \tag{19}$$

for $K{=}\{M,G\}$, where $X_{t,ss}$ captures the evolution of X along the transition absent any shocks, and $\Lambda_{t,t+s,ss} = \beta^s \frac{U'(C_{t+s,ss})}{U'(C_{t,ss})}$ is the stochastic discount factor (SDF) along the transition with no shocks. The first component captures the effect of changes in cash flows, holding the discount factor fixed (see Proposition 3.2). The second component captures changes in the discount rate, keeping the cash flows at the trajectory absent any shocks.

While the cash flow channel unambiguously generates countercyclicality in V_t^G/V_t^M, the discount rate channel depends on the cyclicality of the SDF. As we show in Appendix D, a procyclical stochastic discount factor dampens the countercyclicality of the relative valuation of green patents while a countercyclical SDF amplifies it. The intuition is straightforward. If the discount factor falls in a recession—making agents discount the future more—the IP values of green innovations are hurt *more* and not less than those of non-green innovations because of the more backloaded structure.

The cyclicality of the SDF depends on the underlying shock driving the business cycle. Our empirical evidence conditional on monetary policy shocks suggests that the cash flow channel dominates: such shocks imply a procyclical SDF, which works against the countercyclicality of green innovation. In Section 3.5, we allow for the SDF to be endogenously determined and show that the relative value of green innovation, net of setup costs, is generally countercyclical.

The net values of green and non-green innovation determine the incentives to innovate over the cycle. In the next section, we study the corresponding problem of the innovators.

3.3. Innovators

There is a continuum of innovators indexed by $i \in [0, 1]$. Each existing green or non-green variety, as described in the previous section, is created by one of these innovators. Because the innovation decisions for each variety are independent of one another, we need not track which innovator creates and owns which variety.

In each period, each innovator i engages in R&D to *create* new varieties. Upon successfully developing a new variety, the innovator sells its IP rights at the price $\mathcal{G}_t^K \equiv \mathbb{E}_t[\Lambda_{t,t+1} V_{t+1}^K]$, since production begins in period $t+1$. We now describe this innovation process in more detail.

Let $L_{it,K}^S$ denote the skilled labor employed in R&D by innovator i in materials and green-energy innovation, K=$\{M, G\}$. Let $L_{t,K}^S \equiv \int_0^1 L_{it,K}^S \, di$ denote aggregate sector-K R&D input. φ_t^K is the number of new technologies that each unit of skilled labor can create. Following Romer (1990), we assume the innovation productivity depends on aggregate conditions, meant to capture knowledge spillover effects:

$$\varphi_t^K = \zeta_K A_t^K \left(L_{t,K}^S\right)^{-(1-\nu)} \tag{20}$$

where the terms A_t^K capture positive externalities from knowledge accumulation, respectively. There is also a congestion externality: as more firms engage in R&D, each one's contribution becomes less effective due to competition for similar innovation targets. The strength of this congestion externality is governed by $\nu \in [0, 1)$ and prevents corner solutions in which all innovation is concentrated in a single type.

We assume that innovators pay a fixed setup cost, $c\bar{\mathcal{G}}_t^K$, for each unit of new innovation. These costs are proportional to the counterfactual value of intellectual property in the absence of aggregate shocks. Specifically, $\bar{\mathcal{G}}_t^K$ represents the expected discounted value of new IP rights, where production profits are evaluated at their no-shock values along the economy's actual technology path. This modeling choice, similar to the calibration strategy in Barlevy (2007), allows the model to generate realistic cyclical responses of innovation investment while maintaining internal consistency between setup costs and expected value. We denote the net value of innovation by $\mathcal{V}_t^K = \mathcal{G}_t^K - c\bar{\mathcal{G}}_t^K$.

In summary, innovator i's optimization problem can be written as:

$$\max_{L_{it,K}^S} \quad \varphi_t^K L_{it,K}^S \mathcal{V}_t^K - W_t^S L_{it,K}^S, \tag{21}$$

taking wages W_t^S and innovation productivity φ_t^K as given.

The free-entry condition is therefore

$$\zeta_K A_t^K \left(L_{t,K}^S\right)^{\nu-1} \mathcal{V}_t^K = W_t^S, \qquad K \in \{G, M\}. \tag{22}$$

Aggregation. Let $S_t^K = \varphi_t^K L_{t,K}^S$ denote the aggregate successful innovation in $K = \{M, G\}$. The total amount of varieties then evolves as $A_{t+1}^K = \phi A_t^K + S_t^K$.

3.4. General Equilibrium

We now embed the production and innovation blocks into a general equilibrium setting. This allows us to incorporate business cycle shocks, as examined in the empirical part of the paper, and to analyze the cyclicality of innovation *outcomes*, rather than just their incentives. More importantly, within this general equilibrium setting, a key mechanism emerges that explains the notable countercyclical pattern of the number of green patents uncovered in our empirical analysis. To close the economy, we detail the household sector and discuss market clearing.

Households. All households are identical, which is why we focus on the problem of a representative household. The household derives utility over consumption C_t and labor. They maximize lifetime utility

$$\mathbb{E}_t \sum_{t=0}^{\infty} \beta^t \left(\varrho_t^d \log C_t - \frac{\bar{\omega}}{1+\eta} L_t^{1+\eta} - \frac{\bar{\omega}^S}{1+\psi} (L_t^S)^{1+\psi} \right), \tag{23}$$

where ϱ_t^d is the time-preference shock which follows: $\log \varrho_t^d = \rho_d \log \varrho_{t-1}^d + \sigma_d \varepsilon_t^d$.

The household faces the following budget constraint:

$$P_t C_t + Q_t B_{t+1} = B_t + W_t L_t + W_t^S L_t^S + D_t. \tag{24}$$

Here, L_t is the supply of unskilled labor and L_t^S is the supply of skilled labor with corresponding wages W_t and W_t^S, B_t is a risk-free bond and D_t are transfers.

Market clearing. In general equilibrium, all markets must clear. Unskilled labor market clearing requires the final-good producer's labor demand to equal the household's supply, $L_t^d = L_t$, while skilled labor market clearing requires

$$\int_0^1 \left(L_{it,G}^S + L_{it,M}^S \right) di = L_t^S. \tag{25}$$

Final-good market clearing requires

$$C_t + \int_0^{A_t^M} m_{ht}\, dh + \int_0^{A_t^G} g_{jt}\, dj + \xi_f^{-1} f_t = Y_t. \tag{26}$$

The bond market then clears by Walras' law, i.e. $B_{t+1} = 0$.

Balanced growth. We assume that a BGP exists and that the economy is on a green transition path, or equivalently that the conditions stated in Lemma 3.1 hold. This assumption is not restrictive. In our model, we will always be on a green transition path in the absence of technological obsolescence—i.e., when $\phi = 1$. With technological obsolescence

($\phi < 1$), the green transition condition requires that the parameters governing green innovation are such that the pace of green innovation exceeds the rate of obsolescence. In our quantitative analysis, we confirm that this condition holds for empirically plausible calibrations. In Appendix C.2, we provide a detailed discussion on existence.

3.5. The Role of General Equilibrium Effects

We now study the cyclicality of green and non-green patenting in general equilibrium. We first start with our real model and consider preference ϱ_t^d and TFP shocks Z_t. In a next step, we introduce nominal rigidities and also study monetary policy shocks. For the analytical results in this section, we set $\phi = 1$; we relax this assumption in the quantitative analysis in Section 4.1.

A key prediction from our partial equilibrium analysis is that the relative value of green varieties is countercyclical during the green transition. In general equilibrium, innovation depends on patent values net of setup costs. The countercyclicality of the relative net value of green innovation then implies that firms' R&D investment in green, relative to non-green, is countercyclical as well. As a result, the green share of new varieties, $\frac{S_t^G}{S_t^G+S_t^M}$, is itself countercyclical. Proposition 3.3 formalizes this result.

Proposition 3.3 (**Countercyclical Green Share of New Varieties**). *Under a regularity condition, during the green transition, the green share of new varieties, $\frac{S_t^G}{S_t^G+S_t^M}$, is countercyclical conditional on both preference and TFP shocks.*

Proof. See Appendix D. ■

Proposition 3.3, however, does not only apply for shocks that imply a countercyclical SDF: it also holds for technology and preference shocks that imply a procyclical SDF in our model. In these cases, the discount rate channel could potentially overturn the cash flow channel. However, we show that the relative net value of green innovation remains countercyclical. Key to this result is the assumption of log utility. If the intertemporal elasticity of substitution is much lower, the discount rate channel becomes more powerful and the result could be potentially overturned. In Section 4.1, we show that under empirically plausible parameterizations, the discount rate channel is dominated. The regularity condition is $0 < \rho_U < 1 - \nu(1-\beta)/[\beta(1-\nu+\psi)]$. It holds provided that business-cycle shocks are not quasi-permanent. Intuitively, our mechanism relies on heterogeneous exposure to business-cycle shocks—and on the non-permanent nature of these shocks. Under our baseline calibration, the condition requires shock persistence below approximately 0.998. This condition also applies to the subsequent results in this section.

So far, we showed that the green duration channel can account for the countercyclical share of green varieties. However, this channel alone is not enough to explain the countercyclicality in the *number* of green varieties.

In general equilibrium, there is an additional effect at play, driven by changes in equilibrium skilled wages. During recessions, skilled wages decline due to both increased labor supply—households' endogenous response to reduced consumption—and diminished labor demand, resulting from lower non-green innovation. The lower wage reduces the cost of green R&D, incentivizing firms to undertake more green innovation and thereby offsetting the partial-equilibrium effect. Proposition 3.4 shows that, if the elasticity of skilled wages with respect to either a TFP shock or a preference shock is sufficiently large, the number of new green varieties becomes countercyclical in general equilibrium.

Proposition 3.4 (**General Equilibrium Effects**). *During the green transition, there exists a threshold $\bar{\epsilon}_U$ such that green innovation is countercyclical, i.e.,*

$$\frac{\partial \log S_t^G}{\partial \log U_t} < 0,$$

if and only if the elasticity of skilled wages with respect to the shock, $\frac{\partial \log W_t^S}{\partial \log U_t}$, exceeds $\bar{\epsilon}_U$ for $U = Z, \varrho^d$. By contrast, non-green innovation is procyclical:

$$\frac{\partial \log S_t^M}{\partial \log U_t} > 0.$$

Moreover, the threshold $\bar{\epsilon}_U$ is lower when the net value of green innovation, $\mathcal{V}_t^G$, is less procyclical.

Proof. See Appendix D. ■

For green innovation to be countercyclical, as observed in the data, the general equilibrium effects through wages must offset the partial equilibrium effect of a recession on the value of green patents. The latter depends on the strength of the green duration channel. Therefore, the condition is more easily satisfied when the net value of green innovation is less procyclical.

To further build intuition, Corollary 3.1 provides a *sufficient* condition, showing that when the supply of skilled labor is sufficiently inelastic—that is, when the labor supply curve is steep—the general equilibrium effect dominates, rendering the number of new green varieties countercyclical.

Corollary 3.1. *During the green transition, there exists a threshold $\overline{\psi}_U$. If the Frisch elasticity of labor supply ψ^{-1} is less than $\overline{\psi}_U^{-1}$, then in equilibrium:*

$$\frac{\partial \log S_t^M}{\partial \log U_t} > 0, \qquad \frac{\partial \log S_t^G}{\partial \log U_t} < 0 \qquad \textit{for } U = Z,\ \varrho^d. \tag{27}$$

Proof. See Appendix D. ∎

Generalization to alternative innovation inputs. Our baseline specification generates cyclical innovation costs through the inelastic supply of skilled labor, a margin we view as empirically meaningful. The theoretical mechanism, however, does not depend on labor being the relevant input. Appendix C.4 generalizes the model to a generic scarce innovation input, X_t, with price P_t^X. This input may represent R&D capital, laboratory services, or any other scarce input required for innovation. What matters for our mechanism is not the identity of the input per se, but rather how its equilibrium price responds when innovation demand shifts over the business cycle. We show that the qualitative implications of Proposition 3.4 extend to this broader setting.

Monetary policy shocks. So far, we have focused on a real economy in which money is neutral. To be able to study the effects of monetary policy shocks, we extend the model to include nominal rigidities, with retailers facing Rotemberg price adjustment costs (see Appendix C.1 for details). We introduce monetary policy through a Taylor rule and incorporate a monetary shock ϱ_t^m, which follows: $\log \varrho_t^m = \rho_m \log \varrho_{t-1}^m + \sigma_m \varepsilon_t^m$.

A result similar to Proposition 3.4 holds conditional on monetary policy shocks:

Corollary 3.2. *During the green transition, there exists a threshold $\bar{\epsilon}_m > 0$. If the absolute value of the elasticity of skilled wages, $\left|\frac{\partial \log W_t^S}{\partial \log \varrho_t^m}\right|$, is greater than $\bar{\epsilon}_m$, then in equilibrium:*

$$\frac{\partial \log S_t^M}{\partial \log \varrho_t^m} < 0, \qquad \frac{\partial \log S_t^G}{\partial \log \varrho_t^m} > 0. \tag{28}$$

Proof. See Appendix D. ∎

4. Evaluating Model Predictions

The previous section analytically demonstrates that the model can qualitatively rationalize our empirical findings. In this section, we assess the model's predictions quantitatively. First, we show that under standard calibrations, the model can quantitatively match the empirical findings. Second, we confront key model predictions with the data and provide direct evidence supporting the model mechanisms.

4.1. A Quantitative Exploration

Calibration. We set the annual discount factor β to 0.99. The final good technology parameters α_L, α_M are set to 0.5 and 0.42, respectively, which corresponds to a 50% income share of intermediate inputs (Comin and Gertler 2006) and matches an 8% energy share of income, the average for the United States since 1970 reported by the U.S. Energy Information Administration (EIA). The markup parameters μ_M and μ_G are set to 2 to ensure the existence of a balanced growth path.

Following Acemoglu et al. (2012), we set the elasticity of substitution between green energy and fossil fuels, ρ, to 3. The extraction productivity ξ_f is normalized to 1. The congestion externality parameter ν is set to 0.5, within the range of panel and cross-sectional estimates from Griliches (1990). The technology obsolescence rate $1-\phi$ is set to 0.03, consistent with Comin and Gertler (2006) and recent estimates from Ma (2021).

For labor supply elasticities, we set the Frisch elasticity of labor supply, $1/\eta$, to 2, in line with standard RBC calibrations (Kydland and Prescott 1982; King and Rebelo 1999), to generate meaningful business cycle fluctuations. The inverse Frisch elasticity of skilled labor supply—the key parameter determining the strength of the GE effects—is set to $\psi = 2$. This is motivated by Chetty et al. (2011) and Elminejad et al. (2023) that estimate a low labor supply elasticity for skilled, higher-wage workers. The scale parameters of labor $\bar{\omega}$ and $\bar{\omega}^S$ are set to normalize the skilled and unskilled labor to 1 on the BGP.

Following Ottonello and Winberry (2020), we set $\varphi = 90$ and $\sigma = 10$. The Taylor rule coefficient is set to $\phi_\pi = 1.69$. We assume that supply and demand shocks are equally important in driving the business cycle. For the underlying contributions of demand shocks, we assume that preference shocks account for 45% and monetary policy shocks for 5%. We assume that all shocks are equally persistent, with $\rho_x = 0.6$. To jointly generate a 1.2% standard deviation of output at business cycle frequency, we calibrate the standard deviations of the shocks to $\sigma_z = 0.007$, $\sigma_d = 0.009$, and $\sigma_m = 0.002$.

We start the green transition at an initial state where fossil fuel consumption accounts for 80% of the total energy consumption—a value comparable to the figure reported by the EIA. Balanced growth requires the two technology stocks to grow at a common rate, which restricts the innovation-productivity parameters to $\zeta_G/\zeta_M = (\alpha_M/(1-\alpha_L-\alpha_M))^\nu$. At this initial state we therefore calibrate ζ_G to match the growth of the U.S. non-fossil energy share, which has averaged 1.2% per year (EIA), and this ratio then determines ζ_M. The fixed setup cost for innovation, $c = 0.89$, is calibrated to match a 2% standard deviation in aggregate R&D expenditures from the national accounts at business cycle frequencies.

Impulse responses. We now turn to the model's quantitative predictions. We focus on the effects of a monetary policy shock for more direct comparison with the empirical evidence. Figure 8 shows the impulse responses of green and non-green patenting to a 25 basis point monetary policy shock.

The net IP value of a non-green new variety is significantly more sensitive to shocks than that of a green variety, falling by around 1.5 times as much after a contractionary

Figure 8: Green and non-green patenting responses in the model

(a) Net IP value of new varieties (b) Green share (c) Number of new varieties

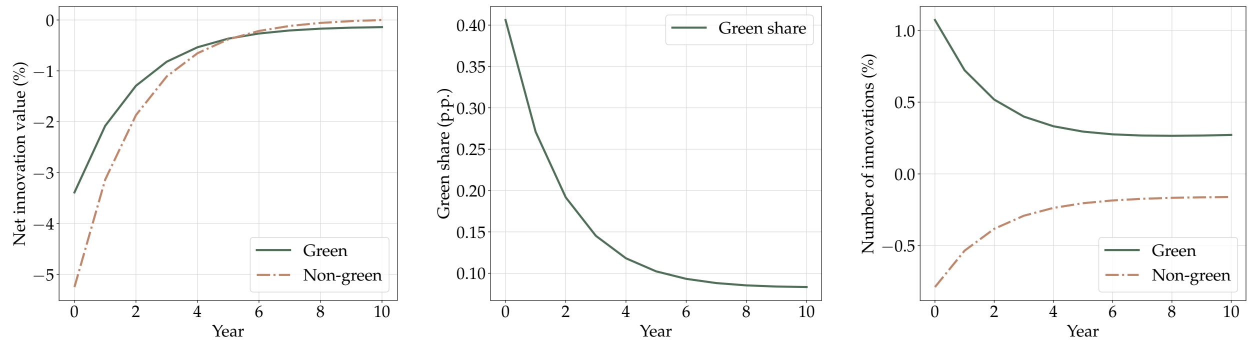

Notes: Impulse responses of the net value and number of varieties of green and non-green patents to a 25 basis point monetary policy shock, based on the green business cycle model calibrated to the U.S. economy.

monetary policy shock. This result demonstrates the quantitative significance of our green duration channel underlying Proposition 3.2.

Consistent with the change in the relative values of green and non-green varieties, the green share among new varieties increases. The magnitude of this increase is around 0.4 percentage points on impact—in line with the empirical response. Importantly, these moments are not targeted in our calibration, illustrating the quantitative success of the model.

The model not only produces the countercyclicality of the green share, it also generates the countercyclical response of the number of green varieties and the procyclical response of the number of non-green varieties.[12] This is the additional general equilibrium effect via the inelastic supply of skilled labor at play. After a recessionary shock, innovative activity falls, with a disproportionately larger drop in the non-green sector. This reduces the demand for skilled labor, leading to a decline in wages for skilled workers. The lower wages in turn decrease the cost of green R&D, incentivizing firms to undertake more green innovation.

These short-run reallocations also have permanent effects on the composition of technology. The intuition is that a transitory shock changes the flow of innovation today. Once extra green varieties are created, they do not disappear when the monetary shock fades. They raise the stock of green technology, lower the relative cost of green energy, and therefore leave the economy with a higher green patent share along the transition path. In our baseline calibration, ten years after the monetary tightening, green patenting remains about 0.27% above its no-shock path, and the green patent share remains close to 0.1 percentage points higher. Thus, by reallocating innovation between green and

[12]Since there is no clear quantitative mapping between new varieties and new patents, we cannot directly compare the magnitude of these responses to their empirical counterparts.

Figure 9: Decomposition: Cash flow vs. discount factor channel

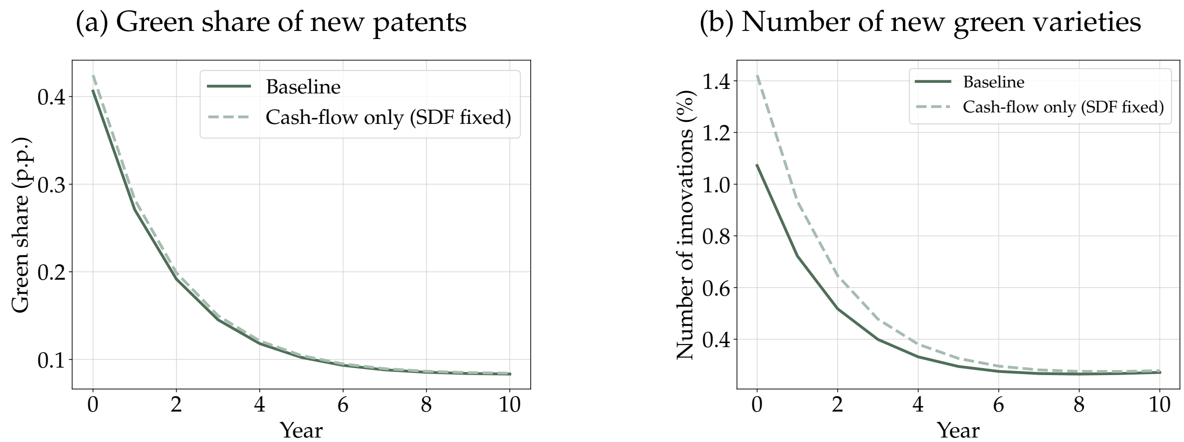

Notes: Impulse responses of the green share of new varieties and the number of new green varieties to a 25 basis point monetary policy shock. We compare the baseline model (with both cash flow and discount factor channels) to a counterfactual in which the discount factor channel is shut down.

non-green technologies, monetary policy can have permanent effects on the direction of technical change and on the green patent share.

How powerful is the discount rate channel in our simulations? To shed light on this, we perform a counterfactual exercise where we keep the discount rate fixed at its no-shock trajectory.

Figure 9 shows the results. We see that for monetary policy shocks the discount rate channel works against the green countercyclicality. The reason is that these shocks imply a procyclical SDF. When we shut the discount rate channel down, the green share increases by 0.42 percentage points on impact, around 0.02 percentage points more relative to our baseline response. The difference is even more pronounced when we look at the response of the number of new green varieties.

Overall, these results illustrate that while the discount factor channel goes against the cash flow channel, its quantitative impact is relatively modest. In Appendix C.6, we examine the sensitivity of these results with respect to the intertemporal elasticity of substitution. We show that the results are robust when we use a lower intertemporal elasticity of substitution of 0.5, even though the magnitudes are somewhat smaller due to the amplified discount rate channel.

In Appendix C.5, we study the responses to alternative shocks. Preference shocks are of particular interest, as they can generate a countercyclical SDF such that the discount rate channel reinforces the green countercyclicality. We find that a negative preference shock produces stronger countercyclicality than a monetary shock with the same impact on the output gap (see Appendix Figure C.2).

How does the green duration channel depend on the starting point and speed of the transition? Our baseline calibration implies that green energy accounts for half of energy expenditure after about 41 years. The further along in the transition, the weaker the countercyclicality of the green patent share: as green energy takes over, the current cash flow of a green variety grows relative to its patent value, and the green duration effect fades. See Appendix C.7 for details. For similar reasons, the countercyclicality of the green patent share is also amplified when the overall speed of the transition is accelerated, see Appendix C.8.

4.2. Empirical Evidence Supporting the Model Mechanism

In this section, we provide empirical evidence supporting our key model mechanisms. We start by looking into the green duration channel. As discussed in Section 3.2, this channel is active when the values of green patents are less cyclical than those of non-green patents. This is a testable prediction that we can confront with the data.

To test this prediction, we use the market-implied values of USPTO patents constructed by Kogan et al. (2017) from stock market responses to patent news. We merge these values with our PATSTAT data (see Appendix A for details).

Based on this data, we can then test the model's prediction about the cyclicality of patent values. We conduct two complementary exercises. First, we exploit panel variation in the patent data to estimate the relative cyclicality of green and non-green patent values:

$$\text{value}_{j,i,t} = \alpha_i + \delta_t + \theta \mathrm{r}_t \times \text{green}_{j,i,t} + \gamma' \mathbf{x}_{j,i,t} + \varepsilon_{j,i,t}, \tag{29}$$

where $\text{value}_{j,i,t}$ corresponds to the (log) real value of patent j filed by firm i. We focus on the federal funds rate, instrumented using high-frequency monetary surprises, but also report results using GDP growth instead without conditioning on a specific shock. $\mathbf{x}_{j,i,t}$ are additional patent-level controls. α_i and δ_t are firm and time fixed effects, respectively. Since our goal is to estimate the relative cyclicality of green and non-green patent values, captured by θ, the inclusion of time fixed effects allows us to flexibly control for any time-varying common shocks. We also control for the baseline green-patent indicator. As quality is homogeneous in the model, we include dummy variables for biadic patents, as well as for patents with at least one citation.

Table 3 reports the estimated coefficients. Consistent with the model's prediction, green patent values are less cyclical than non-green patent values: after a recessionary shock, the value of green patents falls by significantly less than that of non-green patents. This holds true unconditionally using GDP growth as well as when conditioning on monetary policy shocks. The results are robust to excluding the quality controls.

Second, we construct firm-level patent valuations by tracking the market-implied value of firms' stock of green and non-green patents over time. Using these valuations, we estimate firm-level green and non-green patent value responses to monetary policy

Table 3: Relative cyclicality of green and non-green patent values in the data

	Dependent variable: 100×log(patent value$_{j,i,t}$)			
	(1)	(2)	(3)	(4)
$\Delta\text{GDP}_t \times \text{green}_{j,i,t}$	-2.12***	-2.05***		
	(0.48)	(0.61)		
$\text{r}_t \times \text{green}_{j,i,t}$			2.48***	2.47***
			(0.52)	(0.52)
Observations	1,256,917	1,256,917	1,256,917	1,256,917
Firm fixed effects	Yes	Yes	Yes	Yes
Time fixed effects	Yes	Yes	Yes	Yes
Quality controls	No	Yes	No	Yes

Notes: The relative cyclicality of green and non-green patent values, estimated based on (29). ΔGDP_t is real GDP growth and r_t is the policy rate, instrumented with monetary surprises. $\text{green}_{j,i,t}$ is a dummy denoting green patents. We consider a 1 percentage point increase in GDP growth and a 25 basis point policy rate increase. Robust standard errors in parentheses, significance levels denoted by *** $p < 0.01$, ** $p < 0.05$, * $p < 0.10$.

shocks using panel local projections (3). To control for quality, we focus only on biadic patents that received at least one citation in the construction of the firm-level value indices.

Figure 10a shows that non-green patent values fall significantly and persistently after a contractionary monetary policy shock. By contrast, the values of green patents are much less affected: while they also tend to decline, the response is weaker and insignificant.

Next, we aim to shed light on the general equilibrium effects via the market of skilled labor. Our model predicts a decline in non-green patenting during business cycle downturns, depressing the equilibrium wage of skilled workers (scientists). This reduces the cost for firms to engage in green innovation and increases labor demand. We confront these predictions using two different datasets.

First, we construct a real quarterly earnings index of scientists in STEM occupations by combining relevant waves of the U.S. Current Population Survey over our sample period (see e.g. Autor, Katz, and Kearney, 2008; Autor and Dorn, 2013). For details, see Appendix A.6. To test how this aggregate earnings index responds to monetary policy, we rely on the local projections approach (2). In line with the model prediction, Figure 10b shows that scientists' earnings decrease following a monetary tightening.

Second, we explore USPTO data on inventors referenced in patent filings. Importantly, this dataset disambiguates inventor names (see e.g. Li et al., 2014), enabling us to classify inventors as green or non-green based on their patenting activity. We aggregate the number of green inventors at the firm-level and trace their dynamic responses to monetary shocks, using the panel local projections model (3). Figure 10c shows a significant

Figure 10: Responses of patent values, scientists' earnings and green inventors

(a) Patent values

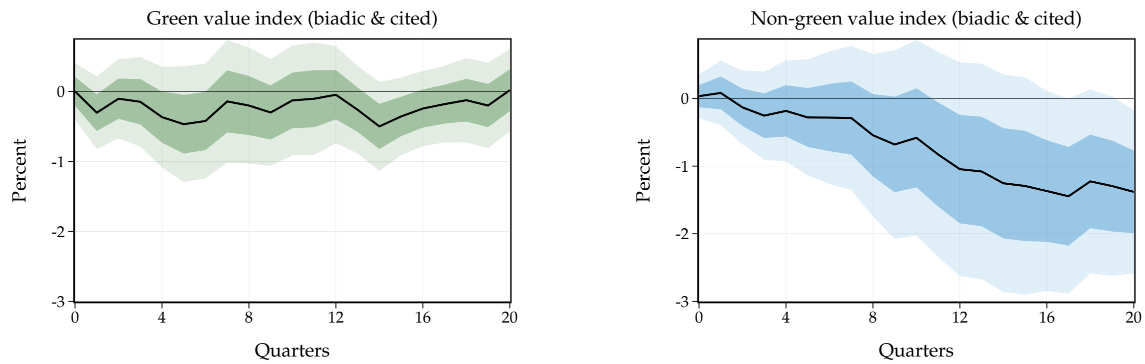

(b) Scientist earnings index

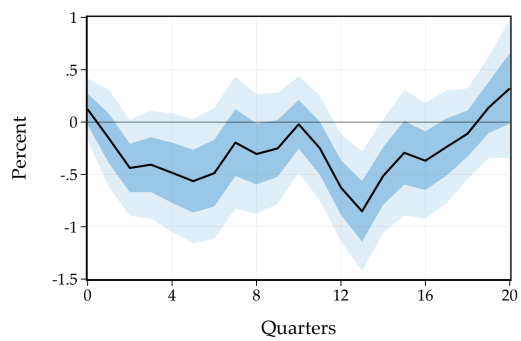

(c) Number of green inventors

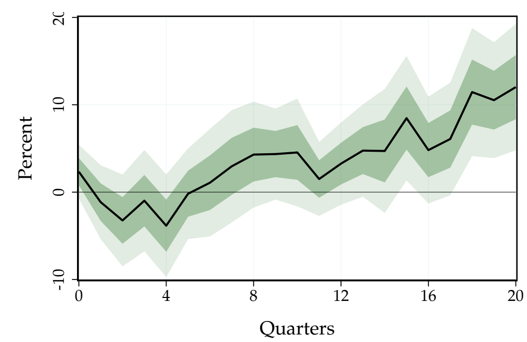

Notes: Responses of patent values (Panel a) and green inventors (Panel c) to a monetary policy shock, estimated based on (3). Panel b: response of scientist earnings index, estimated based on (2). Shock is normalized to increase the federal funds rate by 25 basis points on impact. Solid line: the point estimate. Dark and light shaded areas: 68 and 95% confidence bands.

increase in the number of green inventors. We find that at least part of this increase is driven by new inventors, i.e. inventors that have not patented at the firm previously (see Appendix B.2.2). These results are consistent with the general equilibrium effects via the skilled labor market that operate in our model.

Overall, this evidence corroborates our model mechanisms that generate the countercyclicality of the green patent share and the number of green patents.

5. State-Dependent Effects of R&D Subsidies

The main result of the paper is that green innovation is countercyclical. A direct policy implication is that a given dollar of R&D subsidy spending can generate more innovation during downturns, when the skilled R&D wage is lower. This section formalizes this state dependence and asks whether it is stronger for green innovation. We consider TFP and preference shocks and assume that skilled R&D wages are sufficiently procyclical.

Countercyclical innovation subsidies. We introduce an unanticipated, one-period general innovation subsidy, and let τ_t^N denote the neutral subsidy rate. Skilled R&D workers receive the real wage W_t^S, while innovators in both sectors face the effective wage cost $(1-\tau_t^N)W_t^S$. The free-entry conditions become

$$\zeta_K A_t^K \left(L_{t,K}^S\right)^{\nu-1} \mathcal{V}_t^K = (1-\tau_t^N)W_t^S, \qquad K \in \{G, M\}. \tag{30}$$

The fiscal cost of the policy, financed by a contemporaneous lump-sum tax, is

$$B_t^N = \tau_t^N W_t^S (L_{t,G}^S + L_{t,M}^S). \tag{31}$$

We define the innovation subsidy multiplier as $\mathscr{M}_t \equiv \frac{\partial S_t}{\partial B_t^N}$, evaluated at zero subsidy, that is, the increase in total innovation generated by one additional dollar of neutral R&D wage subsidies. Similarly, $\mathscr{M}_t^K \equiv \frac{\partial S_t^K}{\partial B_t^N}$, for $K \in \{G, M\}$, denotes the sector-specific innovation multiplier.

For the analytical results in this section, we again assume zero depreciation of ideas ($\phi = 1$) and impose the regularity condition requiring that business-cycle shocks are not quasi-permanent.

Proposition 5.1 (Countercyclical Subsidy Multipliers). *The innovation subsidy multipliers are countercyclical:*

$$\frac{d\log \mathscr{M}_t}{d\log Y_t} < 0, \qquad \frac{d\log \mathscr{M}_t^G}{d\log Y_t} < 0, \qquad \frac{d\log \mathscr{M}_t^M}{d\log Y_t} < 0. \tag{32}$$

Moreover, along the transition path we have $\left|\frac{d\log \mathscr{M}_t^G}{d\log Y_t}\right| > \left|\frac{d\log \mathscr{M}_t^M}{d\log Y_t}\right|$*, implying that a given dollar of subsidies allocated during downturns generates relatively more green patents.*

Proof. See Appendix D. ∎

The intuition behind Proposition 5.1 is straightforward. During downturns, lower skilled R&D wages reduce the cost of creating new varieties, allowing a given subsidy expenditure to generate more innovation. Moreover, the green duration channel makes the green component of the subsidy multiplier rise more strongly than the non-green part. Thus, relative to the same expenditure in a boom, a neutral subsidy deployed during a downturn generates more patents overall and a larger absolute increase in green patents.

The timing of innovation subsidies therefore matters for their effectiveness. Subsidies deployed during downturns generate more aggregate and green innovation per dollar than subsidies deployed during booms.

Green-targeted subsidies. We now consider targeted subsidies. Let τ_t^G denote a wage subsidy that applies only to skilled labor used in green R&D. Skilled R&D workers receive the common real wage W_t^S. Green innovators pay $(1-\tau_t^G)W_t^S$, while non-green innovators pay W_t^S. The free-entry conditions become

$$\zeta_G A_t^G \left(L_{t,G}^S\right)^{\nu-1} \mathcal{V}_t^G = (1-\tau_t^G) W_t^S, \qquad \zeta_M A_t^M \left(L_{t,M}^S\right)^{\nu-1} \mathcal{V}_t^M = W_t^S. \tag{33}$$

The fiscal cost of the policy is

$$B_t^G = \tau_t^G W_t^S L_{t,G}^S. \tag{34}$$

Let $\mathscr{M}_t^{GS} \equiv \frac{\partial [S_t^G/(S_t^G+S_t^M)]}{\partial B_t^G}$ denote the effect of green-targeted R&D wage subsidies on the green innovation share.

Proposition 5.2 (Countercyclical Effects of Green-Targeted Subsidies). *Green-targeted subsidies increase the green share $\mathscr{M}_t^{GS} > 0$. More importantly, along the green transition, this effect is stronger during downturns:*

$$\frac{d \log \mathscr{M}_t^{GS}}{d \log Y_t} < 0. \tag{35}$$

Proof. See Appendix D. ■

Proposition 5.2 delivers two results. First, green-targeted wage subsidies increase the green share of innovation. Second, this directional effect is stronger during economic downturns: when innovation costs are lower, a dollar of targeted support shifts the composition of innovation more strongly toward green technologies.

Therefore, if a policymaker's objective is to accelerate the green transition, the timing of green-targeted subsidies matters. In particular, the model implies that introducing such subsidies during downturns is especially effective, even though green innovation is already relatively strong in recessions absent policy intervention.

Quantification. The results above establish that R&D subsidy multipliers are state dependent. We now use the calibrated model from Section 4.1 to assess the magnitude of this state dependence. This quantitative exercise relaxes the zero-depreciation assumption, allowing ideas to depreciate at the calibrated rate $1 - \phi = 0.03$.

In the calibrated model, the neutral-subsidy multiplier is countercyclical. A 1% decline in GDP raises the total innovation subsidy multiplier by 2.0%. The effect is larger for green innovation: the green multiplier rises by 2.2%, compared with 1.8% for non-green innovation. To put these elasticities into perspective, consider a recession in which GDP is 3% below its no-shock path and a boom in which GDP is 3% above it. The total innovation subsidy multiplier is approximately 12.5% larger in the recession than in the boom. The difference is about 14.4% for green innovation, compared with 11.5% for non-green innovation. The effect of green-targeted subsidies on the green innovation share is approximately 8.2% larger in the recession.

6. Conclusion

This paper documents a novel empirical fact: while non-green innovation is procyclical, green innovation is countercyclical. Not only is green patenting less affected by recessionary shocks, the number of green patents even tends to rise during downturns. This pattern holds across aggregate and firm-level data, within the U.S. and internationally, and when conditioning on different macroeconomic shocks. These findings challenge the conventional view that innovation declines uniformly in recessions and call for a deeper understanding of the distinct economic forces shaping green technological progress.

To explain these patterns, we develop a business cycle model with endogenous green and non-green innovation. At the core of the model is the green duration channel: along the transition, green patents yield profits that are more backloaded, making their value less sensitive to transitory macroeconomic shocks. In general equilibrium, this effect is reinforced through reallocation in the skilled labor market. When downturns depress non-green innovation, the resulting decline in skilled wages lowers the cost of green R&D, further boosting green innovation. Our model not only accounts for the relative and absolute cyclicality observed in the data, but is also supported by empirical evidence on the underlying mechanisms—specifically, the weaker cyclicality of green patent values and the reallocation of inventors toward green technologies during recessions.

Our results underscore how short-run macroeconomic fluctuations can shape the long-run green transition. Two implications stand out. First, transitory shocks can leave a permanent technological legacy: by changing the level and composition of innovative activity, even short-lived downturns can alter the path of green and non-green technologies after economic activity has recovered. Second, the effects of innovation subsidies are state dependent. A dollar of R&D subsidies generates more innovation during downturns, when innovation costs are lower, and produces relatively more green patents. Conditioning innovation subsidies on macroeconomic conditions can therefore improve their cost-effectiveness and strengthen their contribution to the green transition. More broadly, macroeconomic conditions are central not only to understanding the evolution of green innovation, but also to designing effective innovation policy.

References

Acemoglu, Daron, Philippe Aghion, Lint Barrage, and David Hémous (2023). *Climate change, directed innovation, and energy transition: The long-run consequences of the shale gas revolution*. Tech. rep. National Bureau of Economic Research.

Acemoglu, Daron, Philippe Aghion, Leonardo Bursztyn, and David Hémous (2012). "The environment and directed technical change". *American Economic Review* 102.1, pp. 131–166.

Acemoglu, Daron, Ufuk Akcigit, Douglas Hanley, and William Kerr (2016). "Transition to clean technology". *Journal of Political Economy* 124.1, pp. 52–104.

Aghion, Philippe, George-Marios Angeletos, Abhijit Banerjee, and Kalina Manova (2010). "Volatility and growth: Credit constraints and the composition of investment". *Journal of Monetary Economics* 57.3, pp. 246–265.

Aghion, Philippe, Philippe Askenazy, Nicolas Berman, Gilbert Cette, and Laurent Eymard (2012). "Credit constraints and the cyclicality of R&D investment: Evidence from France". *Journal of the European Economic Association* 10.5, pp. 1001–1024.

Aghion, Philippe, Antonin Bergeaud, Maarten De Ridder, and John Van Reenen (2026). "Lost in transition: Financial barriers to green growth".

Aghion, Philippe, Antoine Dechezleprêtre, David Hémous, Ralf Martin, and John Van Reenen (2016). "Carbon taxes, path dependency, and directed technical change: Evidence from the auto industry". *Journal of Political Economy* 124.1, pp. 1–51.

Aghion, Philippe and Peter Howitt (1992). "A model of growth through creative destruction". *Econometrica* 60.2.

Aghion, Philippe and Gilles Saint-Paul (1998). "Uncovering some causal relationships between productivity growth and the structure of economic fluctuations: a tentative survey". *Labour* 12.2, pp. 279–303.

Angeletos, George-Marios, Fabrice Collard, and Harris Dellas (2020). "Business-cycle anatomy". *American Economic Review* 110.10, pp. 3030–3070.

Angelucci, Stefano, F Javier Hurtado-Albir, and Alessia Volpe (2018). "Supporting global initiatives on climate change: The EPO's "Y02-Y04S" tagging scheme". *World Patent Information* 54, S85–S92.

Antolin-Diaz, Juan and Paolo Surico (2022). *The long-run effects of government spending*. Centre for Economic Policy Research.

Anzoategui, Diego, Diego Comin, Mark Gertler, and Joseba Martinez (2019). "Endogenous technology adoption and R&D as sources of business cycle persistence". *American Economic Journal: Macroeconomics* 11.3, pp. 67–110.

Arora, Ashish, Sharon Belenzon, and Lia Sheer (2021). "Knowledge spillovers and corporate investment in scientific research". *American Economic Review* 111.3, pp. 871–898.

Autor, David H and David Dorn (2013). "The growth of low-skill service jobs and the polarization of the US labor market". *American economic review* 103.5, pp. 1553–1597.

Autor, David H, Lawrence F Katz, and Melissa S Kearney (2008). "Trends in US wage inequality: Revising the revisionists". *The Review of economics and statistics* 90.2, pp. 300–323.

Barlevy, Gadi (Sept. 2007). "On the Cyclicality of Research and Development". *American Economic Review* 97.4, pp. 1131–1164.

Bauer, Michael D. and Eric T. Swanson (2023). "A reassessment of monetary policy surprises and high-frequency identification". *NBER Macroeconomics Annual* 37.1, pp. 87–155.

Benedetti-Fasil, Cristiana, Giammario Impullitti, Omar Licandro, Petr Sedláček, and Adam Hal Spencer (2025). "Heterogeneous Firms, Growth and the Long Shadows of Business Cycles". Working paper.

Benigno, Gianluca and Luca Fornaro (2018). "Stagnation traps". *The Review of Economic Studies* 85.3, pp. 1425–1470.

Bianchi, Francesco, Howard Kung, and Gonzalo Morales (2019). "Growth, slowdowns, and recoveries". *Journal of Monetary Economics* 101, pp. 47–63.

Bilal, Adrien and Diego R. Känzig (2024). *The Macroeconomic Impact of Climate Change: Global vs. Local Temperature*. Tech. rep. National Bureau of Economic Research.

Bornstein, Gideon, Per Krusell, and Sergio Rebelo (2023). "A world equilibrium model of the oil market". *The Review of Economic Studies* 90.1, pp. 132–164.

Burke, Marshall, Mustafa Zahid, Noah Diffenbaugh, and Solomon M Hsiang (2023). *Quantifying climate change loss and damage consistent with a social cost of greenhouse gases*. Tech. rep. National Bureau of Economic Research.

Calel, Raphael and Antoine Dechezleprêtre (2016). "Environmental policy and directed technological change: evidence from the European carbon market". *Review of Economics and Statistics* 98.1, pp. 173–191.

Chen, Ziqiao, Giovanni Marin, David Popp, and Francesco Vona (2021). "The Employment Impact of Green Fiscal Push: Evidence from the American Recovery and Reinvestment Act". *Brookings Papers on Economic Activity*.

Chetty, Raj, Adam Guren, Day Manoli, and Andrea Weber (2011). "Are micro and macro labor supply elasticities consistent? A review of evidence on the intensive and extensive margins". *American Economic Review* 101.3, pp. 471–475.

Cohen, Lauren, Umit G. Gurun, and Quoc H. Nguyen (2020). *The ESG-innovation disconnect: Evidence from green patenting*. Tech. rep. National Bureau of Economic Research.

Colmer, Jonathan, Ralf Martin, Mirabelle Muûls, and Ulrich J. Wagner (2024). "Does pricing carbon mitigate climate change? Firm-level evidence from the European Union Emissions Trading System". *Review of Economic Studies*, rdae055.

Comin, Diego and Mark Gertler (2006). "Medium-term business cycles". *American Economic Review* 96.3, pp. 523–551.

Driscoll, John C. and Aart C. Kraay (1998). "Consistent covariance matrix estimation with spatially dependent panel data". *Review of Economics and Statistics* 80.4, pp. 549–560.

Elminejad, Ali, Tomas Havranek, Roman Horvath, and Zuzana Irsova (2023). "Intertemporal substitution in labor supply: A meta-analysis". *Review of Economic Dynamics* 51, pp. 1095–1113.

Engle, Robert F., Stefano Giglio, Bryan Kelly, Heebum Lee, and Johannes Stroebel (2020). "Hedging climate change news". *The Review of Financial Studies* 33.3, pp. 1184–1216.

Fornaro, Luca, Veronica Guerrieri, Will Hotten, and Lucrezia Reichlin (2026). *Financial Conditions and Green Innovation*. Tech. rep. Centre for Economic Policy Research.

Fornaro, Luca, Veronica Guerrieri, and Lucrezia Reichlin (2024). *Monetary policy for the energy transition*. Tech. rep. Technical report, Working Paper.

— (2025). "Monetary policy for the green transition".

Furlanetto, Francesco, Antoine Lepetit, Ørjan Robstad, Juan Rubio-Ramırez, and Pål Ulvedal (2025). "Estimating hysteresis effects". *American Economic Journal: Macroeconomics* 17.1, pp. 35–70.

Gazzani, Andrea Giovanni, Joseba Martinez, Filippo Natoli, and Paolo Surico (2026). "The public origins of American innovation". *Bank of Italy Temi di Discussione (Working Paper) No* 1521.

Gertler, Mark and Peter Karadi (2015). "Monetary policy surprises, credit costs, and economic activity". *American Economic Journal: Macroeconomics* 7.1, pp. 44–76.

Gilchrist, Simon and Egon Zakrajšek (2012). "Credit spreads and business cycle fluctuations". *American Economic Review* 102.4, pp. 1692–1720.

Gornemann, Nils, Pablo Guerrón-Quintana, and Felipe Saffie (2021). "Real Exchange Rates and Endogenous Productivity".

Griliches, Zvi (1990). "Patent statistics as economic indicators: A survey". *Journal of Economic Literature* 28.4, pp. 1661–1707.

Hall, Bronwyn H., Adam B. Jaffe, and Manuel Trajtenberg (2001). *The NBER patent citation data file: Lessons, insights and methodological tools*.

Hassler, John, Per Krusell, and Conny Olovsson (2021). "Directed technical change as a response to natural resource scarcity". *Journal of Political Economy* 129.11, pp. 3039–3072.

Hémous, David, Morten Olsen, Carlo Zanella, and Antoine Dechezleprêtre (2025). "Induced Automation Innovation: Evidence from Firm-level Patent Data".

Ilzetzki, Ethan (2024). "Learning by necessity: Government demand, capacity constraints, and productivity growth". *American Economic Review* 114.8, pp. 2436–2471.

Jarociński, Marek and Peter Karadi (2020). "Deconstructing monetary policy surprises—the role of information shocks". *American Economic Journal: Macroeconomics* 12.2, pp. 1–43.

Jordà, Òscar (2005). "Estimation and inference of impulse responses by local projections". *American Economic Review* 95.1, pp. 161–182.

Jordà, Òscar, Sanjay R. Singh, and Alan M. Taylor (2024). "The long-run effects of monetary policy". *Review of Economics and Statistics*, pp. 1–49.

Kahle, Kathleen M. and René M. Stulz (2017). "Is the US public corporation in trouble?" *Journal of Economic Perspectives* 31.3, pp. 67–88.

Känzig, Diego R. (2023). "The unequal economic consequences of carbon pricing". *Available at SSRN 3786030*.

King, Robert G. and Sergio T. Rebelo (1999). "Resuscitating real business cycles". *Handbook of macroeconomics* 1, pp. 927–1007.

Kogan, Leonid, Dimitris Papanikolaou, Amit Seru, and Noah Stoffman (2017). "Technological innovation, resource allocation, and growth". *The Quarterly Journal of Economics* 132.2, pp. 665–712.

Kose, M. Ayhan, Naotaka Sugawara, and Marco E. Terrones (2020). "Global recessions". *CEPR Discussion Paper No. 14397*.

Kung, Howard and Lukas Schmid (2015). "Innovation, growth, and asset prices". *The Journal of Finance* 70.3, pp. 1001–1037.

Kydland, Finn E. and Edward C. Prescott (1982). "Time to build and aggregate fluctuations". *Econometrica: Journal of the Econometric Society*, pp. 1345–1370.

Li, Guan-Cheng, Ronald Lai, Alexander D'Amour, David M Doolin, Ye Sun, Vetle I Torvik, Amy Z Yu, and Lee Fleming (2014). "Disambiguation and co-authorship networks of the US patent inventor database (1975–2010)". *Research Policy* 43.6, pp. 941–955.

Ma, Song (2021). *Technological obsolescence*. Tech. rep. National Bureau of Economic Research.

Ma, Yueran and Kaspar Zimmermann (2023). *Monetary policy and innovation*. Tech. rep. National Bureau of Economic Research.

Miranda-Agrippino, Silvia and Hélene Rey (2020). "US monetary policy and the global financial cycle". *The Review of Economic Studies* 87.6, pp. 2754–2776.

Montiel Olea, José Luis and Mikkel Plagborg-Møller (2021). "Local projection inference is simpler and more robust than you think". *Econometrica* 89.4, pp. 1789–1823.

Nagaoka, Sadao, Kazuyuki Motohashi, and Akira Goto (2010). "Patent statistics as an innovation indicator". *Handbook of the Economics of Innovation*. Vol. 2. Elsevier, pp. 1083–1127.

Nakamura, Emi and Jón Steinsson (2018). "High-frequency identification of monetary non-neutrality: The information effect". *The Quarterly Journal of Economics* 133.3, pp. 1283–1330.

Ottonello, Pablo and Thomas Winberry (2020). "Financial heterogeneity and the investment channel of monetary policy". *Econometrica* 88.6, pp. 2473–2502.

Popp, David (2002). "Induced innovation and energy prices". *American Economic Review* 92.1, pp. 160–180.

Queralto, Albert (2020). "A model of slow recoveries from financial crises". *Journal of Monetary Economics* 114, pp. 1–25.

Romer, Paul M. (1990). "Endogenous technological change". *Journal of Political Economy* 98.5, Part 2, S71–S102.

Veefkind, Victor, Javier Hurtado-Albir, Stefano Angelucci, Konstantinos Karachalios, and Nikolaus Thumm (2012). "A new EPO classification scheme for climate change mitigation technologies". *World Patent Information* 34.2, pp. 106–111.

Wang, Lixing and Donghai Zhang (2025). "A Theory of Lumpy Innovation and Aggregate Dynamics". *Available at SSRN 4818040*.

Online Appendix

Innovation, Business Cycles, and the Climate Transition

Diego R. Känzig
Maximilian Konradt
Lixing Wang
Donghai Zhang

A. Data

In this appendix, we provide additional information on the sources and the construction of our sample. We discuss the sources for the patent and firm-level data as well as how we match patents to firms. Finally, we provide details on how we aggregate the patent data, as well as the supplementary macroeconomic and financial data used in our analyses.

A.1. Patent Data

Our main source of patent data is the World Patent Statistical Database (PATSTAT), which encompasses bibliographic information for close to the universe of patents globally. We use the autumn 2023 edition (version 5.22).

We follow the previous literature (e.g. Hémous et al., 2025) to focus on patent families, i.e. patents representing the same innovation filed at different patent offices. For each patent family we use the original application date to capture the time of the innovation and assign nationality based on the respective filing office.

To measure green innovation, we use International Patent Classification (IPC) and Cooperative Patent Classification (CPC) codes. Specifically, we apply the EPO tagging scheme (see Veefkind et al., 2012; Angelucci, Hurtado-Albir, and Volpe, 2018) to classify patent families in the Y02 class of the CPC, which includes technologies that reduce greenhouse gases. We treat patent families with multiple C/IPC codes as green if any of the respective codes meet our criteria. We treat the remaining patent families as non-green.

Table A.1: Green patents by CPC code, 1986-2019

CPC code	Description	Number of patents	Share of sample	Incl. in baseline
Y02E	Production, distribution and transport of energy	109,682	35.93	✓
Y02T	Transportation	63,053	20.66	✓
Y02P	Industry and agriculture	61,760	20.23	✓
Y02A	Adaptation to climate change	34,258	11.22	✓
Y02B	Buildings	32,598	10.68	✓
Y02D	ICT aiming at reduction of own energy use	31,350	10.27	✓
Y02W	Wastewater treatment or waste management	14,995	4.91	✓
Y04S	Smart grids	9,832	3.22	
Y02C	Capture and storage of greenhouse gases	4,416	1.45	✓

Notes: Based on USPTO patent families. Note that CPC categories are non-mutually-exclusive and thus the shares need not to sum to a 100%.

What are the most salient green subclasses? Table A.1 shows that the majority of green patent filings in our data are associated with production, distribution and transport of energy (Y02E), transportation (Y02T), and industry and agriculture (Y02P).

In Table A.2, we provide a number of examples of green patents, specifically related to photovoltaic and solar technologies.

PATSTAT also reports information on patent citations. We compute citation counts at the family level, excluding any self citations within the same family. To measure quality, we additionally define biadic patents, filed with at least two of the three major patent offices (USPTO, EPO and JPO).

Table A.2: Examples of green patents related to photovoltaic and solar technologies

Patent number	Patent name	Applicant	Filing date	CPC codes
US5959787	Concentrating coverglass for photovoltaic cells	The Boeing Company	26.11.1996	Y02E
US6461947	Photovoltaic device and making of the same	Hitachi, Ltd.	07.09.2000	Y02E, Y02P
US20070267290	Photovoltaically powered cathodic protection system for automotive vehicle	Ford Global Technologies, LLC	16.05.2006	Y02T
US20180054064	Smart main electrical panel for energy generation systems	Tesla, Inc.	29.09.2016	Y02B, Y02E

A.2. Firm Data

We rely on Compustat North America for accounting data on listed U.S. companies. Following Cloyne et al. (2023) we exclude Compustat companies in the finance, insurance, real estate and public administration sectors and drop firms which report data for fewer than 20 quarters, or have missing investment or sales figures for more than 20 quarters. We measure firm age using the date of incorporation, which we supplement from Thomson Reuter's WorldScope.

In contrast to Cloyne et al. (2023), we only exclude firms with negative or missing age when we explicitly study firm heterogeneity, including the effects on younger and older firms. Otherwise, we retain firms even if the age variable is negative.[1] We limit our attention to years with consistent reporting, starting in 1986Q1.

Table A.3 shows how we construct the key firm-level variables of interest based on the Compustat data. To limit the impact of outliers, we winsorize the book-to-market ratio, short-term debt and leverage ratio and Tobin's Q at the 1^{st} and 99^{th} percentile in each year. We also merge data on firm-level emissions from Trucost using company ISIN codes. We focus on the Scope 1 GHG emission intensity (scaled by revenue), which is available for roughly half of the companies in our dataset.

Table A.3: Definitions of firm-level variables

Variable	Compustat definition
Size	atq
Investment	capxq/ppentq
Leverage ratio	(dlcq+dlttq)/atq
Book-to-market	ceqq/(prccq*cshoq)
R&D intensity	xrdq/atq
Short term debt	dlcq/(dlcq+dlttq)
Tobin's Q	(atq + prccq*cshoq - ceqq + txditcq) / atq

[1] The age data are noisy, e.g. because of firm mergers and acquisitions.

A.3. Matching Patents to Firms

Measuring U.S. firms' innovation activity requires matching patents to firm-level data. To maximize the number of successful matches, we rely on two different datasets. The first is Orbis Intellectual Property, which links global patent portfolios to Orbis companies (see Hémous et al., 2025). We map Orbis to Compustat companies using the ISIN identifier, which implies we are measuring innovation at the U.S. group level.

Second, we also employ the mapping by Arora, Belenzon, and Sheer (2021), which establishes a link between USPTO patents and Compustat firms based on a fuzzy matching approach and extends the NBER patent database (Hall, Jaffe, and Trajtenberg, 2001). For more details on the approach, see Arora et al. (2024). Combining the matches in both datasets we are able to link 1.7 million distinct patent families to Compustat firms, including about 103,000 green patents.[2] In our main analysis, a patent can be matched to multiple U.S. companies as the result of co-inventions. Our results, available upon request, are robust to excluding, or appropriately weighting such joint patents.

We use the unique patent application number encompassed in both datasets to merge the relevant information from PATSTAT. In particular, we construct firm-level patent counts for green and non-green patents at quarterly frequency. To that end, we retain patents filed with the USPTO and international filings.

In addition to patent counts, we are also interested in quantifying patent values. We therefore match our firm-level data with market-implied patent value data constructed by Kogan et al. (2017), extended to 2020. Consistent with our earlier definition, we focus on the first patent in a patent family to infer its value, but verify that taking an average value does not impact our results. Lastly, to dynamically study the value of firms' innovation, we construct cumulative value indices for green and non-green patents at the firm-level.

A.4. Aggregate Patent Counts

In order to assess the correlation of innovation activity with the business cycle, we compute aggregate patent counts. First, we construct separate series for U.S. green and non-green patents based on USPTO filings recorded in PATSTAT.[3] Second, we compute similar patent counts for OECD countries, including filings with the respective national offices and the EPO. For the OECD, we also include international applications filed under the Patent Cooperation Treaty, but verify that excluding them does not impact our estimates. Finally, we construct counts at the global level, exploiting all available information in PATSTAT.

Third, since Compustat covers close to the universe of listed companies in the U.S., we can also aggregate our matched firm-level patents to compute separate counts for listed

[2] Reassuringly, the two mappings overlap significantly: Orbis identifies 1.444 million total (89,800 green) patents, while applying Arora, Belenzon, and Sheer (2021) results in 1.275 million total (75,600 green) matched patents.

[3] As patent counts can vary across the two sources due to different procedures in how patent applications are recorded and PCT patent applications are treated, we verify that our findings are robust to using USPTO data. The results are available upon request.

and unlisted U.S. firms. Compustat accounts for 97-99% of market capitalization of all listed firms in the U.S. between 1975-2015 according to Kahle and Stulz (2017). Because we assign patent nationality based on the original patent office, we expect that filings by foreign corporations are modest.

To control for potential seasonality, we apply an X-11 filter to our constructed aggregate patent counts.

Figure A.1 compares the evolution of green patenting among listed and unlisted U.S. companies. The green patent share evolves similarly across the two groups, both in terms of its long-run trend and its shorter-run fluctuations. This close co-movement suggests that the aggregate dynamics of green patenting are not driven solely by listed firms but extend more broadly to unlisted companies.

Figure A.1: Green patenting across U.S. listed and unlisted firms

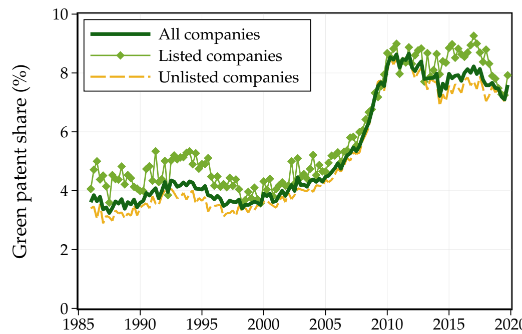

Notes: Share of green patents for U.S. listed and unlisted companies.

A.5. Macroeconomic Data

We complement the innovation and firm-level data with a set of aggregate macroeconomic and financial variables, listed in Table A.4.

One important control in our local projections refers to RD&D spending on renewables by the U.S. Department of Energy. As this series is only reported annually, we temporally disaggregate it using the approach of Chow and Lin (1971). As the relevant quarterly indicator, we use U.S. government spending, which is highly correlated with the RD&D series ($\rho = 0.70$). Figure A.2 shows the resulting interpolated series closely tracks the naive estimate obtained by uniformly distributing the annual total to each quarter.

Table A.4: Macro data description and sources

Variable	Description	Source
U.S. data		
Monetary surprise	Purified high-frequency monetary surprises from Bauer and Swanson (2023)	Michael Bauer's website
Excess bond premium	Gilchrist and Zakrajšek (2012)	FRB website
Monetary surprise	Jarociński and Karadi (2020)	Marek Jarocinski's website
Oil supply shock	Känzig (2021)	Diego Känzig's website
Climate news index	Engle et al. (2020)	Johannes Stroebel's website
Renewables RD&D spending	Disaggregated from annual DOE series	Climate Policy Lab
Federal funds rate	FEDFUNDS	FRED
Real GDP	GDPC1	FRED
GDP deflator	GDPDEF	FRED
Unemployment rate	UNRATE	FRED
Industrial production	INDPRO	FRED
1-year rate	GS1	FRED
Investment	A008RA3Q086SBEA	FRED
Oil price	WTISPLC	FRED
Government spending	GCEC1	FRED
OECD data		
Real GDP	Based on 19 OECD countries	OECD
GDP deflator	Based on 19 OECD countries	OECD
Unemployment rate	Based on 9 OECD countries with consistent data	OECD
European data		
Real GDP	Based on 15 European countries	OECD
GDP deflator	Based on 2 European countries with consistent data	OECD
Unemployment rate	Based on 3 European countries with consistent data	OECD
German 3-month rate	IR3TIB01DEQ156N	FRED
ECB monetary surprise	Jarociński and Karadi (2020)	see above

Notes: Due to data limitations, we construct the unemployment series based on data from 9 major OECD countries that consistently report since 1986. These countries include the United States, Germany, Japan, Australia, Austria, the United Kingdom, New Zealand, Chile and Canada.

Figure A.2: Quarterly Renewables RD&D Series

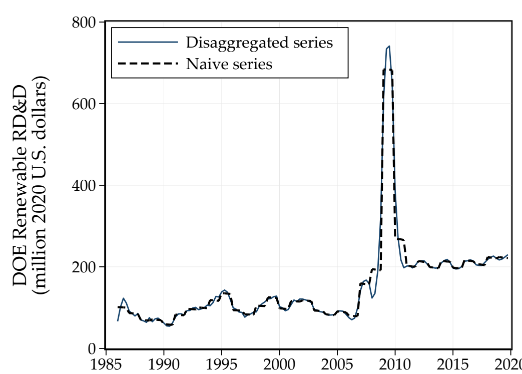

Notes: Disaggregated U.S. DOE RD&D spending, constructed with the Chow and Lin (1971) approach using government spending as the relevant monthly indicator. The dashed line shows the naive estimate, obtained by uniformly distributing the annual total.

A.6. CPS Earnings Data

To empirically test the general equilibrium effect operating via the skilled labor market, we require earnings data of scientists. To that end, we combine data from the 1986–2019 waves of the U.S. Current Population Survey Merged Outgoing Rotation Group (MORG), which includes detailed information on earnings and demographics for a large, representative sample of U.S. workers.

We classify scientists based on 122 occupations in O*NET "Research, Development, Design & Practitioners" category of Science, Technology, Engineering, and Mathematics (STEM). To harmonize these occupations over time, we map the underlying SOC-2018 codes into the consistent occupation codes of Autor and Dorn (2013).

There are two main challenges in constructing an aggregate index over time. First, earnings are top-coded in different vintages of the survey. In line with the literature, we multiply each top-coded observation by 1.5 (e.g. Autor, Katz, and Kearney, 2008). Second, the composition of the workforce is not constant over time. To account for compositional changes, we follow Acemoglu and Autor (2011) and partition workers into 40 cells based on sex, education and experience. Lastly, we compute the hours-weighted mean of log earnings by cell, and aggregate using fixed weights for each cell computed over the full sample.

B. Sensitivity and Additional Results

B.1. Additional Time Series Results

In this appendix, we report some additional results based on the time series.

Figure B.1: Macroeconomic effects of a U.S. monetary policy shock

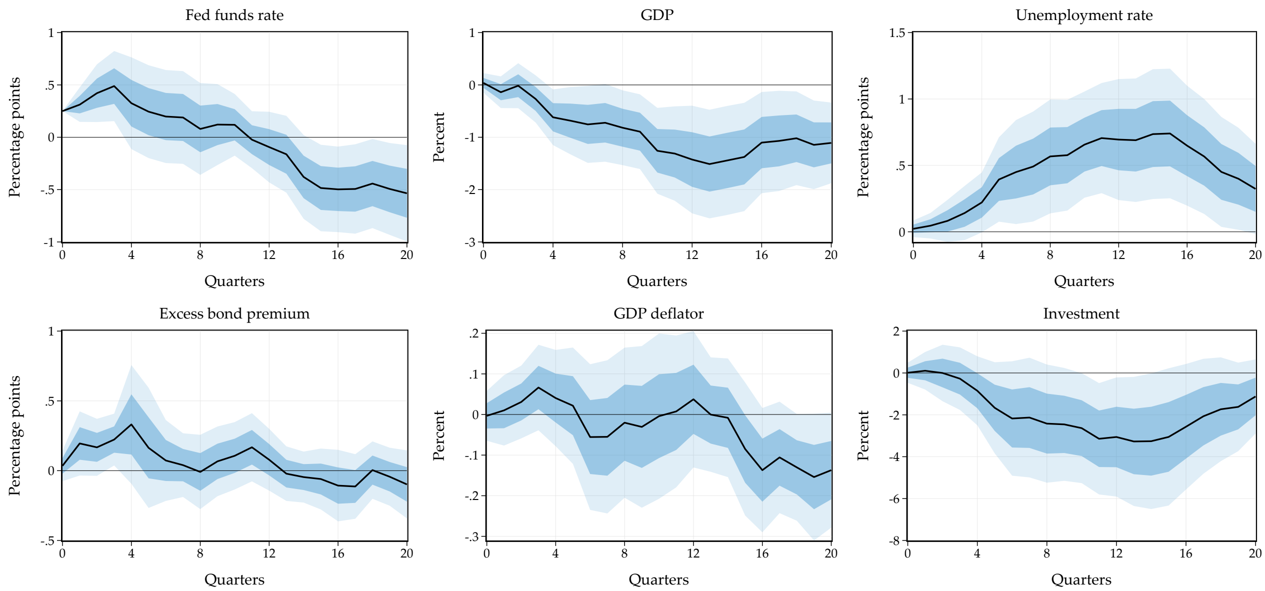

Notes: Macroeconomic effects of a U.S. monetary policy shock, estimated based on the LP-IV model (2).

Figure B.2: Patenting responses to business cycle shock

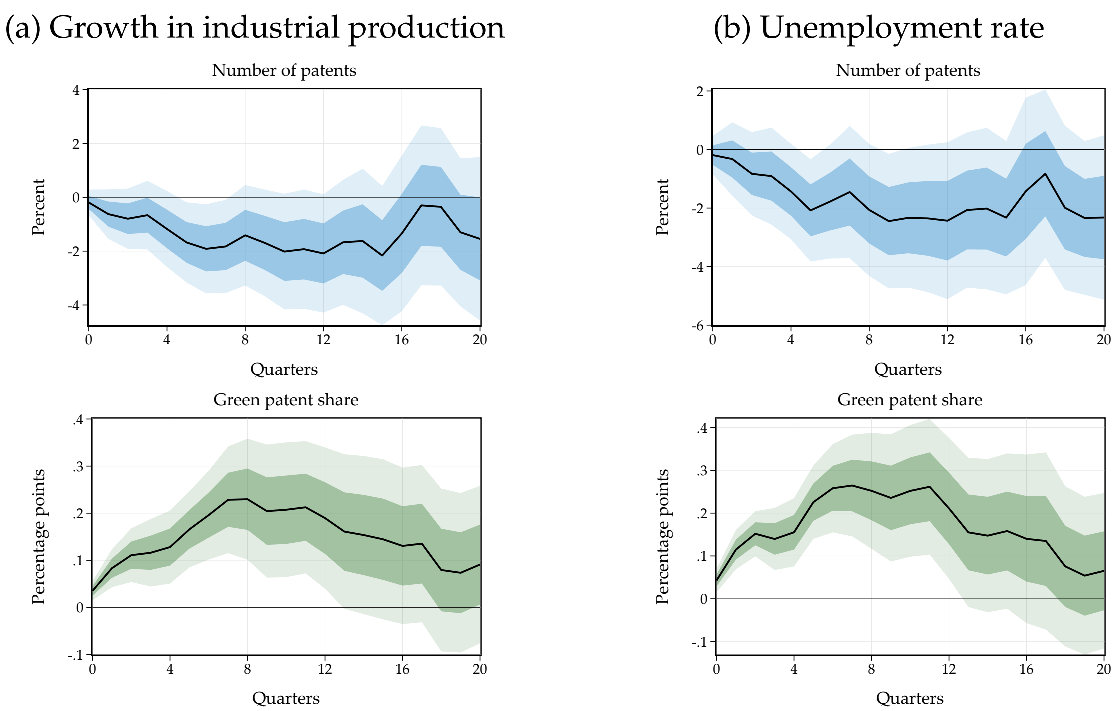

Notes: Responses of total patents and the green patent share in the U.S. to a recessionary innovation to IP growth (normalized to a 1% decrease) and the unemployment rate (normalized to a 25 basis points increase), estimated based on the reduced-form local projections (1).

B.1.1. Alternative Shock Measures

Our baseline analysis relies on a local projections approach using the monetary surprises by Bauer and Swanson (2023) as an instrument. The left panel in Figure B.3 shows similar dynamic responses of the U.S. green patent share, estimated using the monetary surprises by Jarociński and Karadi (2020) as an instrument.

As alternative shock measures, the right panel in Figure B.3 considers the impacts of oil supply shocks on the green patent share. Specifically, we use the oil supply shock identified in Känzig (2021) as an instrument for the real oil price in an otherwise identical empirical setup. The responses, normalized to increase the real oil price by 10 USD, display a similarly persistent increase as in our main analysis.

Figure B.3: Patenting responses to alternative macroeconomic shocks

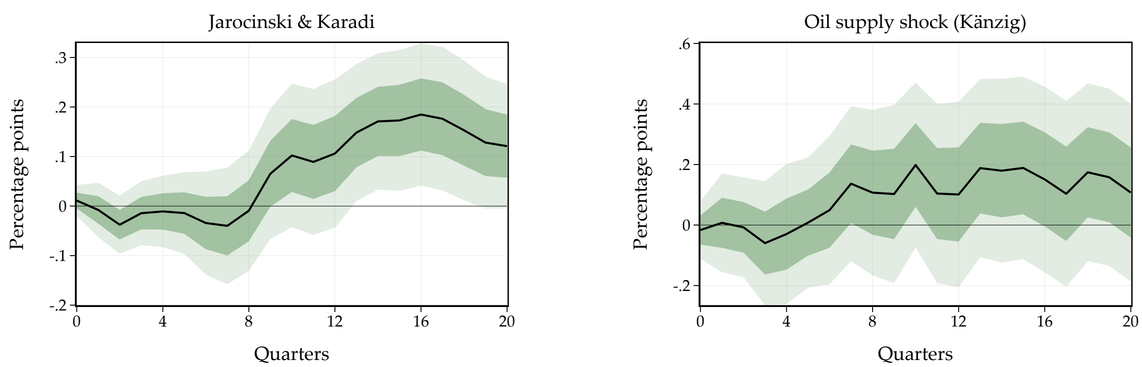

Notes: Green patenting responses to alternative monetary policy and oil supply shocks. Left panel: monetary policy shock, identified using Jarociński and Karadi (2020) monetary surprises. Right panel: Oil supply news shock, identified using the OPEC surprise series by Känzig (2021).

B.1.2. Alternative Green Classifications and Controlling for Quality

Our baseline classification of green patents includes all subclasses of Y02.

Figure B.4: Patenting responses using alternative green patent classifications

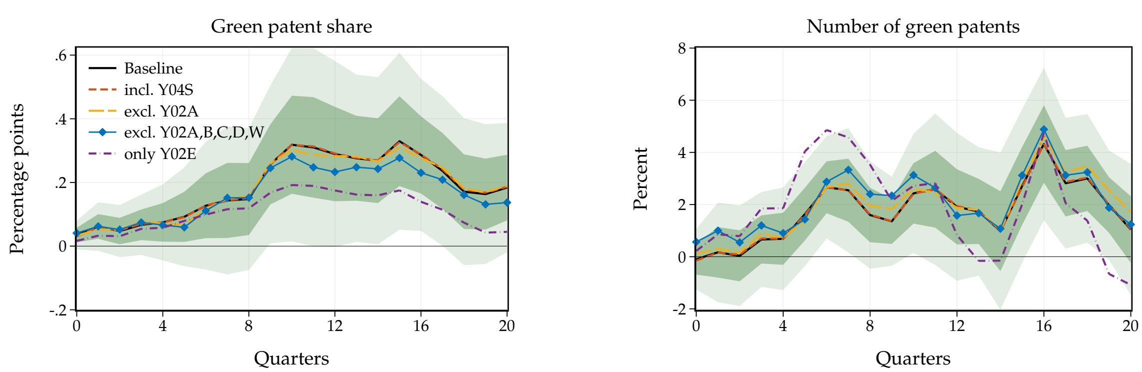

Notes: Responses of the share and number of green patents to a monetary policy shock for alternative definitions of green patents. Responses are estimated based on LP-IV model (2). Compared to the baseline (including all Y02 subclasses), we include Y04S (orange dotted line), exclude Y02A (yellow dashed line), exclude Y02A, Y02B, Y02C, Y02D and Y02W (blue dotted line) and include only Y02E (purple dashed line).

Figure B.4 verifies that the responses in the U.S. are robust to alternative classifications.

First, we drop subclasses not directly competing with fossil fuels (Y02A, B, C, D and W) and include only energy-related subclasses (Y02E), which leads to comparable responses. Second, following Calel and Dechezleprêtre (2016), we check that including smart grid technologies (Y04S) does not meaningfully impact our estimates.

In the baseline estimation we include all patent families, irrespective of their quality. To control for patent quality, we closely follow Hémous et al. (2025) to focus on biadic patents (filed in at least two of the three major patent offices) with at least one citation. Figure B.5 shows that the estimated responses for the U.S. sample are very similar.

Figure B.5: Robustness with respect to patent quality

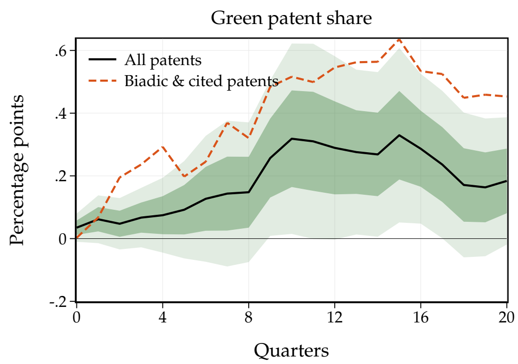

Notes: Green patenting responses to a monetary policy shock when controlling for patent quality. Responses are estimated based on LP-IV model (2). We control for quality by only using biadic patent families with at least one citation.

B.1.3. Sensitivity of Responses to Outliers and Pre-trends

In Figure 6 we find little evidence that extreme observations are responsible for the positive correlation between green patenting and monetary shocks. To formally assess the influence of individual observations, we perform a jackknife exercise, setting one quarterly shock observation to zero at a time. Figure B.6 shows our baseline responses, together with the responses from the jackknife exercise in gray. We see that the estimated effects are not driven by any single shock.

Figure B.6: Sensitivity of green patenting responses to a monetary policy shock

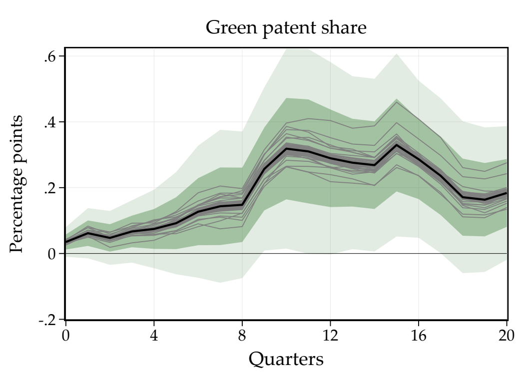

Notes: Green patenting responses to a monetary policy shock, estimated based on LP-IV model (2), together with the responses obtained from the jackknife exercise, censoring one shock value at a time (in gray). Shaded areas: 68 and 95% confidence bands for baseline model.

Figure B.7: Sensitivity of green patenting responses to a business cycle shock

(a) Pre-trends

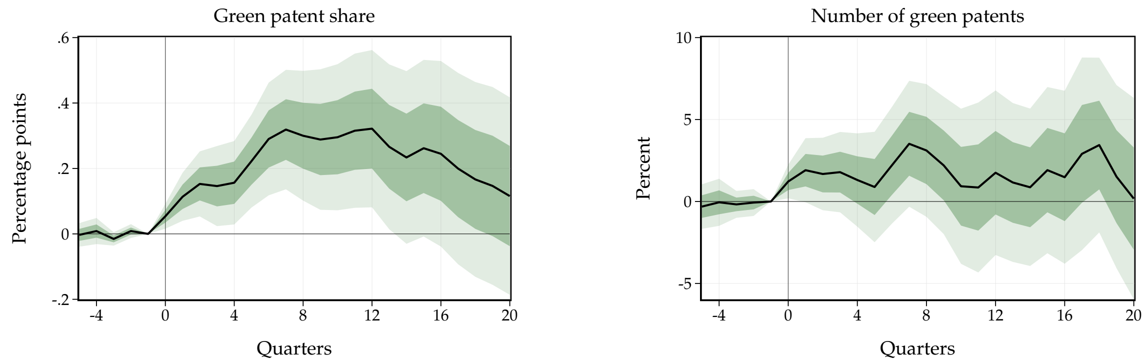

(b) Jackknife

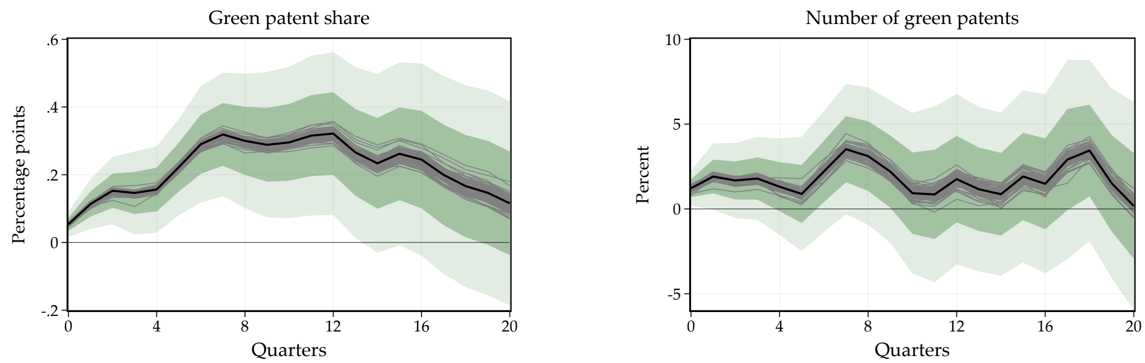

(c) Scatter plot at $h = 8$

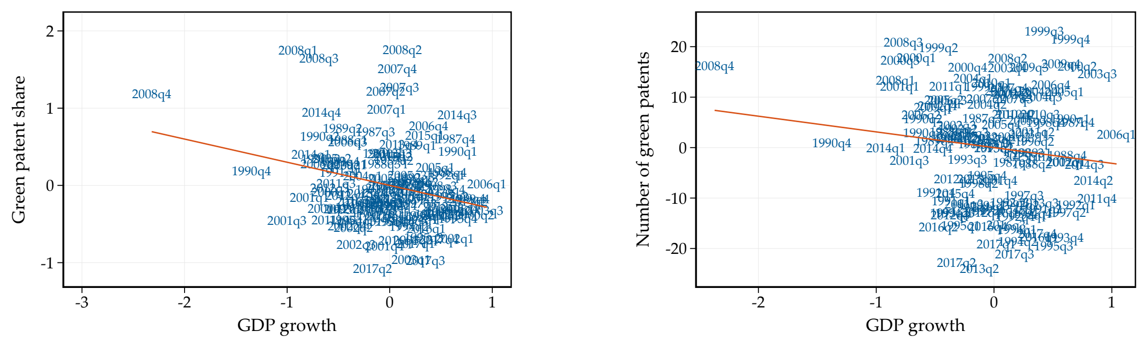

Notes: Sensitivity of green patenting responses in the U.S. to a recessionary innovation to GDP growth (normalized to a 1% decrease). Left panels: responses of the green patent share. Right panels: responses of the number of green patents. Top panels: baseline responses with pre-trends. Estimate for $h{=}-1$ is zero by construction. For $h{=}-4, \ldots, -2$ the lag corresponding to the horizon is excluded from the specification. Middle panels: Jackknife exercise, censoring one shock value at a time (in gray). Lines: point estimates. Dark and light shaded areas: 68 and 95% confidence bands for baseline estimates based on lag-augmented standard errors. Bottom panels: Scatter plot of GDP growth shock against the cumulative change in the outcomes after 8 quarters, conditional on our set of controls.

Figure B.7 presents similar diagnostics for green patenting responses to business cycle shocks based on GDP growth. The top panels suggest no evidence of pre-trends, while the middle and bottom illustrate that the responses of green patenting are not driven by any single extreme value.

B.1.4. Alternative Sample: OECD vs. Europe

How does the response of green patenting activity to monetary policy shocks compare between OECD countries and Europe? Evidence from Aghion et al. (2026), based on German data, suggests that interest rate increases reduce green patenting by tightening financial constraints that limit small firms' ability to invest in R&D.

To test this, we construct a separate series of green patents filed by European countries and estimate their response to monetary policy by the European Central Bank. We closely follow our baseline specification, using analogous controls for the European sample (see Table A.4 for details). As the interest rate measure, we use the German 3-month rate, instrumented with monetary surprises from Jarociński and Karadi (2020).

Figure B.8: Green patenting responses in OECD and Europe

(a) OECD excluding U.S.　　(b) European countries

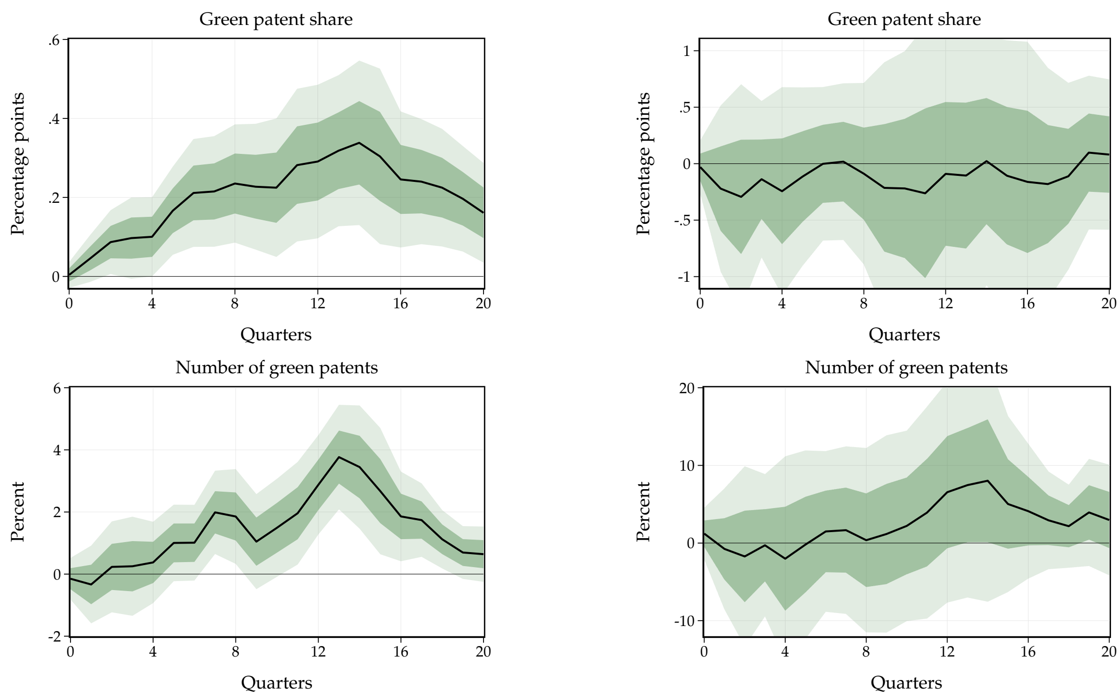

Notes: Responses of green and non-green patents to a monetary policy shock, estimated based on the LP-IV model (2). Panel a: Sample of OECD countries excluding the U.S., using the Fed funds rate and U.S. monetary surprises. Panel b: Sample of European countries, using German 3-month rate and ECB monetary surprises (Jarociński and Karadi, 2020). Solid line: point estimate. Dark and light shaded areas: 68 and 95% confidence bands based on lag-augmented standard errors.

Figure B.8 presents the estimated responses alongside the OECD results. Panel (b) shows no comparable increase in green patenting in the European data, although the estimates are also less precise. This suggests that the European results are more in line with Aghion et al. (2026), possibly reflecting tighter financial constraints facing European firms after a monetary tightening.

B.2. Additional firm-level results

Table B.1: Green patenting by the 20 largest green innovators

	Patenting measure		
Company	Total patents	Green patents	Green patent share
GENERAL MOTORS CO	29,130	6,528	22.41
RTX CORP	33,745	6,467	19.16
FORD MOTOR CO	24,447	6,324	25.87
INTEL CORP	59,594	4,293	7.20
INTL BUSINESS MACHINES CORP	131,497	4,216	3.21
QUALCOMM INC	39,383	3,310	8.40
BOEING CO	20,802	2,984	14.34
HP INC	52,929	2,076	3.92
CATERPILLAR INC	12,375	1,925	15.56
APPLE INC	26,418	1,872	7.09
DU PONT (E I) DE NEMOURS	20,441	1,835	8.98
MOTOROLA SOLUTIONS INC	27,632	1,676	6.07
EXXON MOBIL CORP	10,764	1,492	13.86
MICROSOFT CORP	55,263	1,329	2.40
CUMMINS INC	4,036	1,317	32.63
TEXAS INSTRUMENTS INC	25,166	1,259	5.00
CORNING INC	12,615	1,185	9.39
APPLIED MATERIALS INC	16,224	1,010	6.23
ALPHABET INC	26,418	1,002	3.79
DUPONT DE NEMOURS INC	14,456	989	6.84

Notes: The table reports patent measures for the 20 largest innovators in the U.S. between 1986 to 2019, based on green patent counts.

B.2.1. Evidence on USPTO Patent Renewals

We argue that green patents have a more backloaded profit structure along the green transition. To corroborate this assumption, we exploit information on the maintenance fee payments recorded by the USPTO. Patents need to be renewed after 3.5, 7.5 and 11.5 years in order to remain active. Therefore, patent renewal decisions reflect the value that firms assign to a given innovation over time.

We begin by estimating a logistic regression at the patent-level:

$$\Pr\Big[\text{Renewal}_{j,t} = 1 \mid \delta_t, \text{green}_j, X_j\Big] = \frac{\exp\Big(\delta_t + \theta\,\text{green}_j + \gamma' X_j\Big)}{1 + \exp\Big(\delta_t + \theta\,\text{green}_j + \gamma' X_j\Big)}, \tag{1}$$

where $\Pr\Big[\text{Renewal}_{j,t} = 1 \mid \delta_t, \text{green}_j, X_j\Big]$ corresponds to the conditional probability that patent j filed in quarter t is renewed at least once. δ_t denotes a set of time fixed effects. To control for patent quality, X_j includes dummy variables for biadic patents and patents with at least one citation.

In addition, we estimate OLS regressions using patent duration (expressed in years) as the dependent variable. Lastly, we construct patent maintenance scores, which take on a value between 0 and 3 depending on the number of renewals (Porter et al., 2023). We focus on patents filed before 2010 to allow for up to three recorded renewal decisions.

Table B.2: Evidence on patent renewal decisions

	Logit	OLS	
Dependent variable:	$\text{Renewal}_{j,t}$	$\text{Duration}_{j,t}$	$\text{Maintenance score}_{j,t}$
	(1)	(2)	(3)
green_j	0.36***	0.36***	0.09***
	(0.01)	(0.01)	(0.00)
Observations	3,652,350	3,652,350	3,652,350
Pseudo R^2	0.08	0.07	0.06
Quality controls	Yes	Yes	Yes
Time fixed effects	Yes	Yes	Yes

Notes: Coefficients from regression of patent renewal metrics on green dummy variable, green_j. Column (1) is estimated by logistic regression, with the coefficient reported in log-odds. Columns (2)–(3) are estimated by OLS. Quality controls include dummy variables for biadic patents and patents with at least one citation. All regressions include a constant. Robust standard errors in parentheses, significance levels denoted by *** $p < 0.01$, ** $p < 0.05$, * $p < 0.10$.

Table B.2 presents the results. We find that green patents are more likely to be renewed and remain active for longer relative to non-green patents, controlling for patent quality. These results suggest that green patents carry a higher value at later stages of their life cycle compared to non-green patents.

B.2.2. Evidence on Green Inventors

One key insight from the model is that during business cycle downturns, a decline in non-green patenting depresses wages of skilled workers, making it cheaper for firms to engage in green innovation. We have seen some evidence that the share and number of non-green inventors increase at the firm-level.

Figure B.9: Firm-level responses of new green inventors

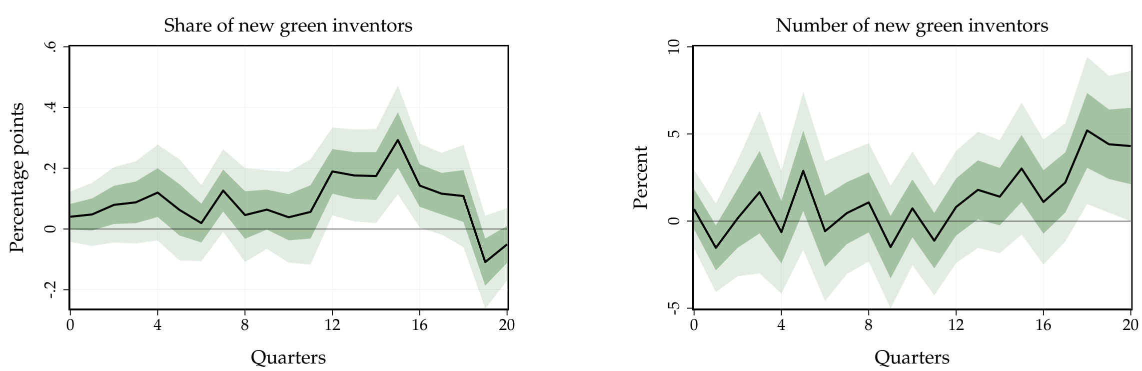

Notes: Responses of new green inventors to a monetary policy shock, estimated based on the panel LP-IV model (3). The measures are restricted to inventors who have not been linked to a green patent before.

One drawback of this approach is that it does not distinguish between existing and new green inventors. To address this issue, we separately analyze the number of new green inventors who are linked to a green patent for the first time in a given quarter. Lastly, we construct the share of new green inventors relative to the total number of inventors who have not been linked to a green patent before. Consistent with the channel emphasized in the model, Figure B.9 suggests an increase in both measures in response to a monetary shock.

B.2.3. Additional Results on Firm-level Heterogeneity

Do the firm-level patenting responses in Table 2 also vary with other firm characteristics? To explore this, Table B.3 considers several additional firm-level characteristics, including proxies for financial constraints—such as leverage, firm age, size, and short-term debt—as well as firms' R&D intensity.

Table B.3: Heterogeneity by firms' financial constraints

Dep. var.:	Green patents$_{it+h}$						Non-green patents$_{it+h}$					
	(1)	(2)	(3)	(4)	(5)	(6)	(7)	(8)	(9)	(10)	(11)	(12)
r_t	0.013**	0.008	0.016**	0.012**	0.018***	0.018***	-0.034**	-0.043***	-0.040**	-0.034**	-0.034**	-0.036**
	(0.006)	(0.006)	(0.006)	(0.006)	(0.006)	(0.006)	(0.015)	(0.016)	(0.016)	(0.015)	(0.015)	(0.016)
$r_t \times \overline{\text{leverage}}_i$	0.006***					0.007***	0.004					-0.001
	(0.002)					(0.002)	(0.003)					(0.002)
$r_t \times \overline{\text{age}}_i$		0.003***				0.008***		0.005***				0.008***
		(0.001)				(0.001)		(0.001)				(0.001)
$r_t \times \overline{\text{size}}_i$			-0.002**			-0.008***			0.004**			-0.004***
			(0.001)			(0.001)			(0.001)			(0.001)
$r_t \times \overline{\text{st debt}}_i$				0.000		-0.000				0.003**		0.003***
				(0.001)		(0.001)				(0.001)		(0.001)
$r_t \times \overline{\text{R\&D int.}}_i$					0.012***	0.012***					-0.001	0.005***
					(0.004)	(0.004)					(0.002)	(0.002)
$r_t \times \overline{\text{btm}}_i$						-0.007***						0.001*
						(0.001)						(0.001)
Observations	84,616	75,910	84,616	83,833	72,850	64,684	84,247	75,499	84,247	83,462	72,962	64,666
Firms	1,526	1,279	1,526	1,500	1,342	1,104	1,526	1,276	1,526	1,499	1,347	1,104

Notes: Patenting semi-elasticities for additional interaction terms with proxies for firms' financial constraints, estimated based on PPML-IV model (4). Dependent variables: firm's cumulative, 20-quarter ahead number of green and non-green patents. Shock is normalized to increase the federal funds rate by 25 basis points. We include interaction terms with average, standardized variables proxying for financial constraints: leverage ratio, age, size (log assets), short-term debt ratio and R&D intensity. Driscoll and Kraay (1998) standard errors in parentheses. Significance levels denoted by *** $p < 0.01$, ** $p < 0.05$, * $p < 0.10$.

Overall, we find limited systematic evidence that these characteristics account for the differential green and non-green patenting responses to monetary policy. While several of the additional interactions are statistically significant, they generally have the same sign for green and non-green patents and therefore cannot explain the divergence in patenting responses across the two technologies. Consistent with the evidence in Aghion et al. (2026), the green patenting response is stronger for more mature firms. At the same time, however, we find that more levered and younger firms display a larger increase in green patenting, possibly reflecting the fact that leverage and age are negatively correlated with the book-to-market ratio in our data. One important distinction is our focus on listed firms, which tend to be larger and more mature and therefore less likely to be financially constrained. Financial constraints may play a more important role for smaller, younger, and unlisted firms (see Aghion et al., 2026).

Consistent with growth firms showing a larger green patenting response, we estimate a positive interaction for firms with higher R&D intensity. Importantly, Column 6 shows that the book-to-market interaction remains robust when all of these firm characteristics are included jointly and, if anything, becomes slightly larger.

C. Model Appendix

C.1. Nominal Rigidities and Monetary Policy

To study monetary policy shocks, we add a retail sector with nominal price rigidities. Households purchase the CES retail basket $C_u = [\int_0^1 c_{iu}^{(\sigma-1)/\sigma} di]^{\sigma/(\sigma-1)}$, where $\sigma > 1$. Cost minimization gives demand and the retail price index:

$$c_{iu} = \left(\frac{p^r_{iu}}{P^r_u}\right)^{-\sigma} C_u, \qquad P^r_u = \left[\int_0^1 (p^r_{iu})^{1-\sigma} di\right]^{1/(1-\sigma)}. \tag{C.1}$$

Retailers. A unit mass of retailers transforms the wholesale final good into retail goods one-for-one. Retailer i chooses its price subject to (C.1) and pays the Rotemberg adjustment cost $\varphi(p^r_{iu}/p^r_{i,u-1} - 1)^2 C_u/2$, where $\varphi > 0$. Its objective, in units of the retail consumption basket, is

$$\max_{\{p^r_{iu}\}_{u\geq t}} \mathbb{E}_t \sum_{h\geq 0} \Lambda_{t,t+h} \left[\frac{p^r_{i,t+h} - P_{t+h}}{P^r_{t+h}} c_{i,t+h} - \frac{\varphi}{2}\left(\frac{p^r_{i,t+h}}{p^r_{i,t+h-1}} - 1\right)^2 C_{t+h}\right]. \tag{C.2}$$

In a symmetric equilibrium, gross inflation is $\Pi_u = P^r_u/P^r_{u-1}$ and the retailer markup is $\mathcal{M}_u = P^r_u/P_u$. For the monetary experiment, log utility and no preference shock imply $\Lambda_{u,u+1}C_{u+1}/C_u = \beta$. The price-setting condition is

$$0 = 1 - \sigma + \frac{\sigma}{\mathcal{M}_u} - \varphi(\Pi_u - 1)\Pi_u + \beta\varphi\mathbb{E}_u[(\Pi_{u+1} - 1)\Pi_{u+1}]. \tag{C.3}$$

The flexible-price markup is $\mathcal{M}^n = \sigma/(\sigma - 1)$.

Households and monetary policy. In the household budget constraint, consumption expenditure is now $P^r_u C_u$ and the bond price is $Q_u = R_u^{-1}$. The SDF and labor supply follow (D.23), with nominal wages deflated by P^r_u. Throughout the valuation and labor-market calculations for this extension, wages, operating profits, patent values and setup payments are measured in units of the retail consumption basket; the superscript r is suppressed when there is no ambiguity.

Actual wholesale operating profits are converted using the actual markup. Benchmark profits are evaluated at their no-shock values at the actual technology (A^M_u, A^G_u), using the markup $\mathcal{M}^n$:

$$\Pi^{K,r}_u = \frac{\Pi^K_u}{\mathcal{M}_u}, \qquad \Pi^{K,r,0}_u = \frac{\Pi^{K,0}_u}{\mathcal{M}^n}, \qquad K \in \{M, G\}. \tag{C.4}$$

Both actual and benchmark values use the actual retail-real SDF. Actual markup does not enter the reference cash flows. The Euler equation for the one-period nominal bond is

$$1 = \mathbb{E}_u \left[\Lambda_{u,u+1} \frac{R_u}{\Pi_{u+1}} \right]. \tag{C.5}$$

Final-good market clearing becomes

$$C_u + \int_0^{A_u^M} m_{hu}\, dh + \int_0^{A_u^G} g_{ju}\, dj + \xi_f^{-1} f_u + \frac{\varphi}{2}(\Pi_u - 1)^2 C_u = Y_u. \tag{C.6}$$

The adjustment cost absorbs the retail basket, produced one-for-one from the wholesale good. Write $s_u = s_u^G$ and $\chi(s) = \alpha_L + k_M + k_G s$, with k_M, k_G defined in (D.16). Equivalently, (C.6) is $[1 + \varphi(\Pi_u - 1)^2/2]C_u = \chi(s_u)Y_u$. Adjustment costs have zero first derivative at zero inflation.

Let C_u^n, Y_u^n be the zero-inflation flexible-price allocation associated with the same endogenous technology path. It satisfies

$$(L_u^n)^{1+\eta} = \frac{\alpha_L}{\bar{\omega}\mathcal{M}^n \chi(s_u)}, \qquad C_u^n = \chi(s_u) Y_u^n, \tag{C.7}$$

where Y_u^n follows (D.24) with $L_u = L_u^n$. The natural gross interest rate and Taylor rule are

$$(R_u^n)^{-1} = \beta \mathbb{E}_u \left[\frac{C_u^n}{C_{u+1}^n} \right], \qquad R_u = R_u^n \Pi_u^{\phi_\pi} \varrho_u^m, \qquad \phi_\pi > 1. \tag{C.8}$$

For a deterministic path, $R_u^n = \beta^{-1} C_{u+1}^n / C_u^n$. This intercept accounts for endogenous changes in natural consumption growth. The monetary disturbance follows

$$\log \varrho_u^m = \rho_m \log \varrho_{u-1}^m + \sigma_m \varepsilon_u^m. \tag{C.9}$$

Monetary transmission. Linearize in shock size around the zero-inflation transition and let $\widetilde{y}_u = \widehat{Y}_u - \widehat{Y}_u^n = \widehat{C}_u - \widehat{C}_u^n$ denote the output and consumption gap; the equality follows to first order from (C.6). Write $m_u = \widehat{\mathcal{M}}_u$ and $\pi_u = \widehat{\Pi}_u$. Labor supply gives $m_u = -(1+\eta)\widetilde{y}_u$. With $K_p = (\sigma - 1)(1+\eta)/\varphi > 0$, the Euler equation, Taylor rule and price-setting condition imply

$$\begin{aligned} \widetilde{y}_u &= \mathbb{E}_u \widetilde{y}_{u+1} - \phi_\pi \pi_u + \mathbb{E}_u \pi_{u+1} - \widehat{\varrho}_u^m, \\ \pi_u &= \beta \mathbb{E}_u \pi_{u+1} + K_p \widetilde{y}_u. \end{aligned} \tag{C.10}$$

The natural-rate intercept cancels the change in natural consumption growth even when research changes future technology. The forward matrix is

$$T = \frac{1}{1 + \phi_\pi K_p} \begin{pmatrix} 1 & 1 - \phi_\pi \beta \\ K_p & \beta + K_p \end{pmatrix}.$$

It has determinant $\beta/(1+\phi_\pi K_p) < 1$ and $1 - \operatorname{tr} T + \det T = K_p(\phi_\pi - 1)/(1+\phi_\pi K_p) > 0$; $1 + \operatorname{tr} T + \det T > 0$ as well. Both eigenvalues lie inside the unit circle, so the bounded fundamental solution is unique. Put $p = \rho_m$, $0 \le p < 1$. For $\widehat{\varrho}^m_{t+h} = p^h \widehat{\varrho}^m_t$, the solution is

$$
\begin{aligned}
\widetilde{y}_{t+h} &= -\xi_m p^h \widehat{\varrho}^m_t, & m_{t+h} &= (1+\eta)\xi_m p^h \widehat{\varrho}^m_t, \\
\pi_{t+h} &= -\frac{K_p \xi_m}{1-\beta p} p^h \widehat{\varrho}^m_t, & \xi_m &= \left[1 - p + \frac{(\phi_\pi - p)K_p}{1-\beta p}\right]^{-1} > 0.
\end{aligned}
\tag{C.11}
$$

A positive monetary disturbance contracts the output gap and raises the markup. With technology held fixed, the output-gap response is also the response of output and consumption. These responses are used in Corollary 3.2.

C.2. Balanced Growth Path

In this appendix, we define the notion of balanced growth in our model and provide conditions for its existence.

Definition C.1 (Balanced Growth Path)**.** *A* ***balanced growth path (BGP)*** *is a sequence of allocations and prices such that: (a) All equilibrium conditions are satisfied at each t; (b) Y_t, C_t, M_t, E_t grow at constant rates as $t \to \infty$; (c) the final-good input used to produce the varieties in each sector grows at the same rate as the corresponding number of varieties: $\int_0^{A_t^M} m_{ht}\, dh$ grows at the rate of A_t^M, and $\int_0^{A_t^G} g_{jt}\, dj$ at the rate of A_t^G.*

Condition (c) is the standard expanding-variety property: on a balanced growth path, growth comes from the number of varieties rather than their scale (Romer, 1990; Kung and Schmid, 2015). To characterize the BGP after the green transition, consider the production function:

$$
Y_t = L_t^{\alpha_L} M_t^{\alpha_M} G_t^{1-\alpha_L-\alpha_M}. \tag{C.12}
$$

The FOCs and CES prices imply:

$$
M_t = \frac{\alpha_M}{\mu_M}(A_t^M)^{\mu_M - 1} Y_t, \qquad G_t = \frac{1-\alpha_L-\alpha_M}{\mu_G}(A_t^G)^{\mu_G - 1} Y_t. \tag{C.13}
$$

Substituting (C.13) into (C.12), we obtain:

$$
Y_t = \bar{Z} L_t (A_t^M)^{\frac{\alpha_M(\mu_M - 1)}{\alpha_L}} (A_t^G)^{\frac{(1-\alpha_L-\alpha_M)(\mu_G-1)}{\alpha_L}}, \tag{C.14}
$$

where $\bar{Z} = (\alpha_M/\mu_M)^{\alpha_M/\alpha_L}[(1-\alpha_L-\alpha_M)/\mu_G]^{(1-\alpha_L-\alpha_M)/\alpha_L}$. On the balanced growth path, $\int_0^{A_t^M} m_{ht}\, dh$ and $\int_0^{A_t^G} g_{jt}\, dj$ must grow at the same rate as A_t^M and A_t^G, respectively. Moreover, A_t^M, A_t^G have to be growing such that $f_t \to 0$ in the long run.

Assumption C.1. *To ensure the existence of a BGP, the following conditions hold:*

1. *In the long run, A_t^M and A_t^G have to be growing over time.*

2. *In the long run, the technology levels satisfy* $A_t^M = \iota A_t^G$.
3. *The exponents satisfy the constraint:* $\frac{\alpha_M}{\alpha_L}(\mu_M - 1) + \frac{1-\alpha_L-\alpha_M}{\alpha_L}(\mu_G - 1) = 1$.

Let Γ denote the common gross growth rate. With k_M, k_G as defined in (D.16), free entry and the stock laws imply, for $K \in \{M, G\}$,

$$\frac{L_K^S}{L^S} = \frac{k_K}{k_M + k_G}, \qquad \frac{\zeta_G}{\zeta_M} = \left(\frac{k_M}{k_G}\right)^{\nu}, \qquad \Gamma = \phi + \zeta_M \left(\frac{k_M}{k_M + k_G} L^S\right)^{\nu}. \tag{C.15}$$

Combining new-patent valuation, free entry, and skilled-labor supply gives

$$\bar{\omega}^S (L^S)^{\psi+1-\nu}(\Gamma - \beta\phi) = \frac{(1-c)\beta\zeta_M k_M}{\alpha_L + k_M + k_G}\left(\frac{k_M}{k_M + k_G}\right)^{\nu-1}.$$

Substituting (C.15), the left-hand side increases strictly from zero to infinity with $L^S > 0$, while the right-hand side is positive, yielding a unique positive research allocation and an associated growth rate Γ. Positive growth requires $\zeta_M (L_M^S)^{\nu} > 1 - \phi$, which holds automatically for $\phi = 1$. The calibration in Section 4.1 satisfies these conditions.

C.3. Equilibrium Conditions and Model Solution

We present here the equilibrium conditions under nominal rigidity and monetary policy shocks, in line with the empirical analysis which focuses on the impulse responses to monetary policy shocks. The real-economy version excludes the retail sector and monetary policy. In this subsection, prices and wages are nominal, while patent cash flows and values are measured in retail-consumption units.

Households. The consumption Euler equation:

$$1 = \beta \mathbb{E}_t \left[\frac{\varrho_{t+1}^d C_t}{\varrho_t^d C_{t+1}} \Pi_{t+1}^{-1} R_t\right]. \tag{C.16}$$

Unskilled/Skilled Labor Supply:

$$\varrho_t^d W_t = \bar{\omega} C_t P_t^r L_t^{\eta}, \qquad \varrho_t^d W_t^S = \bar{\omega}^S C_t P_t^r (L_t^S)^{\psi}. \tag{C.17}$$

Final good producer. The optimization of the final good producer yields the following FOCs:

$$\alpha_L \frac{P_t Y_t}{L_t} = W_t, \qquad \alpha_M \frac{P_t Y_t}{M_t} = P_t^M,$$
$$(1-\alpha_L-\alpha_M)\frac{P_t Y_t}{E_t}\left(\frac{E_t}{f_t}\right)^{1/\rho} = P_t^f, \qquad (1-\alpha_L-\alpha_M)\frac{P_t Y_t}{E_t}\left(\frac{E_t}{G_t}\right)^{1/\rho} = P_t^G. \tag{C.18}$$

Production and intermediate-input demand are given by (6)–(7) and (10). The energy price index is

$$P_t^E = \left[(P_t^f)^{1-\rho} + (P_t^G)^{1-\rho} \right]^{1/(1-\rho)}. \tag{C.19}$$

Intermediate good producer.

$$p_{ht}^m = \mu_M P_t, \qquad\qquad p_{jt}^g = \mu_G P_t. \tag{C.20}$$

Thus $P_t^M = \mu_M P_t (A_t^M)^{1-\mu_M}$ and $P_t^G = \mu_G P_t (A_t^G)^{1-\mu_G}$. Using the profit coefficients in (D.16), per-variety profits are

$$\Pi_t^{M,r} = \frac{k_M Y_t}{\mathcal{M}_t A_t^M}, \qquad \Pi_t^{G,r} = \frac{k_G s_t^G Y_t}{\mathcal{M}_t A_t^G}, \qquad \mathcal{M}_t = \frac{P_t^r}{P_t}. \tag{C.21}$$

Fossil fuel. The price-setting condition of fossil fuel producer:

$$P_t^f = \xi_f^{-1} P_t. \tag{C.22}$$

Innovation. Existing and newly created patents satisfy

$$V_t^K = \Pi_t^{K,r} + \phi \mathbb{E}_t[\Lambda_{t,t+1} V_{t+1}^K], \qquad \mathcal{G}_t^K = \mathbb{E}_t[\Lambda_{t,t+1} V_{t+1}^K], \qquad K \in \{M, G\}. \tag{C.23}$$

Let $\Pi_u^{K,r,0}$ denote no-shock profits evaluated at the actual date-u technology stocks. The setup-cost benchmark discounts these profits using the actual household SDF:

$$\bar{\mathcal{G}}_t^K = \sum_{h=1}^{\infty} \phi^{h-1} \mathbb{E}_t[\Lambda_{t,t+h} \Pi_{t+h}^{K,r,0}], \qquad \mathcal{V}_t^K = \mathcal{G}_t^K - c\bar{\mathcal{G}}_t^K. \tag{C.24}$$

Free entry and the laws of motion are

$$\begin{aligned} \zeta_K A_t^K (L_{t,K}^S)^{\nu-1} \mathcal{V}_t^K &= \frac{W_t^S}{P_t^r}, & S_t^K &= \zeta_K A_t^K (L_{t,K}^S)^{\nu}, \\ A_{t+1}^K &= \phi A_t^K + S_t^K, & K &\in \{M, G\}. \end{aligned} \tag{C.25}$$

Retailers, monetary policy, and market clearing. Retail pricing and monetary policy follow (C.3) and (C.8). The goods market clears according to (C.6); skilled labor and bond market clearing require $L_{t,M}^S + L_{t,G}^S = L_t^S$ and $B_{t+1} = 0$.

Definition of equilibrium. Given an initial value of (A_0^M, A_0^G) and a sequence of exogenous shocks $\{Z_t, \varrho_t^d, \varrho_t^m\}_{t=0}^{\infty}$, a Competitive Equilibrium consists of sequences of household allocations $\{C_t, L_t, L_t^S, B_{t+1}\}_{t=0}^{\infty}$; firm decisions $\{Y_t, L_t, M_t, E_t, m_{ht}, g_{jt}, f_t\}_{t=0}^{\infty}$; innovation choices $\{L_{it,M}^S, L_{it,G}^S\}_{t=0}^{\infty}$; a price system $\{P_t, P_t^r, P_t^M, P_t^G, P_t^f, P_t^E, W_t, W_t^S, R_t\}_{t=0}^{\infty}$; and aggregate state variables $\{A_t^M, A_t^G\}_{t=0}^{\infty}$. Such that: (a) Households optimize consumption and labor supply subject to budget constraints; (b) Firms optimize their respective objectives—profit maximization; Innovators choose R&D to maximize expected returns; (c) Monetary policy follows the specified Taylor rule; (d) Variety stocks A_t^M, A_t^G evolve according to innovation and obsolescence; (e) All markets clear: goods, labor, bond, and intermediate inputs.

Solution method. In solving the model, we adopt the MIT shock approach to study the causal effect of a specific shock on the economy's dynamic transition path. An unanticipated shock is followed by its deterministic AR(1) decay. The numerical solution proceeds as follows:

1. Solve the no-shock transition from the initial technology stocks.
2. Initialize the post-shock technology paths, keeping (A_0^M, A_0^G) fixed. Given these paths, solve the Euler and retailer pricing equations backward, evaluate actual and benchmark patent values, and determine skilled wages and research allocation.
3. Update technology stocks forward using (C.25), and repeat until the equilibrium conditions are satisfied.

Terminal values are computed along a no-shock continuation toward the balanced growth path. Impulse responses are measured relative to the no-shock transition.

C.4. External Funding for R&D

This appendix develops an alternative microfoundation in which the effective input price P_t^X is pinned down by an external funding constraint on R&D activity rather than by the skilled R&D wage. The setup leaves the form of the innovator free-entry condition unchanged, and supports the conclusions of Proposition 3.4 under fixed funding capacity. Throughout this appendix we use the shorthand $\eta_t^K \equiv d \log \mathcal{V}_t^K / d \log Y_t$ for the cyclicality of sector-K patent values.

C.4.1. Setup

Innovators purchase the physical R&D input at price $\tilde{P}_t^X$ and rely on external finance to do so. The input consists of the skilled research services in the main text. Innovators must finance these services through a specialized lending market before selling new patents, and repay the loans from the sale proceeds. The aggregate supply of external R&D funding is a fixed capacity $\bar{F} = 1$, measured in the original units of R&D services. Rather than micro-founding the portfolio-allocation and intermediation decisions that channel savings to innovators, we take $\bar{F}$ as a reduced-form funding capacity that summarizes frictions making the effective supply of external R&D finance less than perfectly elastic.[4]

[4]Examples include search and matching frictions in venture-capital and other specialized financing markets, asymmetric information between innovators and financiers, limited pledgeability of early-stage R&D, and institutional segmentation of funding sources.

The aggregate physical R&D input $X_t \equiv X_{t,G} + X_{t,M}$ is subject to the funding constraint

$$\tilde{P}_t^X X_t \leq \tilde{P}_t^X \bar{F}, \tag{C.26}$$

with Kuhn–Tucker multiplier $\lambda_t \geq 0$ and complementary slackness

$$\lambda_t \big[\tilde{P}_t^X \bar{F} - \tilde{P}_t^X X_t\big] = 0. \tag{C.27}$$

Define the funding wedge

$$q_t \equiv 1 + \lambda_t \geq 1. \tag{C.28}$$

The effective input price faced by innovators is the composite

$$P_t^X \equiv q_t \, \tilde{P}_t^X, \tag{C.29}$$

which collapses to $\tilde{P}_t^X$ when the funding constraint is slack ($\lambda_t = 0$) and exceeds it whenever the constraint binds. The wedge has a natural Tobin's q interpretation: by free entry, $q_t = \varphi_t^K \mathcal{V}_t^K / \tilde{P}_t^X$, the value of the patents created per unit of R&D input relative to its physical replacement cost. Hence $q_t = 1$ when funding is slack and $q_t > 1$ when it binds, capturing the scarcity value of external R&D finance. We consider the strictly binding regime, so $X_t = \bar{F}$ and P_t^X adjusts to clear the market. The production and household blocks and the innovation specification are unchanged.

C.4.2. Proposition 3.4 under external funding

We first establish the equivalence between the fixed-capacity funding equilibrium and the inelastic-labor benchmark (Lemma C.1). Applied to the external-funding closure of Section C.4.1, this yields Proposition C.1, the funding-closure counterpart of Proposition 3.4.

Lemma C.1 (Observational equivalence). *In any closure of the innovation-input market for which the innovator's free-entry condition takes the form $\zeta_K A_t^K X_{t,K}^{\nu-1} \mathcal{V}_t^K = P_t^X$ with $K \in \{G, M\}$, the impact responses of innovation satisfy*

$$\frac{d \log S_t^K}{d \log Y_t} = \frac{\nu(\eta_t^K - \varepsilon_t^X)}{1-\nu}, \qquad K \in \{G, M\}, \tag{C.30}$$

where $\varepsilon_t^X \equiv d \log P_t^X / d \log Y_t$. Under the strictly binding fixed-capacity closure above, equilibrium allocations and innovation responses coincide with those of the inelastic-labor benchmark, with P_t^X replacing W_t^S.

Proof. See Appendix D. ■

Proposition C.1 (**Proposition 3.4 under external funding**). *Under the external-funding closure of Section C.4.1 and the maintained transition and shock conditions, the conclusions of Proposition 3.4 hold, with P_t^X replacing the skilled wage W_t^S. The input-price elasticity decomposes as*

$$\varepsilon_t^X = \frac{d \log q_t}{d \log Y_t} + \frac{d \log \tilde{P}_t^X}{d \log Y_t}. \tag{C.31}$$

Proof. See Appendix D. ■

C.5. Impulse Responses

In the main text, we report the impulse response of green and non-green innovation to a 25 basis point monetary policy shock. To provide a comprehensive overview of the model's quantitative results, Figure C.1 presents the impulse responses of a range of other aggregate variables. The contractionary monetary policy shock leads to a decline in aggregate demand, resulting in a short-term reduction in output and deflationary pressures. Simultaneously, it lowers the profitability of innovation and skilled employment in R&D, with a delayed decline in total factor productivity.

Figure C.1: Model impulse responses

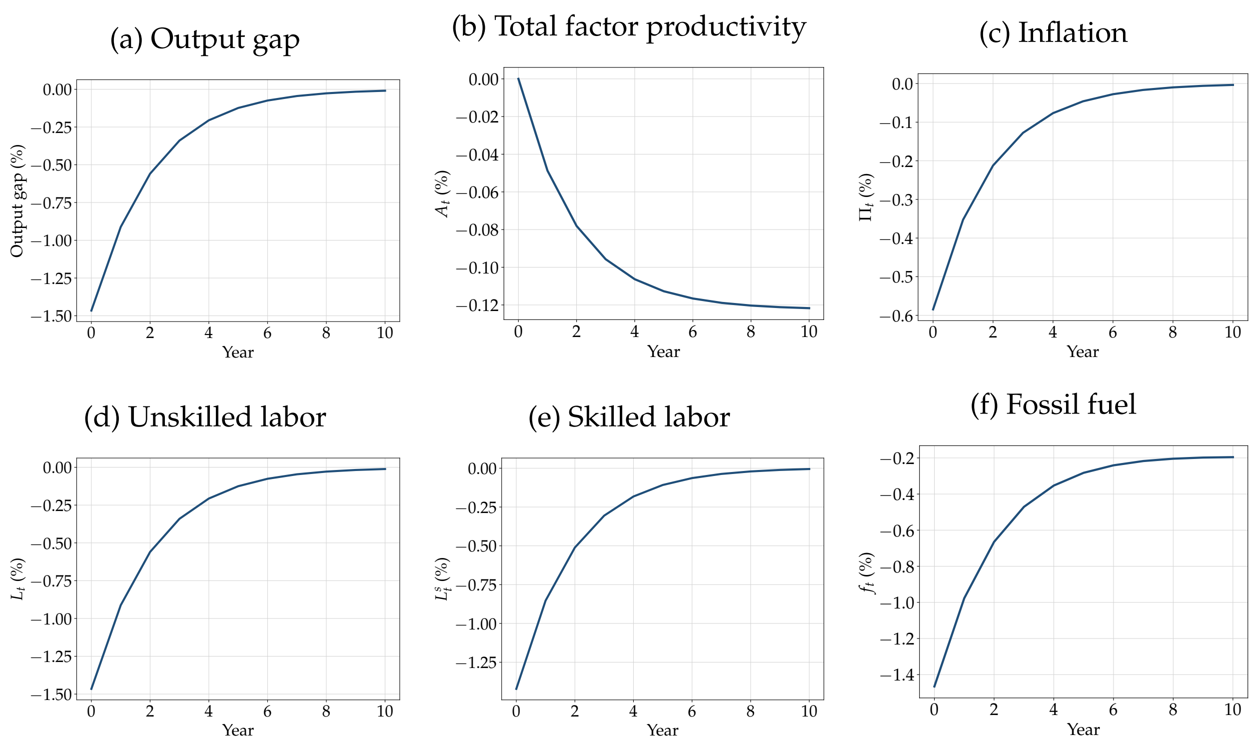

Notes: Figure C.1 illustrates the impulse response of aggregate variables to a 25-basis-point monetary policy shock.

Preference shocks. In Section 3, we model monetary shocks as demand-side disturbances to allow for better comparability with the empirical analysis. In this appendix, we look into the implications of the preference shock, altering the marginal utility of consumption. In this comparison, the policy intercept responds to technology but not directly to preference shocks.

Unlike monetary shocks, preference shocks influence not only the level of marginal utility but also intertemporal substitution by shifting the relative valuation of consumption today versus in the future. Specifically, the stochastic discount factor becomes:

$$\Lambda_{t,t+1} = \beta \frac{\varrho_{t+1}^{d} C_t}{\varrho_t^{d} C_{t+1}}. \tag{C.32}$$

As a result, the SDF becomes less procyclical—or even countercyclical—compared to the case of TFP or monetary shocks. This distinction implies that the discount rate channel may contribute to countercyclical movements in the relative valuation of intellectual property associated with green versus non-green technologies.

Figure C.2 compares the responses of green innovation to a preference shock and to a comparable monetary shock. Both shocks generate an impact decline in the output gap of one percent.

Figure C.2: Preference shocks

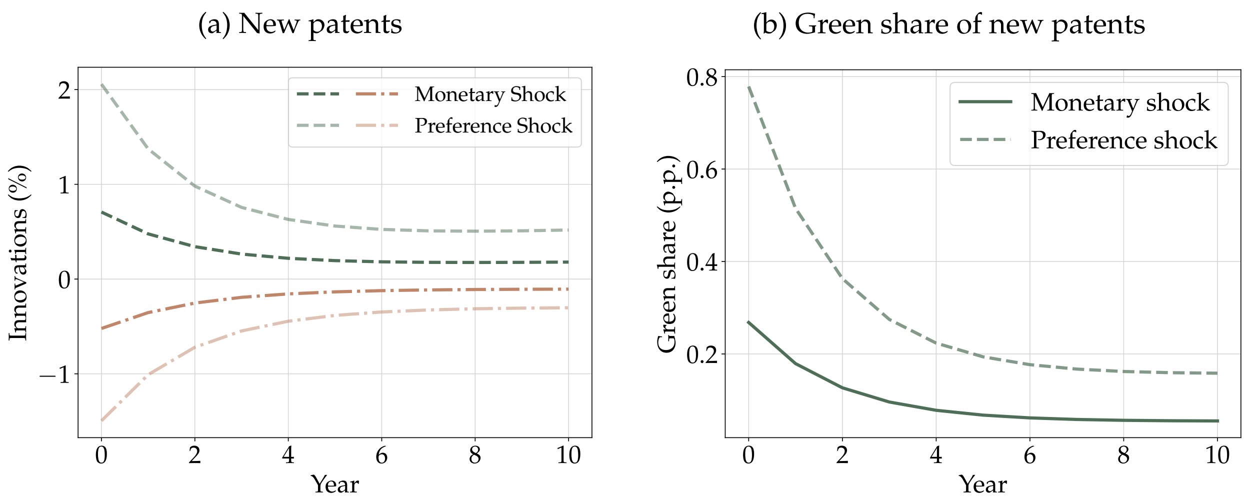

Notes: Impulse responses of new patents and the green share of new patents to a preference shock and a monetary shock that reduces the output gap by approximately 1% at $t = 0$.

We can see the countercyclicality of green patenting is stronger under a preference shock, consistent with the intuition that a countercyclical stochastic discount factor—induced by such shocks—gives rise to a discount rate channel that reinforces, rather than offsets, the countercyclicality raised by the cash flow channel.

C.6. The Role of Intertemporal Elasticity of Substitution

In Section 3, we demonstrate that under log utility, the cash flow channel dominates the discount rate channel in general equilibrium. In this section, we extend the analysis to a more general CRRA utility specification and examine how different values of the intertemporal elasticity of substitution (IES) influence the cyclicality of green innovation. Specifically, we modify the household's objective to:

$$\mathbb{E}_t \sum_{t=0}^{\infty} \beta^t \left(\varrho_t^d \frac{C_t^{1-\sigma_c}}{1-\sigma_c} - \frac{\bar{\omega}}{1+\eta} L_t^{1+\eta} - \frac{\bar{\omega}^S}{1+\psi} (L_t^S)^{1+\psi} \right), \tag{C.33}$$

where σ_c denotes the coefficient of relative risk aversion. All other parameters remain unchanged.

Figure C.3: The role of intertemporal elasticity of substitution

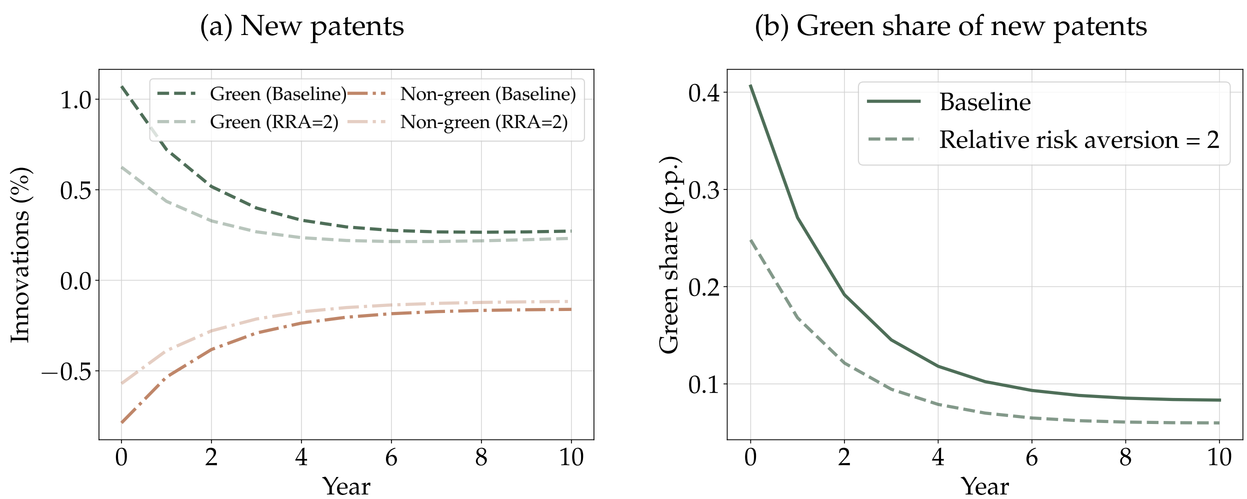

Notes: Impulse responses of new patents and the green share of new patents to a 25 basis point monetary policy shock. We compare the baseline model ($\sigma_c = 1$) to the case where $\sigma_c = 2$, keeping other parameterizations the same.

Figure C.3 compares the results under $\sigma_c = 2$ to the baseline specification with log utility (i.e., $\sigma_c = 1$). Intuitively, a higher value of σ_c implies a lower intertemporal elasticity of substitution, which strengthens the discount rate channel and thereby dampens the countercyclicality of green innovation.

Panel a shows that when $\sigma_c = 2$, the countercyclicality of new green patenting declines considerably, while the cyclicality of new non-green patents changes little by comparison. As a result, the countercyclicality of the green share of new patents declines by about 40% on impact under the same parameterization, see Panel b.

C.7. Green Is in the Future Along the Transition Path

In Section 4, we present the impulse response of the green share of patents at $t = 0$, which is calibrated to the green share of energy in the 2010s. The results show that, due to the 'green is in the future' effect, the green share of new patents is countercyclical. How does the green is in the future effect evolve, and how does it affect the countercyclicality of the green share of new patents along the transition path?

Figure C.4: The role of the base period along the transition path

(a) Green share of energy (b) Profit of green production (c) Green share of new patents

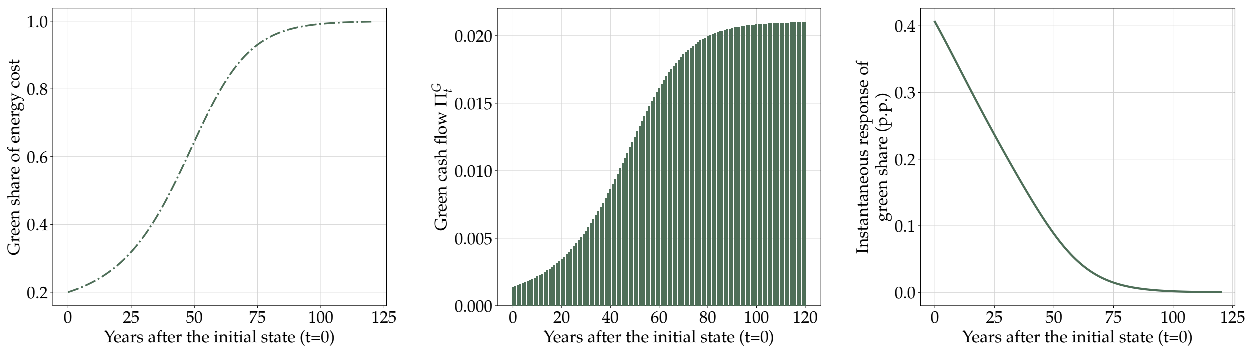

Notes: Sensitivity of the results depending on the initial period t along the transition path when the monetary policy shock hits.

Figure C.4a first depicts the green share of energy cost along the transition path. The green energy input gradually takes over the energy market. Panel b plots the cash flow from producing green varieties. Its trend tracks the trajectory of the green transition, initially growing slowly, then accelerating as the transition progresses, and eventually flattening out as green energy dominates the entire energy market. Panel c shows the instantaneous response of the green share of new patents to a 25 basis point monetary policy shock along the transition path. The countercyclicality is strongest at the initial state and declines monotonically as the transition proceeds. At the initial state, the current cash flow of a green variety is only about 45% as large, relative to its patent value, as that of a non-green variety, which is what makes green patent values insensitive to current conditions. As green energy takes over the market, this ratio rises towards one, and the green is in the future effect gradually vanishes.

C.8. Varying Speed of Green Transition

In Section 4.1, we calibrate the model to U.S. data, and the model suggests that it takes 41 years for the economy to reach a point where green energy occupies half of the energy market. What if the green transition is accelerated? How does an accelerated green transition influence the cyclicality of green innovation? Figure C.5a shows the green transition path based on our baseline calibration, as well as an accelerated path where we increase the scale parameters of innovation ζ_G and ζ_M by 20%. Figure C.5b illustrates the impulse response of the green share of new patents to a 25-basis-point monetary policy shock under both transition scenarios. This figure shows that if the green transition is accelerated, the green share of new patents exhibits stronger countercyclicality. This is because a faster transition means that, within a relatively short period, the proportion of current cash flow to value is smaller, thereby strengthening the green is in the future effect. Figure C.5c plots the cumulative response of the green share of new patents over the first ten years against the years required for the green share of energy cost to reach 50%. We find that the faster the green transition, the stronger the countercyclicality.

Figure C.5: Varying speed of green transition

(a) Green share of energy (b) IRF of green share $t = 0$ (c) Green share of new patents

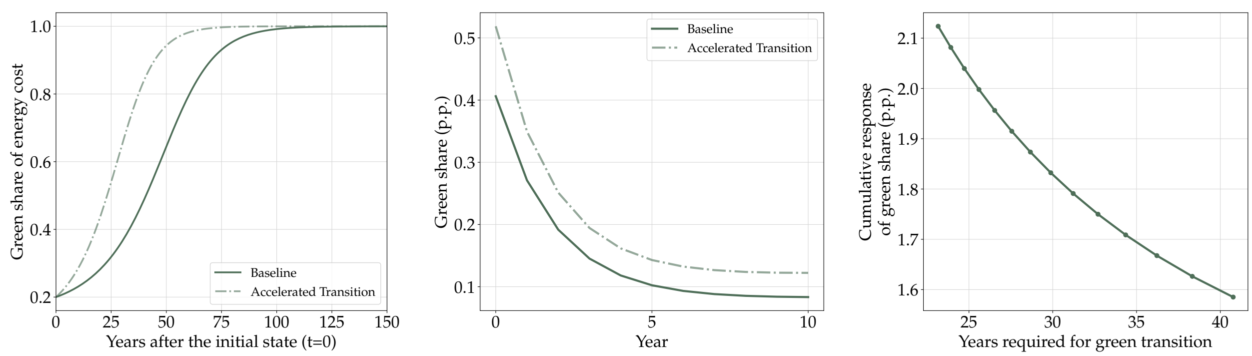

Notes: Panels a and b consider an accelerated path where we increase the scale parameters of innovation ζ_G and ζ_M by 20%. Panel c plots the cumulative response of the green share of new patents over the first ten years against the years required for the green share of energy cost to reach 50%.

C.9. Model with Brown Innovation

In Section 3, we abstract from innovation in fossil fuel (brown) inputs. This simplification allows us to focus on the endogenous dynamics of green innovation. However, empirical evidence suggests that a considerable fraction of energy-related innovation continues to target improvements in the efficiency and productivity of traditional fossil fuels. For instance, Aghion et al. (2016) documents that firms facing weak environmental regulation tend to innovate more in brown technologies rather than shifting towards green alternatives. To capture this pattern, we extend the model by allowing for endogenous innovation in brown energy. In this section, we relax the assumption of a fixed measure of brown inputs and introduce entry dynamics for fossil-based energy varieties.

Endogenous brown innovation. We modify the baseline specification by allowing the measure of brown energy varieties to evolve endogenously. The final energy input is produced by aggregating green and brown components through a CES aggregator:

$$E_t = \left(G_t^{\frac{\rho-1}{\rho}} + F_t^{\frac{\rho-1}{\rho}} \right)^{\frac{\rho}{\rho-1}}, \quad F_t = \left(\int_0^{A_t^F} f_{st}^{\frac{1}{\mu_F}} \, ds \right)^{\mu_F}. \tag{C.34}$$

From the optimization problem of final good producer, demand for each brown energy variety $s \in [0, A_t^F]$ is given by

$$f_{st} = \left(\frac{p_{st}^f}{P_t^F} \right)^{\frac{\mu_F}{1-\mu_F}} F_t, \tag{C.35}$$

where P_t^F denotes the associated price index, $P_t^F = \left(\int_0^{A_t^F} (p_{st}^f)^{\frac{1}{1-\mu_F}} \, ds \right)^{1-\mu_F}$.

The evolution of the fossil reserve is modified to account for the endogenous measure of brown varieties:

$$R_{t+1} = R_t - \int_0^{A_t^F} f_{st} \, ds. \tag{C.36}$$

Each brown energy variety is produced by a monopolistic firm that sets price p_{st}^f to maximize profits $\Pi_{st}^F = \max_{p_{st}^f} \{ p_{st}^f f_{st} - \xi_f^{-1} f_{st} \}$, with value $V_t^F = \sum_{h=0}^{\infty} \phi^h \mathbb{E}_t[\Lambda_{t,t+h} \Pi_{t+h}^F]$. The corresponding innovation problem mirrors that of materials and green energy:

$$\max_{L_{it,F}^S} \quad \varphi_t^F L_{it,F}^S (\mathcal{G}_t^F - c\bar{\mathcal{G}}_t^F) - W_t^S L_{it,F}^S, \tag{C.37}$$

where $\varphi_t^F = \zeta_F A_t^F (L_{t,F}^S)^{-(1-\nu)}$. As in Section 3.3, $\mathcal{G}_t^F = \mathbb{E}_t[\Lambda_{t,t+1} V_{t+1}^F]$, and $\bar{\mathcal{G}}_t^F$ uses no-shock profits along the actual technology path. Brown varieties evolve as $A_{t+1}^F = \phi A_t^F + S_t^F$, where $S_t^F = \varphi_t^F L_{t,F}^S$, and skilled-labor clearing becomes $L_{t,M}^S + L_{t,G}^S + L_{t,F}^S = L_t^S$.

Green is in the future. The model with brown innovation preserves the green is in the future properties, provided that there is green transition underway:

Proposition C.2 (Brown Innovation)**.** *Given the green transition, Proposition 3.1, 3.2, and 3.3 hold under the model with brown innovation.*

Proof. See Appendix D. ■

C.10. Alternative Formulation of Extraction Cost

In the baseline model, we assume a linear extraction technology for fossil fuel. To allow for increasing marginal extraction costs, we follow Bornstein, Krusell, and Rebelo (2023) and introduce a convex cost structure, where the extraction cost depends nonlinearly on the extraction rate. Extraction uses final goods, with cost and the associated marginal-cost pricing condition given by

$$c^F(\theta_t) = \psi^F \theta_t^{\eta^F} R_t, \qquad \frac{P_t^f}{P_t} = \psi^F \eta^F \theta_t^{\eta^F - 1}, \tag{C.38}$$

where $\theta_t \equiv f_t / R_t$ denotes the extraction rate, and R_t is the remaining stock of reserves.

We set $\eta^F = 2$ and calibrate ψ^F so that the convex economy starts from the same initial fossil share as the baseline. Both economies start from the same technology stocks; the remaining parameters are held fixed.

Figure C.6: Alternative fossil extraction technology

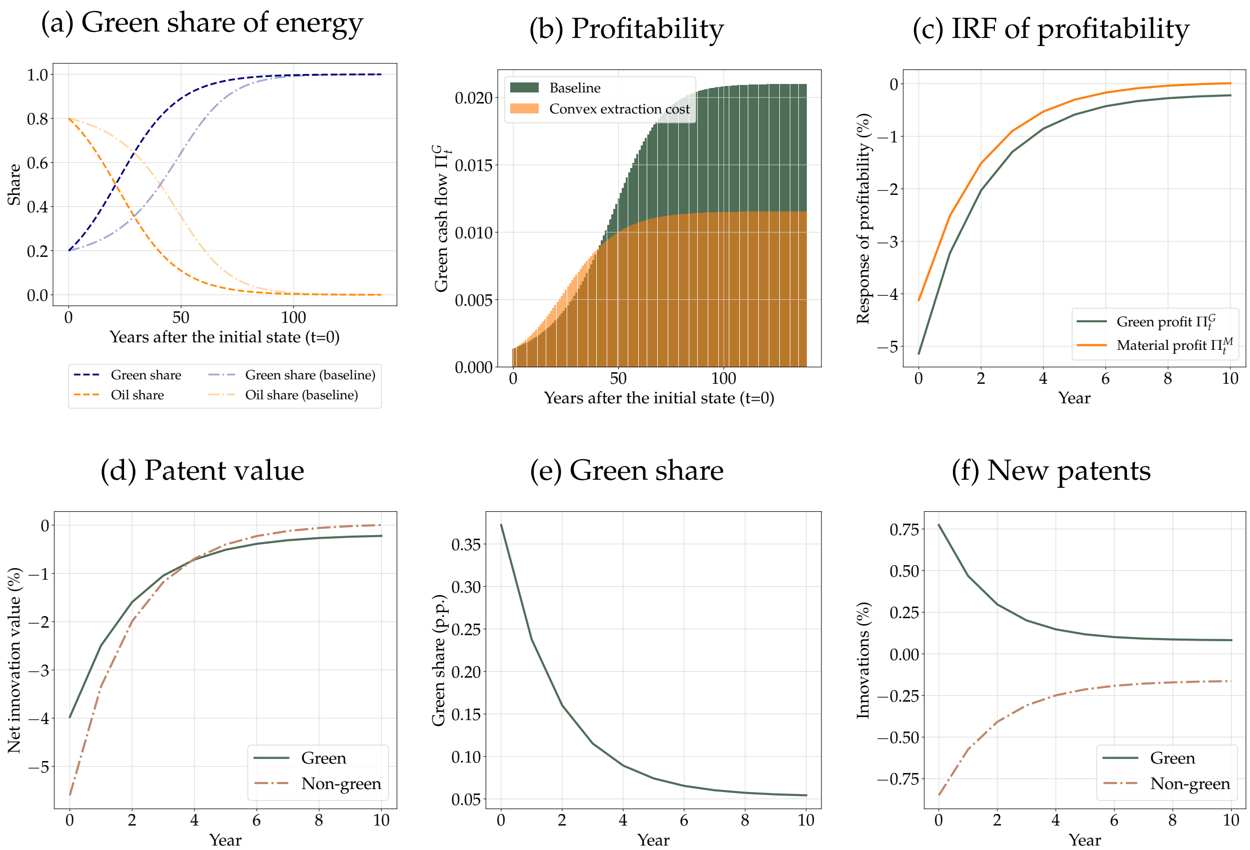

Notes: Panels (a)–(b) show no-shock transition paths; panels (c)–(f) show responses to a 25bp monetary tightening under the alternative extraction technology. The convex cost parameter is set to $\eta^F = 2$. All other parameters follow the baseline calibration in Section 4.1.

Figure C.6a shows that under the convex oil production technology, the green transition accelerates, with the green energy share surpassing fossil fuels within about 21 years—compared to about 41 years in the baseline. Panel b shows that green profits rise more rapidly early in the transition but converge to a lower level. Panel c illustrates that, due to the procyclical behavior of oil prices induced by the convex cost structure, green profitability becomes more procyclical as well. Nevertheless, Panel d shows that the value of green patents remains less procyclical than that of non-green patents, although the gap in cyclicality narrows. Panel f confirms that the countercyclicality of new green patenting still holds, and Panel e shows that the green share of innovation remains countercyclical.

C.11. Model with Creative Destruction

In this appendix, we consider a different model of innovation. Specifically, we endogenize the obsolescence rate to allow for vertical innovation.

Production. The green energy composite G_t and the materials composite M_t each aggregate a continuum of differentiated product lines indexed by $j \in [0,1]$ for green energy and $h \in [0,1]$ for materials:

$$M_t = \left(\int_0^1 A^m_{ht} m_{ht}^{1/\mu_M} \, dh \right)^{\mu_M}, \qquad G_t = \left(\int_0^1 A^g_{jt} g_{jt}^{1/\mu_G} \, dj \right)^{\mu_G}. \tag{C.39}$$

Here, A^m_{ht} and A^g_{jt} represent the qualities of materials and green energy inputs, respectively, while m_{ht} and g_{jt} denote the quantities of each product line. Final-good and energy production are given by (6)–(7), with the same factor shares α_L, α_M and fossil price $P^f_t = \xi_f^{-1}$. All prices and payoffs below are in final goods, with $P_t = 1$. Demand and the composite price indices are

$$m_{ht} = \left(\frac{p^m_{ht} / A^m_{ht}}{P^M_t} \right)^{\mu_M/(1-\mu_M)} M_t, \qquad g_{jt} = \left(\frac{p^g_{jt} / A^g_{jt}}{P^G_t} \right)^{\mu_G/(1-\mu_G)} G_t, \tag{C.40}$$

$$P^M_t = \left[\int_0^1 \left(\frac{p^m_{ht}}{(A^m_{ht})^{\mu_M}} \right)^{1/(1-\mu_M)} dh \right]^{1-\mu_M}, \quad P^G_t = \left[\int_0^1 \left(\frac{p^g_{jt}}{(A^g_{jt})^{\mu_G}} \right)^{1/(1-\mu_G)} dj \right]^{1-\mu_G}.$$

Intermediate input producers. Higher-quality inputs are more costly to produce. Write q for a line's quality and $\xi_q > 0$ for the unit cost parameter. Its marginal cost is $\xi_q q$. The current leader is the sole producer on its line. The producer maximizes profits subject to (C.40):

$$\Pi^I_{kt} = \max_{p^I_{kt}} (p^I_{kt} - \xi_q A^I_{kt}) I_{kt}, \qquad I \in \{m, g\}. \tag{C.41}$$

Optimal prices are $p^m_{ht} = \mu_M \xi_q A^m_{ht}$ and $p^g_{jt} = \mu_G \xi_q A^g_{jt}$. Quantities are common within each sector, denoted by $\bar{m}_t, \bar{g}_t$. With $A^M_t = \int_0^1 A^m_{ht} \, dh$ and $A^G_t = \int_0^1 A^g_{jt} \, dj$, it follows that

$$P^K_t = \mu_K \xi_q (A^K_t)^{1-\mu_K}, \quad K \in \{M, G\}, \qquad M_t = (A^M_t)^{\mu_M} \bar{m}_t, \qquad G_t = (A^G_t)^{\mu_G} \bar{g}_t. \tag{C.42}$$

Using k_M, k_G from (D.16) and the energy expenditure share s^G_t in (D.4), define profit per unit of quality by

$$\pi^M_t = k_M \frac{Y_t}{A^M_t}, \qquad \pi^G_t = k_G \frac{s^G_t Y_t}{A^G_t}, \qquad \Pi^K_t(q) = q \pi^K_t. \tag{C.43}$$

Sectoral profits are therefore $A_t^M \pi_t^M = k_M Y_t$ and $A_t^G \pi_t^G = k_G s_t^G Y_t$.

Innovation and patent values. Both incumbents and entrants conduct research. A successful innovation raises the line's quality from q to λq, where $\lambda = 1 + \delta > 1$. Research takes place after current production, and the new technology becomes available next period. Incumbent and entrant successes are independent. If both succeed, the incumbent retains the line; if only the entrant succeeds, it replaces the incumbent.

Both types of researchers use the sectoral efficiency $\zeta_K = \zeta/\sqrt{k_K}$, with $\zeta > 0$. An incumbent attaining success probability i_t^K employs $\ell_{I,t}^K(q) = (q/A_t^K)(i_t^K/\zeta_K)^2$ units of skilled labor. Entrants undertake research portfolios with labor allocated across lines in proportion to q/A_t^K. Their private success contribution is linear in own labor, with productivity $(\zeta_K A_t^K/q)(L_{E,t}^K)^{-1/2}$, taking total entrant research $L_{E,t}^K$ as given. Thus, at the sectoral level,

$$i_t^K = \zeta_K \sqrt{L_{I,t}^K}, \qquad e_t^K = \zeta_K \sqrt{L_{E,t}^K}, \qquad L_t^S = \sum_{K \in \{G,M\}} (L_{I,t}^K + L_{E,t}^K). \tag{C.44}$$

The probabilities of replacement and realized improvement are $d_t^K = e_t^K(1 - i_t^K)$ and $u_t^K = i_t^K + d_t^K$, respectively. Aggregate technology evolves according to

$$A_{t+1}^K = \Gamma_t^K A_t^K, \qquad \Gamma_t^K = 1 + \delta u_t^K. \tag{C.45}$$

Let qv_t^K be the incumbent's enterprise value, including future own research and its costs. Its benchmark qb_t^K replaces only operating profits by their no-shock values at the same technology. Define

$$F_t^K = \mathbb{E}_t[\Lambda_{t,t+1} v_{t+1}^K], \qquad \bar{F}_t^K = \mathbb{E}_t[\Lambda_{t,t+1} b_{t+1}^K], \qquad N_t^K = F_t^K - c\bar{F}_t^K, \tag{C.46}$$

where $0 < c < 1$. The incumbent pays $c\delta q \bar{F}_t^K$ when only its research succeeds and $c\lambda q \bar{F}_t^K$ when both succeed. The entrant pays $c\lambda q \bar{F}_t^K$ only when it replaces the incumbent. Household preferences and the final-good resource constraint are unchanged.

Proposition C.3 (**Green Is in the Future**). *During the green transition:*

1. *The green energy market share $P_t^G G_t/(P_t Y_t)$ increases.*

2. *The relative operating profits of equal-quality green and material producers, π_t^G/π_t^M, increase.*

For the next two propositions, suppose that $\beta \in (\bar{\beta}, 1)$ and that shocks are sufficiently transitory.

Proposition C.4 (**Countercyclical Green Share of Innovations**). *During the green transition, there exists $\bar{\zeta} > 0$ such that, for $0 < \zeta < \bar{\zeta}$, the green share of realized innovations, $u_t^G/(u_t^G + u_t^M)$, is countercyclical conditional on both preference and TFP shocks.*

Proposition C.5 (General Equilibrium Effects). *During the green transition, there exists* $\bar{\zeta} > 0$ *such that, for* $0 < \zeta < \bar{\zeta}$, *green innovation is countercyclical, i.e.,*

$$\frac{\partial \log u_t^G}{\partial \log U_t} < 0,$$

if and only if the elasticity of skilled wages with respect to the shock, $\partial \log W_t^S / \partial \log U_t$, *exceeds a threshold* $\overline{\epsilon}_U$, *for* $U \in \{Z, \varrho^d\}$. *By contrast, non-green innovation is procyclical:*

$$\frac{\partial \log u_t^M}{\partial \log U_t} > 0.$$

Moreover, holding the non-green net-value elasticity fixed, the threshold $\overline{\epsilon}_U$ *decreases with the degree of countercyclicality of the relative net value of green versus non-green innovation,* N_t^G / N_t^M.

D. Proofs

For the following production-side proofs, normalize the final-good price to one, $P_t = 1$, and assume positive factor shares, $\alpha_L, \alpha_M, 1 - \alpha_L - \alpha_M > 0$, and interior monopoly pricing $\mu_M, \mu_G > 1$. As in Section 3.2, assume that A_t^M / A_t^G is nondecreasing along the transition. Lemma D.1 below establishes this property for the no-shock innovation equilibrium under the parameter restrictions stated there.

Proof of Lemma 3.1. The final-good producer's first-order conditions for fossil fuel and the green composite are

$$P_t^f = (1 - \alpha_L - \alpha_M) \frac{P_t Y_t}{E_t} \left(\frac{E_t}{f_t} \right)^{1/\rho}, \qquad P_t^G = (1 - \alpha_L - \alpha_M) \frac{P_t Y_t}{E_t} \left(\frac{E_t}{G_t} \right)^{1/\rho}. \tag{D.1}$$

Dividing these conditions and substituting into (7) gives

$$\frac{f_t}{G_t} = \left(\frac{P_t^G}{P_t^f} \right)^{\rho}, \qquad \frac{G_t}{E_t} = \left[1 + \left(\frac{P_t^G}{P_t^f} \right)^{\rho - 1} \right]^{-\rho/(\rho-1)}. \tag{D.2}$$

The last expression is strictly increasing in P_t^f / P_t^G because $\rho > 1$ and both prices are positive. Demand in (10) has elasticity $\mu_G / (\mu_G - 1)$, so unit marginal cost implies $p_{jt}^g = \mu_G$. The CES price index then yields $P_t^G = \mu_G (A_t^G)^{1-\mu_G}$, establishing the lemma. ■

Proof of Proposition 3.1. Part (1). For brevity, let s_t^G denote the green expenditure share within energy. Multiplying (D.1) by the respective input quantities and adding, using the homogeneity of (7), gives

$$P_t^f f_t + P_t^G G_t = (1 - \alpha_L - \alpha_M) P_t Y_t, \tag{D.3}$$

$$s_t^G \equiv \frac{P_t^G G_t}{P_t^f f_t + P_t^G G_t} = \left[1 + \left(\frac{P_t^G}{P_t^f} \right)^{\rho - 1} \right]^{-1}, \qquad \frac{P_t^G G_t}{P_t Y_t} = (1 - \alpha_L - \alpha_M) s_t^G. \tag{D.4}$$

Lemma 3.1 implies that s_t^G, and hence the green share of final-good expenditure, strictly increases during the green transition. The quantity ratio $G_t / E_t = (s_t^G)^{\rho/(\rho-1)}$ is distinct from the expenditure share s_t^G.

Part (2). Let m_t and g_t be the common quantities produced by a material and a green variety. Symmetry, monopoly pricing, and the final-good producer's material expenditure condition imply

$$m_t = \frac{\alpha_M}{\mu_M} \frac{Y_t}{A_t^M}, \qquad g_t = \frac{1 - \alpha_L - \alpha_M}{\mu_G} \frac{s_t^G Y_t}{A_t^G}. \tag{D.5}$$

These are quantities per variety: sectoral revenues are $A_t^M \mu_M m_t = \alpha_M Y_t$ and $A_t^G \mu_G g_t = (1 - \alpha_L - \alpha_M) s_t^G Y_t$. With unit marginal cost, per-variety profits therefore satisfy

$$\Pi_t^M = \frac{\alpha_M(\mu_M - 1)}{\mu_M} \frac{Y_t}{A_t^M}, \qquad \Pi_t^G = \frac{(1 - \alpha_L - \alpha_M)(\mu_G - 1)}{\mu_G} \frac{s_t^G Y_t}{A_t^G}, \tag{D.6}$$

$$\frac{\Pi_t^G}{\Pi_t^M} = \frac{(1 - \alpha_L - \alpha_M)(\mu_G - 1)\mu_M}{\alpha_M(\mu_M - 1)\mu_G} s_t^G \frac{A_t^M}{A_t^G}. \tag{D.7}$$

Part (1) gives a strictly increasing s_t^G, while A_t^M / A_t^G is nondecreasing on the maintained transition path. Hence

$$\frac{\Pi_{t+1}^G / \Pi_{t+1}^M}{\Pi_t^G / \Pi_t^M} = \frac{s_{t+1}^G}{s_t^G} \frac{A_{t+1}^M / A_{t+1}^G}{A_t^M / A_t^G} > 1, \tag{D.8}$$

which proves part (2). ■

Proof of Proposition 3.2. Consider a local perturbation of output along a deterministic no-shock transition, holding the entire technology and price paths fixed as in Section 3.2. Hold the common positive SDF path $\Lambda_{t,t+h}$ fixed as well; it may equal the household SDF along this transition and need not equal β^h. For $0 < \phi \leq 1$, assume positive, finite present values and summable local bounds on their derivatives. Define

$$V_t^K = \sum_{h=0}^{\infty} \phi^h \Lambda_{t,t+h} \Pi_{t+h}^K, \quad w_h^K = \frac{\phi^h \Lambda_{t,t+h} \Pi_{t+h}^K}{V_t^K}, \qquad \sum_{h=0}^{\infty} w_h^K = 1, \quad K \in \{M, G\}. \tag{D.9}$$

Here $\Lambda_{t,t} = 1$, and values and weights are evaluated at the unperturbed transition. Consider a transitory local output response

$$\eta_h \equiv \frac{d \log Y_{t+h}}{d \log Y_t}, \qquad \eta_0 = 1, \qquad 1 \geq \eta_h \geq \eta_{h+1} \geq 0, \qquad \lim_{h \to \infty} \eta_h = 0.$$

This includes an impact-only shock and responses $\eta_h = \kappa^h$ for $0 < \kappa < 1$.

Equation (D.6) shows that both sectors' profits at horizon h have elasticity η_h when the technology and price paths are held fixed. Differentiating the present values yields

$$\frac{d \log V_t^K}{d \log Y_t} = \sum_{h=0}^{\infty} w_h^K \eta_h. \tag{D.10}$$

Let $r_h = \Pi_{t+h}^G / \Pi_{t+h}^M$. Its weighted mean and the weight ratio are

$$\bar{r} = \sum_h w_h^M r_h = \frac{V_t^G}{V_t^M} > 0, \qquad \frac{w_h^G}{w_h^M} = \frac{r_h}{\bar{r}}.$$

Proposition 3.1 gives a strictly increasing r_h along the transition. Equation (D.10) and the covariance identity give

$$\begin{aligned}\frac{d\log(V_t^G/V_t^M)}{d\log Y_t} &= \frac{\mathrm{Cov}_{w^M}(r,\eta)}{\bar{r}} \\ &= \frac{1}{2\bar{r}}\sum_{h=0}^{\infty}\sum_{j=0}^{\infty} w_h^M w_j^M (r_h - r_j)(\eta_h - \eta_j) \leq 0. \end{aligned} \tag{D.11}$$

Every summand is nonpositive. Since $\eta_0 = 1$ and $\eta_h \to 0$, some $j > 0$ satisfies $\eta_j < \eta_0$. Both horizons have positive weight and $r_j > r_0$, so the inequality is strict.

Cash-flow and discount-rate decomposition. For the local calculation in (19), evaluate all weights along the no-shock transition, retaining the original meaning of its *ss* subscripts:

$$w_h^K = \frac{\phi^h \Lambda_{t,t+h,ss}\Pi^K_{t+h,ss}}{V^K_{t,ss}}, \qquad \sum_{h=0}^{\infty} w_h^K = 1. \tag{D.12}$$

Now vary profits and the SDF in a differentiable local perturbation. For both contributions, assume local derivative bounds that are summable over horizons. The product rule yields

$$\frac{d\log V_t^K}{d\log Y_t} = \sum_{h=0}^{\infty} w_h^K \frac{d\log \Pi^K_{t+h}}{d\log Y_t} + \sum_{h=0}^{\infty} w_h^K d_h, \qquad d_h \equiv \frac{d\log \Lambda_{t,t+h}}{d\log Y_t}. \tag{D.13}$$

This is (19); it is a first-order identity at the no-shock path.

The cumulative SDF response d_h differs from the response of a one-period SDF. Multiplicativity implies

$$d_0 = 0, \qquad d_{h+1} - d_h = \frac{d\log \Lambda_{t+h,t+h+1}}{d\log Y_t}. \tag{D.14}$$

Under the same relative-profit ordering as in Appendix D, the difference between the two discount-rate components is

$$\sum_h (w_h^G - w_h^M) d_h = \frac{\mathrm{Cov}_{w^M}(r,d)}{\bar{r}}. \tag{D.15}$$

If the response of every one-period SDF to date-t output is nonnegative, d_h is nondecreasing, and the covariance is nonnegative. It is positive when some positive-weight pair satisfies $r_h < r_j$ and $d_h < d_j$. If all one-period responses are nonpositive, the signs reverse, with strictness for a strictly opposed pair. A procyclical SDF in this horizon-specific sense therefore offsets the cash-flow ordering, whereas a countercyclical SDF reinforces it.

■

Endogenous ordering of sectoral growth rates. Consider the no-shock equilibrium of Section 3.4. Define

$$k_M = \frac{\alpha_M(\mu_M - 1)}{\mu_M}, \qquad k_G = \frac{(1-\alpha_L-\alpha_M)(\mu_G - 1)}{\mu_G}, \qquad \Gamma_t^K = \frac{A_{t+1}^K}{A_t^K}. \tag{D.16}$$

The resource constraint gives $C_t/Y_t = \chi(s_t^G) \equiv \alpha_L + k_M + k_G s_t^G$. An existing patent has cum-dividend value V_t^K, whereas a new patent created at date t first produces at $t+1$. Its date-t revenue is

$$\mathcal{G}_t^K = \mathbb{E}_t[\Lambda_{t,t+1}V_{t+1}^K] = \sum_{h=1}^{\infty}\phi^{h-1}\mathbb{E}_t[\Lambda_{t,t+h}\Pi_{t+h}^K]. \tag{D.17}$$

The first payoff is not multiplied by ϕ: new varieties enter $A_{t+1}^K = \phi A_t^K + S_t^K$ without obsolescence at entry. On the no-shock path the benchmark equals this revenue, so $\mathcal{V}_t^K = (1-c)\mathcal{G}_t^K$.

Lemma D.1 (Ordering of sectoral growth rates)**.** *Let* $0 < \nu < 1$, $0 < \beta < 1$, $0 < \phi \leq 1$, *and* $0 \leq c < 1$. *Under the research-productivity restriction associated with a common-growth BGP,*

$$\frac{\zeta_G}{\zeta_M} = \left(\frac{k_M}{k_G}\right)^{\nu}, \tag{D.18}$$

an interior no-shock equilibrium with $s_t^G < 1$ *at every finite transition date satisfies* $\Gamma_t^M > \Gamma_t^G$. *Consequently,* A_t^M/A_t^G *is strictly increasing along the transition.*

Proof of Lemma D.1. Normalize existing values by $\mathscr{P}_t^K \equiv A_t^K V_t^K/(k_K C_t)$ and new-patent revenues by $\mathscr{H}_t^K \equiv A_t^K \mathcal{G}_t^K/(k_K C_t)$. The fundamental value formulas and the household SDF $\Lambda_{t,t+1} = \beta C_t/C_{t+1}$ imply

$$\mathscr{H}_t^M = \frac{\beta}{\Gamma_t^M}\left[\frac{1}{\chi(s_{t+1}^G)} + \phi\mathscr{H}_{t+1}^M\right], \qquad \mathscr{H}_t^G = \frac{\beta}{\Gamma_t^G}\left[\frac{s_{t+1}^G}{\chi(s_{t+1}^G)} + \phi\mathscr{H}_{t+1}^G\right]. \tag{D.19}$$

Here $\mathscr{P}_t^M = 1/\chi(s_t^G) + \phi\mathscr{H}_t^M$ and $\mathscr{P}_t^G = s_t^G/\chi(s_t^G) + \phi\mathscr{H}_t^G$. At the common-growth BGP, $s^G = 1$ and $\mathscr{H}^G = \mathscr{H}^M$. Equal S^K/A^K and free entry give (D.18).

Along the transition, let $\mathscr{R}_t = \mathscr{H}_t^G/\mathscr{H}_t^M$. Free entry (22) and aggregation yield

$$\frac{S_t^G/A_t^G}{S_t^M/A_t^M} = \left(\frac{\zeta_G}{\zeta_M}\right)^{1/(1-\nu)}\left(\frac{A_t^G\mathcal{G}_t^G}{A_t^M\mathcal{G}_t^M}\right)^{\nu/(1-\nu)} = \mathscr{R}_t^{\nu/(1-\nu)}, \qquad \Gamma_t^K = \phi + \frac{S_t^K}{A_t^K}. \tag{D.20}$$

Thus $\mathscr{R}_t \geq 1$ implies $\Gamma_t^M/\Gamma_t^G \leq 1$. Taking the ratio in (D.19) gives

$$\mathscr{R}_t = \frac{\Gamma_t^M}{\Gamma_t^G}[\omega_{t+1}s_{t+1}^G + (1-\omega_{t+1})\mathscr{R}_{t+1}], \qquad \omega_{t+1} \equiv \frac{1}{\chi(s_{t+1}^G)\mathscr{P}_{t+1}^M} \in (0,1). \tag{D.21}$$

Write $\underline{\chi} = \alpha_L + k_M$ and $\overline{\chi} = \alpha_L + k_M + k_G$. Since $\Gamma_t^K > \phi$, the normalized discounted cash flows are bounded by $\beta^h/\underline{\chi}$, and hence

$$\mathscr{P}_t^K \leq \frac{1}{\underline{\chi}(1-\beta)}, \qquad \mathscr{P}_t^M \geq \frac{1}{\overline{\chi}}, \qquad \omega_t \geq \underline{\omega} \equiv \frac{\underline{\chi}(1-\beta)}{\overline{\chi}} > 0. \tag{D.22}$$

If $\mathscr{R}_t \geq 1$, then $\Gamma_t^M/\Gamma_t^G \leq 1$. Equation (D.21) and $s_{t+1}^G < 1$ imply $\mathscr{R}_{t+1} - 1 > (\mathscr{R}_t - 1)/(1-\omega_{t+1})$. After at most one date the deviation is strictly positive and grows by a factor at least $1/(1-\underline{\omega}) > 1$ each period. But at every date on this supposed branch,

$$\mathscr{R}_u = \frac{\Gamma_u^M}{\Gamma_u^G}\frac{\mathscr{P}_{u+1}^G}{\mathscr{P}_{u+1}^M} \leq \frac{\overline{\chi}}{\underline{\chi}(1-\beta)},$$

contradicting that divergence. Hence $\mathscr{R}_t < 1$, and (D.20) gives $\Gamma_t^M > \Gamma_t^G$. ∎

For $\nu = 0$, (D.18) gives $\zeta_G = \zeta_M$ and hence $\Gamma_t^G = \Gamma_t^M$.

Proof of Proposition 3.3. For this proof and the subsequent results, we use $\phi = 1$, $0 < \nu < 1$, $0 < c < 1$, $0 < \beta < 1$, $\eta \geq 0$, and $\psi > 0$. The production parameters and the common-growth restriction (D.18) are unchanged. We study first derivatives with respect to an unexpected date-t shock, evaluated on an interior deterministic no-shock transition. Future shock innovations are zero. A separate small-growth expansion is used below to establish signs, with a bound on its remainder.

Households, production, and new-patent revenues. Write $\alpha_E = 1 - \alpha_L - \alpha_M$, $s = s^G$, and retain k_K and $\chi(s) = \alpha_L + k_M + k_G s$ from Appendix D. In the real economy the household conditions are

$$\Lambda_{u,u+h} = \beta^h \frac{\varrho_{u+h}^d}{\varrho_u^d}\frac{C_u}{C_{u+h}}, \qquad W_u = \frac{\bar{\omega} C_u}{\varrho_u^d} L_u^\eta, \qquad W_u^S = \frac{\bar{\omega}^S C_u}{\varrho_u^d}(L_u^S)^\psi. \tag{D.23}$$

Cost minimization, labor-market clearing, and the resource constraint imply

$$Y_u = Z_u L_u \left(\frac{\alpha_M}{p_u^M}\right)^{\alpha_M/\alpha_L} \left(\frac{\alpha_E}{p_u^E}\right)^{\alpha_E/\alpha_L}, \qquad L_u^{1+\eta} = \frac{\alpha_L \varrho_u^d}{\bar{\omega}\chi(s_u)}, \qquad C_u = \chi(s_u) Y_u, \tag{D.24}$$

where $p^K = P^K/P$, $p^f = \xi_f^{-1}$, $p^M = \mu_M(A^M)^{1-\mu_M}$, and $p^E = [(p^f)^{1-\rho} + (p^G)^{1-\rho}]^{1/(1-\rho)}$. Let $\mathbf{q} = (\log A^M, \log A^G)$ and define

$$\begin{aligned}
\kappa_u &= (\rho-1)(\mu_G-1)(1-s_u), & e_{\chi,u} &= \frac{k_G s_u}{\chi(s_u)},\\
b_M &= \frac{\alpha_M(\mu_M-1)}{\alpha_L}, & b_{G,u} &= \frac{\alpha_E(\mu_G-1)s_u}{\alpha_L},\\
T_{C,u} &= \left(b_M,\ b_{G,u} + \frac{\eta}{1+\eta}e_{\chi,u}\kappa_u\right).
\end{aligned} \tag{D.25}$$

Thus $D_{\mathbf{q}} \log s_u = (0, \kappa_u)$ and $D_{\mathbf{q}} \log C_u = T_{C,u}$, holding the shocks fixed. In particular the technology-price elasticities are $\mu_K - 1$.

Set $F_M(\mathbf{q}) = k_M/\chi(s)$ and $F_G(\mathbf{q}) = k_G s/\chi(s)$. Per-variety profits, not profit pools, satisfy

$$\begin{aligned}
\frac{\Pi_u^K}{C_u} &= \frac{F_K(\mathbf{q}_u)}{A_u^K}, & \widetilde{\mathcal{G}}_u^K &\equiv \frac{A_u^K \mathcal{G}_u^K}{C_u} = \sum_{h\geq 1} \beta^h F_K(\mathbf{q}_{u+h}) \frac{A_u^K}{A_{u+h}^K},\\
\widetilde{\mathcal{G}}_u^K &= \frac{\beta}{\Gamma_u^K}[F_K(\mathbf{q}_{u+1}) + \widetilde{\mathcal{G}}_{u+1}^K], & \Gamma_u^K &= 1 + \zeta_K (L_{u,K}^S)^\nu.
\end{aligned} \tag{D.26}$$

The sum and recursion in (D.26) are for the no-shock path. Their $1/\Gamma_u^K$ is induced by normalization by the number of varieties; new-patent revenue excludes current profits. There is no quality jump or incumbent-improvement payoff.

The benchmark and the full response system. Let $\Pi^{K,0}(\mathbf{q}) = C^0(\mathbf{q})F_K(\mathbf{q})/A^K$ be the per-variety profit with shocks at their no-shock values and technology stocks $\mathbf{q}$. The benchmark is

$$\bar{\mathcal{G}}_u^K = \sum_{h\geq 1} \mathbb{E}_u[\Lambda_{u,u+h}\Pi^{K,0}(\mathbf{q}_{u+h})], \qquad \mathcal{V}_u^K = \mathcal{G}_u^K - c\bar{\mathcal{G}}_u^K. \tag{D.27}$$

Here $\mathbf{q}_{u+h}$ and $\Lambda_{u,u+h}$ follow the actual economy. On a no-shock path $\bar{\mathcal{G}}_u^K = \mathcal{G}_u^K$. For $\phi < 1$, the benchmark uses the same ϕ^{h-1} weights as (D.17). Each infinitesimal innovator takes the aggregate technology path, benchmark, and pricing kernel as given; no benchmark derivative enters its individual free-entry condition.

Let $\omega_{u,h}^K = \beta^h F_K(\mathbf{q}_{u+h})A_u^K/(A_{u+h}^K \widetilde{\mathcal{G}}_u^K)$ be the baseline revenue weights. They are positive and sum to one over $h \geq 1$. Write $\langle z\rangle_{K,u} = \sum_{h\geq 1}\omega_{u,h}^K z_{u+h}$. For a shock derivative ∂, put

$$x_{K,u} = \partial \log A_u^K, \quad \ell_{K,u} = \partial \log L_{u,K}^S, \quad d_{K,u} = \partial \log S_u^K, \quad v_{K,u} = \partial \log \mathcal{V}_u^K, \quad w_u = \partial \log W_u^S.$$

Also let $a_u = \partial \log \varrho_u^d$, $\gamma_u = \partial \log C_u$, $\mathcal{H}_u = \gamma_u - a_u$, and $J_{K,u} = D_{\mathbf{q}} \log F_K(\mathbf{q}_u)$. The symbol c remains the setup parameter. Differentiating profits and the actual SDF gives exactly

$$\begin{aligned}
\partial \log \bar{\mathcal{G}}_u^K &= \mathcal{H}_u + \langle a - \gamma + (J_K - \mathbf{e}_K^\top + T_C)x \rangle_{K,u}, \\
v_{K,u} - \mathcal{H}_u &= \left\langle a + (J_K - \mathbf{e}_K^\top)x + \frac{c}{1-c}(\gamma - T_C x) \right\rangle_{K,u}.
\end{aligned} \tag{D.28}$$

Here $\mathbf{e}_K$ is the sector coordinate vector and $\partial \log \Lambda_{u,u+h} = \mathcal{H}_u + a_{u+h} - \gamma_{u+h}$.

Free entry and aggregation give the following identities at every date:

$$\begin{aligned}
(1-\nu)\ell_{K,u} &= x_{K,u} + v_{K,u} - w_u, \\
d_{K,u} &= x_{K,u} + \nu \ell_{K,u} = \frac{x_{K,u} + \nu(v_{K,u} - w_u)}{1-\nu}, \\
x_{K,u+1} &= x_{K,u} + \nu g_{K,u} \ell_{K,u}, \qquad g_{K,u} = \frac{\Gamma_u^K - 1}{\Gamma_u^K}, \\
\partial \log \Gamma_u^K &= g_{K,u}(d_{K,u} - x_{K,u}).
\end{aligned} \tag{D.29}$$

Here $S^K / A^K = \zeta_K (L_K^S)^\nu$ is an innovation intensity, with no probability cap.

Let $n_u^K = L_{u,K}^S / L_u^S$, and $M_u = (1-\nu)I + \psi \mathbf{1} n_u^\top$. Skilled-labor supply and clearing imply

$$\begin{aligned}
w_u &= \mathcal{H}_u + \psi n_u^\top \ell_u, \qquad M_u \ell_u = x_u + v_u - \mathcal{H}_u \mathbf{1}, \\
M_u^{-1} &= \frac{1}{1-\nu}\left(I - \frac{\psi}{1-\nu+\psi} \mathbf{1} n_u^\top \right), \qquad \|M_u^{-1}\|_\infty \le \frac{2}{1-\nu}.
\end{aligned} \tag{D.30}$$

Thus (D.28)–(D.30), with $x_t = 0$, close the response through innovation, future technology, future profits, the actual SDF, and future benchmark payments. There is no extra ν in the individual free-entry condition.

Speed and persistence restrictions. Work on a regular interior branch with $s_u \ge s_* > 0$, positive net values, and $\varepsilon = \sup_{u,K} g_{K,u}$ small. The upper bound is over the continuations being valued, not just the shock date. The primitive parameters other than the scale governing slow growth are fixed away from $\beta = 1$, $c = 1$, and $\nu = 1$. The restrictions below are sufficient local bounds; slow growth is an additional restriction, not a consequence of shock transience.

For $U_t \in \{Z_t, \varrho_t^d\}$, write $p = \rho_U$ and impose the regularity condition in Proposition 3.3:

$$0 < p < \bar{p}(\psi) \equiv 1 - \frac{\nu(1-\beta)}{\beta(1-\nu+\psi)}, \qquad \nu(1-\beta) < \beta(1-\nu+\psi). \tag{D.31}$$

The latter inequality makes the interval nonempty. The upper bound is derived below.

No-shock path derivatives. Choose $v \in (\sqrt{\beta}, 1)$ and use $\|z\|_v = \sup_{h\geq 0} v^h \|z_{t+h}\|_\infty$. Because F_K is bounded above and away from zero, and $\Gamma^K > 1$,

$$\omega^K_{u,h} \leq C_\omega \beta^{h-1} \quad (h \geq 1), \qquad W_v = \frac{C_\omega}{v - \beta}, \qquad L_F = \sup_{K,u} \|J_{K,u}\|_1 < \infty.$$

All first and second log-state derivatives of F_K and the production functions are bounded on this region. The constants can be obtained directly from (D.25); for example $C_\omega = \max_K(\sup F_K / \inf F_K)$ is sufficient, since the $h = 1$ term bounds $\widetilde{\mathcal{G}}^K_u$ below by $\beta \inf F_K / \Gamma^K_u$.

For a perturbation k_0 of a no-shock initial state, differentiate (D.26) and the normalized free-entry condition. The reference responses satisfy

$$\begin{aligned} k_h &= k_0 + \nu \sum_{v<h} \operatorname{diag}(g_v) \ell^0_v, \\ M_u \ell^0_u &= \left(\sum_{h\geq 1} \omega^K_{u,h} \left[J_{K,u+h} k_{u+h} - \nu \sum_{v=u}^{u+h-1} g_{K,v} \ell^0_{K,v} \right] \right)_K . \end{aligned} \tag{D.32}$$

Consumption cancels from normalized free entry. In particular, no term proportional to the level of A^K remains in this reference equation. Accumulation has norm at most $\nu\varepsilon/(1-v)$. A sufficient bound for the resulting linear reference operator is

$$q_{\text{ref}} = \frac{2\nu\varepsilon W_v (L_F + 1)}{(1-\nu)(1-v)} < q_* < 1, \qquad L_\ell = \frac{2 L_F W_v}{(1-\nu)(1-q_*)}. \tag{D.33}$$

It gives $\|D_{\mathbf{q}} \log L^{S,0}_K\| \leq L_\ell$ at the initial date, uniformly also as $\psi \to \infty$. Successive reference states therefore have derivative bounded by $\exp(\nu L_\ell \varepsilon h)$. Impose the summability condition

$$\beta e^{2\nu L_\ell \varepsilon} < 1. \tag{D.34}$$

The same reference system differentiated twice, with the bounded second derivatives of production, supplies uniform second-order bounds: its inverse has norm at most $(1-q_*)^{-1}$ times the datewise bound in (D.30); the remaining terms are products of the bounded first derivatives. Polynomial factors in h are summable under the strict exponential margin in (D.34).

Actual technology feedback. For a response ℓ, write $(\mathcal{A}\ell)_{t+h} = \nu \sum_{v=t}^{t+h-1} \operatorname{diag}(g_v) \ell_v = x_{t+h}$. Define the state operator, component by component, by

$$(\mathcal{K}x)_{K,u} = x_{K,u} + \langle (J_K - \mathbf{e}^\top_K) x \rangle_{K,u}, \qquad \mathcal{T} = M^{-1} \mathcal{K} \mathcal{A}. \tag{D.35}$$

All coefficients are no-shock quantities. This formula retains the future $x_{K,u}$ in free entry and the state dependence of both values. Equations (D.28)–(D.30) reduce to $\ell = f + \mathcal{T}\ell$, where f is the fixed-technology forcing derived below. A sufficient operator bound is

$$\|\mathcal{T}\|_v \le q_{\text{dyn}} \equiv \frac{2\nu\varepsilon}{(1-\nu)(1-v)}[1 + W_v(L_F + 1)] < q_* < 1. \tag{D.36}$$

These component bounds establish invertibility of the full linear response system. They neither assume a response sign nor infer a dynamic contraction from a scalar denominator.

Consequently $x = O(\varepsilon)$ in the discounted norm. The future stock term in free entry changes research by $O(\varepsilon)$ and affects subsequent states through $\nu g_{K,u}\ell_{K,u}$, hence contributes $O(\varepsilon^2)$ to date-t values. The future-state contribution to values themselves is first order and is retained below.

Relative net values. Let

$$(\iota_a, \iota_y) = \begin{cases} (0,1), & U = Z, \\ (1, (1+\eta)^{-1}), & U = \varrho^d. \end{cases} \qquad B_U = \iota_a + \frac{c\iota_y}{1-c} > 0.$$

When technology is held fixed, (D.24) gives $a_{t+h} = \iota_a p^h$ and $\gamma_{t+h} = y_{t+h} = \iota_y p^h$; with endogenous technology, $\gamma_{t+h} = T_{C,t+h}x_{t+h} + \iota_y p^h$. Thus the exact fixed-technology forcing and relative-value response are

$$\begin{aligned} Q_{K,u}(p) &= \sum_{h\ge 1} \omega^K_{u,h} p^h, \\ f_u &= M_u^{-1} B_U p^{u-t} (Q_{M,u}, Q_{G,u})^\top, \\ D_t^{\text{dir}} &\equiv (v_{G,t} - v_{M,t})_{\text{fixed technology}} = B_U(Q_{G,t} - Q_{M,t}) < 0. \end{aligned} \tag{D.37}$$

The covariance argument in Appendix D applies to these $h \ge 1$ weights as well: relative profits increase and p^h strictly decreases over the payoff horizons.

For the technology comparison, freeze date-t coefficients and retain first order in ε, after differentiating once in shock size. Let

$$\begin{aligned} &\delta_t = g_{M,t} + (\kappa_t - 1) g_{G,t} > 0, \\ &\xi_M = -g_M - e_\chi \kappa g_G, \qquad \xi_G = -g_G + (1 - e_\chi)\kappa g_G. \end{aligned} \tag{D.38}$$

The strict sign uses Lemma D.1: $g_M > g_G$ and $\kappa > 0$. Baseline growth rates and ξ_K change by $O(\varepsilon^2)$ per date, by the reference derivative bounds. Normalized value weights therefore have first-order geometric factors $\beta_K = \beta(1 + \xi_K)$, with $\beta_G - \beta_M = \beta\delta_t$. It suffices to take ε small enough that $\beta_K \in (0,1)$; for example $\beta[1 + (\kappa_{\max} - 1)^+\varepsilon] < 1$ is an upper bound. The exact values already converge by (D.26).

The new-patent sums start at one. With $Q = p(1-\beta)/(1-\beta p)$ and $H_h(p) = (1-p^h)/(1-p)$, their expansions are

$$\begin{aligned}
Q_{G,t} - Q_{M,t} &= -\frac{\beta\delta_t p(1-p)}{(1-\beta p)^2} + O(\varepsilon^2), &\qquad \mathbb{E}_{\omega^{(0)}} H_h(p) &= \frac{1}{1-\beta p},\\
\ell_{K,t+h} &= \frac{B_U Q}{1-\nu+\psi} p^h + O(\varepsilon), & x_{K,t+h} &= g_K d^{(0)} H_h(p) + O(\varepsilon^2),\\
d^{(0)} &= \frac{\nu B_U Q}{1-\nu+\psi}.
\end{aligned} \tag{D.39}$$

The error statements apply in the discounted norms and sums, not uniformly without discounting over all future dates. Technology may remain displaced after the exogenous shock has vanished.

At the shock date $x_t = 0$. Subtracting the two equations in (D.28), and using (D.39), gives

$$\begin{aligned}
D_t \equiv v_{G,t} - v_{M,t} &= D_t^{(1)} + O(\varepsilon^2),\\
D_t^{(1)} &= -\frac{B_U\beta\delta_t p}{(1-\beta p)^2}\left[1 - p - \frac{\nu(1-\beta)}{\beta(1-\nu+\psi)}\right].
\end{aligned} \tag{D.40}$$

Indeed the first-order state contribution is

$$\frac{\delta_t d^{(0)}}{1-\beta p}.$$

The common term $-e_\chi \kappa x_G$ enters a difference in sectoral weights of order $O(\varepsilon)$, so its contribution is second order. The direct duration effect and the displayed state contribution are both $O(\varepsilon)$; neither has been discarded.

Condition (D.31) makes the bracket in (D.40) positive. For fixed p, signs in the original differentiated model use a strict persistence margin and a finite transition window with $\delta_t \geq d_* \varepsilon > 0$. The uniform $O(\varepsilon^2)$ bound then proves $D_t < 0$ for all sufficiently small positive ε, not just in the truncated expansion. This restriction can be checked without solving for the shock response, as follows.

Let $\ell^0_{K,t+h} = B_U Q p^h/(1-\nu+\psi)$, and define the impact functional

$$\mathcal{J}_t \ell = \langle (J_G - \mathbf{e}_G^\top)\mathcal{A}\ell\rangle_{G,t} - \langle (J_M - \mathbf{e}_M^\top)\mathcal{A}\ell\rangle_{M,t}.$$

The exact relation is $D_t = B_U(Q_{G,t} - Q_{M,t}) + \mathcal{J}_t\ell$, and a sufficient bound is $\|\mathcal{J}_t\| \leq 2\nu\varepsilon W_v(L_F+1)/(1-v)$. The resolvent of (D.35) gives the computable error certificate

$$|D_t - D_t^{(1)}| \leq E_t \equiv \left| B_U(Q_{G,t} - Q_{M,t}) + \mathcal{J}_t\ell^0 - D_t^{(1)} \right| + \frac{\|\mathcal{J}_t\|}{1-q_{\text{dyn}}} \|f - \ell^0 + \mathcal{T}\ell^0\|_v. \tag{D.41}$$

All terms on the right are reference-path coefficients or residuals of the specified trial response. The condition $E_t < |D_t^{(1)}|$ certifies a given finite growth rate. It bounds a second-order residual after retaining the first-order feedback, rather than assuming feedback is smaller than the direct effect. The bounds above give $E_t = O(\varepsilon^2)$.

At impact, (D.29) now implies

$$d_{G,t} - d_{M,t} = \frac{\nu}{1-\nu} D_t < 0, \qquad \partial \log \frac{S_t^G}{S_t^G + S_t^M} = \frac{S_t^M}{S_t^G + S_t^M} \frac{\nu}{1-\nu} D_t < 0. \tag{D.42}$$

Output rises at impact for either positive shock by (D.24), since technology is predetermined. This proves the proposition on the stated slow-transition domain.

The domain is nonempty: for example $\beta = 0.96$, $\nu = 0.3$, $c = 0.2$, $\psi = 1$ gives $\bar{p} = 1 - 0.012/1.632 > 0.99$. Strictly interior initial energy shares and a common reduction of the two research-productivity scales preserve (D.18) and admit arbitrarily slow regular branches. At zero growth the normalized research block has the nonsingular datewise matrix (D.30); the small-operator bounds continue it locally. Its limiting ratio is $g_G/g_M = s^{\nu/(1-\nu)}$, obtained from normalized free entry and (D.18). On finite windows bounded away from the end of the transition, this ratio and $\kappa > 0$ give the required duration margin. These are analytic examples and restrictions, not changes to the calibration.

At $p = 0$, $Q_{K,u}(0) = 0$ and the forcing is zero. The locally unique response is therefore $x = \ell = d = 0$: an impact-only shock rescales new-patent revenue, the matched setup benchmark, and the labor-supply shifter equally. Strict innovation signs require positive persistence; this boundary also applies to the monetary result below. At $c = 0$ a TFP shock leaves the normalized research system unchanged: on the locally unique branch, $x = \ell = d = 0$ exactly. At $\nu = 0$, $S_t^K = \zeta_K A_t^K$ has zero impact elasticity. Neither boundary supports the stated strict innovation signs for both shocks.

■

Proof of Proposition 3.4. At impact let $\mathcal{H} = \iota_y - \iota_a$ and $D = v_G - v_M$. From free entry and market clearing,

$$w = \frac{(1-\nu)\mathcal{H} + \psi(n^G v_G + n^M v_M)}{1 - \nu + \psi}, \qquad d_G < 0 \iff w > v_G. \tag{D.43}$$

Also $v_M - \mathcal{H} = B_U Q + O(\varepsilon) > 0$. Together with $D < 0$, the convex combination in (D.43) gives $w < v_M$ and $d_M > 0$. These conclusions hold for sufficiently small growth with the strict margins above. The exact threshold is $\bar{\epsilon}_U = v_G$. Hence it is lower when the net value of green innovation is less procyclical.

For TFP, $v_G = 1 + cQ/(1-c) + O(\varepsilon) > 0$. For a preference shock, however,

$$v_G = \frac{1}{1+\eta}\left[-\eta + \frac{1+\eta(1-c)}{1-c}\frac{p(1-\beta)}{1-\beta p}\right] + O(\varepsilon). \tag{D.44}$$

The preference-shock threshold may have either sign; the condition $w > v_G$ applies in both cases. ■

Proof of Corollary 3.1. Fix a finite set $\mathcal{I}$ of transition dates and put $e = \psi^{-1}$. At $e = 0$, the labor-supply equation $\log L_u^S = e(\log W_u^S - \log H_u)$, where $H_u = \bar{\omega}^S C_u / \varrho_u^d$, becomes $L_u^S = 1$. Choose its regular interior no-shock branch. Impose the strict uniform reference and response bounds above on this branch, and a finite-window duration margin. These conditions concern the limiting economy, not a threshold evaluated at an already chosen positive e.

Let $\mathcal{D}_u^K = (\zeta_K A_u^K \mathcal{V}_u^K)^{1/(1-\nu)}$. The level market-clearing equation has the regular representation

$$\frac{1 + e(1-\nu)}{1-\nu} \log W_u^S = e \log H_u + \log(\mathcal{D}_u^M + \mathcal{D}_u^G). \tag{D.45}$$

At the shock date, the exact innovation responses are

$$\begin{aligned} d_G(e) &= \frac{\nu}{1-\nu} \frac{e(1-\nu)[v_G(e) - \mathcal{H}(e)] + n^M(e)D(e)}{1 + e(1-\nu)}, \\ d_M(e) &= \frac{\nu}{1-\nu} \frac{e(1-\nu)[v_M(e) - \mathcal{H}(e)] - n^G(e)D(e)}{1 + e(1-\nu)}. \end{aligned} \tag{D.46}$$

At $e = 0$, the common zeroth-order research response ℓ^0 is zero. The first-order relative response is $-B_U \beta \delta_t p(1-p)/(1-\beta p)^2$. For fixed $0 < p < 1$ and sufficiently small growth, the error certificate therefore gives $D_t(0) < 0$. Interiority then yields exactly

$$d_{G,t}(0) = \frac{\nu}{1-\nu} n_t^M(0) D_t(0) < 0, \qquad d_{M,t}(0) = -\frac{\nu}{1-\nu} n_t^G(0) D_t(0) > 0.$$

The inverse in (D.30), the reference derivative bounds, and (D.45) are uniform at $e = 0$. On the selected nonsingular branch the equilibrium and its shock response are continuous in e, including the derivatives of all future benchmark payments. This follows from the local implicit function theorem and the uniform resolvent bounds, not from differentiating the wage formula while holding values or weights fixed. Moreover

$$\bar{p}(e) = 1 - \frac{\nu(1-\beta)e}{\beta[1 + e(1-\nu)]} \longrightarrow 1.$$

Let $\Delta = \min_{t \in \mathcal{I}}\{-d_{G,t}(0), d_{M,t}(0)\} > 0$. Continuity on this finite set supplies $\bar{e}_U > 0$ such that both responses differ from their limiting values by less than $\Delta/2$ for every $t \in \mathcal{I}$ and $0 \le e < \bar{e}_U$. Set $\overline{\psi}_U^{-1} = \bar{e}_U$. This is a common sufficient neighborhood constructed from the limiting economy; it is not a pointwise threshold depending on the actual e. It need not cover an infinite sequence approaching the BGP, where the duration margin vanishes. No bound $S^K/A^K < 1$ is needed. ■

Proof of Corollary 3.2. Use the retail-consumption numeraire and monetary transmission in Appendix C.1, and put $p = \rho_m$. For a unit monetary innovation, (C.11) and (D.25) give actual consumption, including the endogenous technology response,

$$\gamma_{t+h} = T_{C,t+h} x_{t+h} - \xi_m p^h.$$

Technology changes natural output and consumption, but not the markup response in (C.11). The relevant actual and reference operating profits, in common units, are

$$\Pi_u^{M,r} = \frac{k_M Y_u}{A_u^M \mathcal{M}_u}, \qquad \Pi_u^{G,r} = \frac{k_G s_u Y_u}{A_u^G \mathcal{M}_u},$$
$$\Pi^{K,r,0}(\mathbf{q}_u) = \frac{C^0(\mathbf{q}_u) F_K(\mathbf{q}_u)}{A_u^K \mathcal{M}^n}. \tag{D.47}$$

The benchmark is (D.27) with these reference retail-real cash flows and the *actual* retail-real SDF. Actual markup does not multiply reference profits. In the no-shock value normalization replace F_K by $F_K/\mathcal{M}^n$; the weights still sum to one and J_K is unchanged. This common constant leaves the proof of Lemma D.1 and the duration ordering valid.

For net values, actual markup adds $-\langle m\rangle_{K,u}/(1-c)$ to $v_{K,u} - \mathcal{H}_u$ in (D.28); its other terms are unchanged. At fixed technology, (C.11) therefore gives

$$\mathcal{H}_t = -\xi_m, \qquad v_{K,t} - \mathcal{H}_t = -B_m Q_{K,t}, \qquad B_m = \frac{\xi_m(1+\eta+c)}{1-c} > 0. \tag{D.48}$$

Because the technology component of markup is zero and that of consumption is $T_C x$, the full operator (D.35) is unchanged, evaluated on this nominal no-shock branch. In particular it still contains all future Romer stock effects on actual and benchmark values. Replace B_U by $-B_m$ in (D.37)–(D.41). This yields

$$D_t = \frac{B_m \beta \delta_t p}{(1-\beta p)^2}\left[1 - p - \frac{\nu(1-\beta)}{\beta(1-\nu+\psi)}\right] + O(\varepsilon^2) > 0. \tag{D.49}$$

The strict sign holds under the same persistence cutoff (D.31), uniform small-growth bounds, and remainder margin. Also $v_M < v_G < \mathcal{H}_t < 0$ for sufficiently small growth: the leading common gap below $\mathcal{H}_t$ is $-B_m Q < 0$. The wage equation (D.43) then gives $v_M < w < 0$, and hence $d_M < 0$. Finally free entry gives

$$d_G > 0 \iff w < v_G \iff |w| > \bar{\epsilon}_m, \qquad \bar{\epsilon}_m = |v_G| > 0.$$

This proves the corollary with the natural-rate policy rule. ■

Proof of Proposition 5.1. Use $\phi = 1$ and the regular interior slow-transition domain of Proposition 3.3, including (D.18) and (D.34). Set the policy date to zero and write $\tau = \tau_0^N$,

$k = 1 - \nu$, and $D = k + \psi$. All derivatives are evaluated at zero subsidy and zero macroeconomic shock, holding initial technology fixed. Retain $\varepsilon = \sup_{u,K} g_{K,u}$ over the full continuation, where $g_{K,u} = (\Gamma_{K,u} - 1)/\Gamma_{K,u}$. On the finite transition window, maintain the strict duration margin

$$\delta_t = g_{M,t} + (\kappa_t - 1) g_{G,t} \geq d_* \varepsilon > 0.$$

The wage condition is $\epsilon_W^U = d \log W_t^S / d \log Y_t \geq w_* > 0$ for each shock, uniformly on this window; w_* is independent of the growth scale. All other structural parameters are fixed as growth becomes small.

Valuation and equilibrium responses. Let the macroeconomic shock have log amplitude z and persistence $p = \rho_U \in (0, 1)$. From (D.23)–(D.24),

$$C_u = C^0(\mathbf{q}_u) d_u, \quad d_u = e^{y_U z p^u}, \quad \varrho_u^d = e^{i_U z p^u}, \quad W_u^S = H_u (L_u^S)^\psi, \quad H_u = \bar{\omega}^S C_u / \varrho_u^d,$$

where $C^0(\mathbf{q})$ is no-shock consumption at technology $\mathbf{q} = (\log A^M, \log A^G)$. The subsidy and lump-sum tax cancel in consolidated accounts. Predetermined technology therefore gives $\partial_\tau C_0 = \partial_\tau H_0 = 0$; future consumption adjusts.

Retain $F_M = k_M / \chi(s)$ and $F_G = k_G s / \chi(s)$, and write $P_K(\mathbf{q}) = F_K(\mathbf{q}) / A^K$ for normalized per-variety profits. The actual and matched reference profits are $C_u P_K(\mathbf{q}_u)$ and $C^0(\mathbf{q}_u) P_K(\mathbf{q}_u)$, respectively. Applying the actual household SDF to both gives, throughout the policy–shock neighborhood,

$$\begin{aligned} \mathcal{V}_{K,u} &= (1 - c) \frac{C_u}{\varrho_u^d} \mathcal{Q}_{K,u}, \qquad \mathcal{Q}_{K,u} = \sum_{h \geq 1} \beta^h P_K(\mathbf{q}_{u+h}) R_U(u + h, z), \\ R_U(v, z) &= \frac{\varrho_v^d (1 - c / d_v)}{1 - c}. \end{aligned} \tag{D.50}$$

At $z = 0$, $R_U = 1$ and $R_{U,z} = B_U p^v$, with

U	$y_U = \partial_z \log Y_0$	$h_U = \partial_z \log H_0$	B_U
Z	1	1	$c/(1-c)$
ϱ^d	$(1+\eta)^{-1}$	$-\eta/(1+\eta)$	$1 + c/[(1+\eta)(1-c)]$

so $y_U, B_U > 0$. Free entry and skilled-labor supply reduce to

$$k \log L_{u,K}^S + \psi \log L_u^S = \log \frac{\zeta_K (1 - c)}{\bar{\omega}^S} + q_{K,u} + \log \mathcal{Q}_{K,u} - \log(1 - \tau \mathbf{1}_{\{u=0\}}). \tag{D.51}$$

Use superscripts P, U, PU for derivatives with respect to $\tau, z, \tau z$, and write $\ell = \partial \log L^S$, $x = \partial \mathbf{q}$, $n_{K,u} = L_{u,K}^S / L_u^S$, and $M_u = kI + \psi \mathbf{1} n_u^\top$. Let $J_K = D_{\mathbf{q}} \log F_K$, $t_K = J_K - \mathbf{e}_K^\top$, and $H_K = D^2_{\mathbf{q}} \log F_K$. Brackets denote averages with $\omega^K_{u,h} = \beta^h P_K(\mathbf{q}_{u+h})/\mathcal{Q}^0_{K,u}$. Differentiating (D.51) and technology accumulation gives

$$
\begin{aligned}
M_u \ell^P_u &= x^P_u + (\langle t_K x^P \rangle_{K,u})_K + \mathbf{1}\mathbf{1}_{\{u=0\}}, \\
M_u \ell^U_u &= x^U_u + (\langle t_K x^U + B_U p^v \rangle_{K,u})_K, \\
x^j_{K,u+1} &= x^j_{K,u} + \nu g_{K,u} \ell^j_{K,u}, \qquad j = P, U,
\end{aligned} \tag{D.52}
$$

and the mixed system is

$$
\begin{aligned}
M_u \ell^{PU}_u &= x^{PU}_u + (\langle t_K x^{PU} \rangle_{K,u})_K + \mathcal{C}_u - \psi \mathbf{1} \operatorname{Cov}_{n_u}(\ell^P_u, \ell^U_u), \\
\mathcal{C}_{K,u} &= \langle (x^P)^\top H_K x^U \rangle_{K,u} + \operatorname{Cov}_{\omega^K_{u,\cdot}}(t_K x^P, t_K x^U + B_U p^v), \\
x^{PU}_{K,u+1} &= x^{PU}_{K,u} + \nu g_{K,u} \ell^{PU}_{K,u} + \nu^2 g_{K,u}(1 - g_{K,u}) \ell^P_{K,u} \ell^U_{K,u}.
\end{aligned} \tag{D.53}
$$

Here $v = u + h$ inside the averages, and all initial stock derivatives vanish. The covariance terms retain changes in valuation and labor weights.

Positive multipliers and common cyclicality. Use the operators $\mathcal{A}$, $\mathcal{K}$, and $\mathcal{T}$ from (D.35), so that $\ell^j = (I - \mathcal{T})^{-1} f^j$. For $\sqrt{\beta} < r < 1$ and $b \in \{r, r^2\}$, set

$$
\|f\|_b = \sup_u b^u \|f_u\|_\infty, \qquad W_b = \frac{C_\omega}{b - \beta}, \qquad q_b = \frac{2\nu\varepsilon}{k(1-b)}[1 + W_b(L_F + 1)].
$$

The production derivative bounds in the proof of Proposition 3.3 give $\|\mathcal{T}\|_b \le q_b$. Take growth small enough that $q_r \le 1/3$ and $q_{r^2} < q_* < 1$; the second norm controls products of first responses. The policy forcing is $f^P_u = D^{-1} \mathbf{1}\mathbf{1}_{\{u=0\}}$, hence

$$
\|\ell^P - f^P\|_r \le \frac{q_r}{D(1 - q_r)}, \qquad \ell^P_{K,0} \ge \frac{1}{2D} > 0.
$$

Let $Q = p(1-\beta)/(1-\beta p)$. Since the valuation weights are geometric at zero growth, the macroeconomic forcing is $f^U_u = (B_U Q/D) p^u \mathbf{1} + O(\varepsilon)$ in the r-norm. It follows that

$$
\ell^U_u = \frac{B_U Q}{D} p^u \mathbf{1} + O(\varepsilon), \qquad x^P, x^U = O(\varepsilon).
$$

The leading labor responses are common across sectors, so their labor-share covariance is $O(\varepsilon^2)$. The remaining forcing in (D.53) is $O(\varepsilon)$; its resolvent is bounded by $(1 - q_{r^2})^{-1}$, giving $\ell^{PU} = O(\varepsilon)$.

At impact, $\partial_\tau B^N_0 = W^S_0 L^S_0$ and

$$
\frac{\partial_{\tau z} B^N_0}{\partial_\tau B^N_0} = h_U + (\psi + 1) n^\top \ell^U.
$$

Consequently the multipliers are positive and satisfy

$$\begin{aligned}
\mathscr{M}_K &= \frac{\nu S_K \ell_K^P}{W^S L^S} > 0, \\
E_K := \frac{d\log \mathscr{M}_K}{d\log Y_0} &= \frac{\nu \ell_K^U + \ell_K^{PU}/\ell_K^P - h_U - (\psi+1)n^\top \ell^U}{y_U} \\
&= -\epsilon_W - k\epsilon_L + \frac{\nu(\ell_K^U - n^\top \ell^U)}{y_U} + \frac{\ell_K^{PU}}{y_U \ell_K^P},
\end{aligned} \tag{D.54}$$

where $\epsilon_L = n^\top \ell^U / y_U$ and $\epsilon_W = h_U/y_U + \psi\epsilon_L$. Thus

$$\epsilon_L = \frac{B_U Q}{D y_U} + O(\varepsilon) > 0, \qquad E_K = -\epsilon_W - k\epsilon_L + O(\varepsilon) < 0$$

for sufficiently small growth under $\epsilon_W \geq w_* > 0$. For example, take the labor-response error below $B_U Q/(2Dy_U)$ and the last two terms of (D.54) below $w_*/2$ in absolute value. The total multiplier is positive, and its elasticity is a positive multiplier-weighted average of E_G, E_M.

Relative multipliers and innovation composition. At impact define

$$\begin{aligned}
\xi_M &= -g_M - e_\chi \kappa g_G, & \xi_G &= -g_G + (1-e_\chi)\kappa g_G, & \bar{\xi} &= n^\top \xi, \\
A(p) &= -\frac{\beta p(1-p)}{(1-\beta p)^2} + \frac{\nu Q}{D(1-\beta p)}, & z_K^\xi &= \xi_K - \frac{\psi}{D}\bar{\xi}.
\end{aligned}$$

Then $\xi_G - \xi_M = \delta$. Expanding the valuation weights and (D.52), with path remainders in the weighted norms above, gives

$$\begin{aligned}
\langle p^h \rangle_{K,0} &= Q - \frac{\beta p(1-p)}{(1-\beta p)^2}\xi_K + O(\varepsilon^2), \\
x_{K,h}^P &= \frac{\nu g_K}{D} + O(\varepsilon^2), \qquad h \geq 1, \\
x_{K,h}^U &= \frac{\nu B_U Q}{D} g_K \frac{1-p^h}{1-p} + O(\varepsilon^2), \\
\ell_{K,0}^P &= \frac{1}{D} + \frac{\nu}{Dk} z_K^\xi + O(\varepsilon^2), \\
\ell_{K,0}^U &= \frac{B_U Q}{D} + \frac{B_U A(p)}{k} z_K^\xi + O(\varepsilon^2).
\end{aligned} \tag{D.55}$$

The stock displacement from the subsidy is constant to first order over all future payoff dates. Hence the covariance of $t_K x^P$ with $B_U p^v$ has no first-order term: changes in t_K and in the displacement contribute only at second order. The Hessian, stock–stock covariance, and labor covariance terms in (D.53) are also second order. Mixed accumulation, however, contributes $\nu^2 g_K B_U Q/D^2$ at every future payoff date to first order. Therefore

$$\ell^{PU}_{K,0} = \frac{\nu^2 B_U Q}{D^2 k} z^{\xi}_K + O(\varepsilon^2). \tag{D.56}$$

Substituting into (D.54) and subtracting sectors gives

$$E_G - E_M = -\frac{B_U}{y_U}\frac{\nu\delta p}{k(1-\beta p)^2}\left[\beta(1-p) - \frac{\nu(1-\beta)}{D}(2-\beta p)\right] + O(\varepsilon^2). \tag{D.57}$$

Writing $\theta = \nu(1-\beta)/D$, the bracket is strictly positive under the regularity condition in Proposition 5.1:

$$\beta > 2\theta, \qquad 0 < p < p_N \equiv \frac{\beta - 2\theta}{\beta(1-\theta)}. \tag{D.58}$$

The pure-policy response similarly gives

$$\partial_\tau \log(S_G/S_M) = \nu(\ell^P_G - \ell^P_M) = \frac{\nu^2\delta}{kD} + O(\varepsilon^2). \tag{D.59}$$

For completeness, the error orders follow from the same resolvent bounds, not from the signs being proved. Applying $(I-\mathcal{T})^{-1} = I + \mathcal{T} + \mathcal{T}^2(I-\mathcal{T})^{-1}$ to (D.52) bounds the omitted labor responses by $O(\varepsilon^2)$. Bounded state derivatives give $O(\varepsilon^2)$ changes in g and ξ per date; the resulting polynomial horizon factors are summable in the r- and r^2-norms. In the mixed system, replacing first responses by their leading expressions changes stock accumulation by $O(\varepsilon^2)$. The covariance cancellation just established leaves a second-order valuation residual as well. The mixed resolvent therefore bounds the error in (D.56) by $O(\varepsilon^2)$. Since $\ell^P_{K,0} \geq 1/(2D)$, these bounds give constants $C_E, C_S < \infty$, independent of ε, bounding the remainders in (D.57) and (D.59) by $C_E\varepsilon^2$ and $C_S\varepsilon^2$ uniformly on the transition window. At a strict persistence margin the leading coefficients are bounded away from zero after division by $\delta \geq d_*\varepsilon$. Reducing growth accordingly yields $E_G < E_M < 0$ and $\partial_\tau \log(S_G/S_M) > 0$, including $|E_G| > |E_M|$.

Compatibility of the wage and persistence conditions. The leading wage elasticities are

$$W^0_Z = 1 + \frac{\psi c Q}{(1-c)D} > 1, \qquad W^0_d = -\eta + \frac{\psi[1+\eta(1-c)]}{(1-c)D}Q.$$

Put $j = \eta(1-c)$. The preference-shock wage is positive to leading order precisely when

$$p > p_W \equiv \frac{jD}{\psi(1+j)(1-\beta) + \beta j D};$$

for $\eta = 0$, $p_W = 0$. The joint domain $0 < \rho_Z < p_N$ and $p_W < \rho_d < p_N$ is nonempty if

$$\beta D > 2\nu(1-\beta), \qquad \eta(1-c) < \frac{\psi[\beta D - 2\nu(1-\beta)]}{\beta D + 2\psi\nu(1-\beta)}. \tag{D.60}$$

Indeed, Q is increasing and $Q(p_N) = [\beta D - 2\nu(1-\beta)]/[\beta(1+\psi)]$; $jD < \psi(1+j)Q(p_N)$ is equivalent to the second inequality. For fixed persistence values strictly inside this domain, choose $0 < w_* < \min_U W_U^0/2$ and reduce growth until the wage-response errors are smaller than $\min_U W_U^0/2$. This supplies the assumed wage bound on the same regular equilibrium branch as the relative-multiplier result. All strict signs persist in sufficiently nearby macroeconomic states. ■

Proof of Proposition 5.2. Retain the regular interior branch, $\phi = 1$, finite transition window, notation, and strict joint parameter domain of the preceding proof. In particular, $\epsilon_W^U \geq w_* > 0$ for both shocks, $y_U, B_U > 0$, and $\varepsilon = \sup_{u,K} g_{K,u}$ bounds growth over the full continuations. Fix the other parameters and persistences. Set $\tau = \tau_0^G$ and evaluate derivatives at $(\tau, z) = (0, 0)$ with initial technology fixed.

Targeted equilibrium responses. The resource constraint and matched setup benchmark are unchanged: $\partial_\tau C_0 = \partial_\tau H_0 = 0$, while future consumption and technology adjust, and (D.50) continues to hold. The only direct change to (D.51) is to replace its last term by $-\mathbf{1}_{\{K=G\}} \log(1 - \tau \mathbf{1}_{\{u=0\}})$. Consequently (D.52) holds with policy forcing $\mathbf{e}_G \mathbf{1}_{\{u=0\}}$, and (D.53) holds with the resulting targeted policy response. There is no direct mixed policy–shock forcing.

Let $\ell^P, \ell^U, \ell^{PU}$ denote the $\tau, z, \tau z$ derivatives of log sectoral research labor, respectively, and let x^j denote the corresponding log-technology derivatives. Writing $M_u = kI + \psi \mathbf{1} n_u^\top$, the operators in (D.35) give

$$\ell^j = (I - \mathcal{T})^{-1} f^j, \qquad f_u^P = M_u^{-1} \mathbf{e}_G \mathbf{1}_{\{u=0\}}, \qquad j = P, U,$$
$$f_{G,0}^P = \frac{1 - \psi n_G / D}{k}, \qquad f_{M,0}^P = -\frac{\psi n_G}{kD}. \tag{D.61}$$

The macroeconomic forcing f^U is unchanged. In particular, $f_{G,0}^P - f_{M,0}^P = 1/k$.

Uniform response bounds. Choose $\sqrt{\beta} < \varpi < 1$. For $b \in \{\varpi, \varpi^2\}$, use $\|f\|_b = \sup_u b^u \|f_u\|_\infty$ and set

$$W_b = \frac{C_\omega}{b - \beta}, \qquad L_T = L_F + 1, \qquad K_b = 1 + W_b L_T,$$
$$a_b = \frac{\nu \varepsilon}{1 - b}, \qquad m = \frac{2}{k}, \qquad q_b = m a_b K_b.$$

The constants C_ω, L_F and a bound L_H satisfying $|a^\top H_K b| \leq L_H \|a\|_\infty \|b\|_\infty$ come from the production derivative bounds of Proposition 3.3. They are uniform over the continuations and independent of the growth scale. Equations (D.34) and (D.36) allow a positive growth neighborhood with $q_\varpi \le 1/5$ and $q_{\varpi^2} \le \bar{q}_2 < 1$. Then $\|\mathcal{A}\|_b \le a_b$, $\|\mathcal{K}\|_b \le K_b$, and $\|(I-\mathcal{T})^{-1}\|_b \le (1-q_b)^{-1}$. Since $\|f^P\|_\varpi \le 1/k$,

$$\|\ell^P - f^P\|_\varpi \le e_P := \frac{q_\varpi}{k(1-q_\varpi)}, \qquad d_P := \ell^P_{G,0} - \ell^P_{M,0} \ge \frac{1}{k} - 2e_P \ge \frac{1}{2k}. \tag{D.62}$$

For $Q = p(1-\beta)/(1-\beta p)$, put $u_U = B_U Q/D > 0$ and $\ell^0_u = u_U p^u \mathbf{1}$. The geometric-weight approximation used in the preceding proof is uniform here. To see this directly, let $\mu = L_T[-\log(1-\varepsilon)]$ and reduce growth so that $\beta e^\mu < 1$. Since each log-stock increment is at most $-\log(1-\varepsilon)$,

$$\left|\log \frac{P_K(\mathbf{q}_{u+h})}{P_K(\mathbf{q}_{u+1})}\right| \le \mu(h-1).$$

Comparing the normalized valuation weights with $(1-\beta)\beta^{h-1}$ therefore gives, uniformly in u, K,

$$|Q_{K,u}(p) - Q| \le d_Q(\varepsilon) := \frac{\beta(e^\mu - 1)(1-\beta e^{-\mu})}{(1-\beta e^\mu)(1-\beta)} = O(\varepsilon).$$

Because $M_u^{-1}\mathbf{1} = \mathbf{1}/D$, it follows that

$$\|\ell^U - \ell^0\|_\varpi \le e_U := \frac{m B_U d_Q(\varepsilon) + q_\varpi u_U}{1-q_\varpi} = O(\varepsilon). \tag{D.63}$$

Take $L_P = [k(1-q_\varpi)]^{-1}$, $L_U = u_U + e_U$, $X_P = a_\varpi L_P$, and $X_U = a_\varpi L_U$. These bound $\|\ell^P\|_\varpi, \|\ell^U\|_\varpi, \|x^P\|_\varpi, \|x^U\|_\varpi$, respectively.

Since ℓ^0_u is common across sectors, the targeted labor covariance satisfies

$$\operatorname{Cov}_{n_u}(\ell^P_u, \ell^U_u) = \operatorname{Cov}_{n_u}(\ell^P_u, \ell^U_u - \ell^0_u), \qquad \|\operatorname{Cov}_n(\ell^P, \ell^U)\|_{\varpi^2} \le 2L_P e_U.$$

Retain all other terms of (D.53). Writing $x^{PU} = \mathcal{A}\ell^{PU} + r^{PU}$, geometric summation and the product bound $\|fg\|_{\varpi^2} \le \|f\|_\varpi \|g\|_\varpi$ give

$$\begin{aligned}
\|r^{PU}\|_{\varpi^2} &\le C_a := \frac{\nu^2 \varepsilon L_P L_U}{1-\varpi^2}, \\
\|\mathcal{C}\|_{\varpi^2} &\le C_v := L_H W_{\varpi^2} X_P X_U \\
&\qquad + [W_{\varpi^2} + (W_\varpi)^2] L_T X_P (L_T X_U + B_U).
\end{aligned}$$

Here C_a bounds mixed accumulation; C_v bounds the state Hessian and valuation covariance, including the mean of a product and the product of two means. Eliminating x^{PU} in the mixed entry equation yields

$$\|\ell^{PU}\|_{\varpi^2} \le L_{PU} := \frac{m}{1-q_{\varpi^2}}[K_{\varpi^2} C_a + C_v + 2\psi L_P e_U] = O(\varepsilon). \tag{D.64}$$

All constants in these order bounds can be fixed before reducing growth: on a sufficiently small closed growth interval, $d_Q(\varepsilon)/\varepsilon$ has a finite continuous extension at zero, each q_b/ε is constant, and the two resolvent denominators are bounded away from zero. There are therefore fixed finite C_e, C_m such that $e_U \le C_e\varepsilon$ and $L_{PU} \le C_m\varepsilon$, uniformly over the finite transition window and both shocks.

To justify differentiation, use the existing state smoothness and reference summability bounds. In a small policy–shock neighborhood, R_U and $1-\tau$ remain positive with bounded derivatives. Growth and normalized entry place equilibrium differences in the weighted spaces. First difference quotients of entry and accumulation obey the same bounds with averaged coefficients; a slight enlargement of the constants preserves contraction and bounds these quotients in the ϖ norm. Mixed quotients use bounded state Hessians, the general bounded labor covariance, and products of first responses, controlled by the ϖ^2 norm and its resolvent. The valuation tails are uniformly summable as $\sum_h(\beta/\varpi)^h$ and $\sum_h(\beta/\varpi^2)^h$. Limits therefore solve the unique first and mixed systems in either order, justifying differentiation under the sums and continuity of impact derivatives. Applying this argument to (D.50) retains both actual and matched-reference value responses.

Expenditure and the true innovation share. Suppress impact-date subscripts and use, only within this proof, $r = S_G/S_M$ and $s_I = r/(1+r)$. The free-entry ratio and predetermined technology imply

$$J := 1 + \partial_\tau \log(\mathcal{V}_G/\mathcal{V}_M) = k d_P \ge \frac{1}{2}, \qquad \partial_\tau \log r = \nu d_P.$$

At zero subsidy in each macroeconomic state, $\partial_\tau B^G = W^S L^S_G = \mathcal{V}_G S_G > 0$. Consequently,

$$\begin{aligned} M_r &:= \frac{\partial r}{\partial B^G} = \frac{r\nu d_P}{W^S L^S_G} = \frac{\nu J}{k\mathcal{V}_G S_M}, \\ \mathscr{M}^{GS} &= \frac{M_r}{(1+r)^2} = \frac{\nu J S_M}{k\mathcal{V}_G(S_G+S_M)^2} > 0. \end{aligned} \tag{D.65}$$

The green expenditure denominator has macro response

$$\frac{\partial_{\tau z} B^G}{\partial_\tau B^G} = h_U + \psi n^\top \ell^U + \ell^U_G.$$

Let $d_U = \ell^U_G - \ell^U_M$, $d_{PU} = \ell^{PU}_G - \ell^{PU}_M$, $\epsilon_L = n^\top \ell^U / y_U$, and $\epsilon_W = h_U/y_U + \psi\epsilon_L$. Differentiating the first expression for M_r, and then the share transformation, gives the exact decomposition

$$\begin{aligned}
E_r &:= \frac{d\log M_r}{d\log Y} = -\epsilon_W - \epsilon_L + \frac{(n_G - k)d_U}{y_U} + \frac{d_{PU}}{y_U d_P},\\
E_s &:= \frac{d\log \mathscr{M}^{GS}}{d\log Y} = E_r - \frac{2\nu s_I d_U}{y_U}\\
&= -\epsilon_W - \epsilon_L + \frac{(n_G - k - 2\nu s_I)d_U}{y_U} + \frac{d_{PU}}{y_U d_P}. \qquad \text{(D.66)}
\end{aligned}$$

By (D.63)–(D.64), $|d_U| \le 2e_U$ and $|d_{PU}| \le 2L_{PU}$. Since $0 < n_G, s_I < 1$, $|n_G - k - 2\nu s_I| \le 1 + \nu$. Using (D.62) therefore gives

$$|E_s + \epsilon_W + \epsilon_L| \le R_s := \frac{2(1+\nu)e_U + 4kL_{PU}}{y_U}.$$

Set $L^0_U = u_U/y_U > 0$, $y_{\min} = \min_U y_U > 0$, and $L_{\min} = \min_U L^0_U > 0$. With the fixed constants above, take $C_s = [2(1+\nu)C_e + 4kC_m]/y_{\min}$, so $R_s \le C_s\varepsilon$. If $\varepsilon_0 > 0$ is the preliminary growth bound used above, including the existing regularity and wage bounds, choose

$$0 < \varepsilon \le \bar\varepsilon := \min\left\{\varepsilon_0, \frac{y_{\min}L_{\min}}{2C_e}, \frac{w_*}{2C_s}\right\}.$$

A zero error constant imposes no corresponding restriction. Each other entry is strictly positive and independent of the growth scale. Thus this is a nonempty common neighborhood, in which $\epsilon_L \ge L^0_U/2$ and $R_s \le w_*/2$. Equation (D.66) now yields

$$\frac{d\log \mathscr{M}^{GS}}{d\log Y} \le -\frac{w_*}{2} - \frac{L^0_U}{2} < 0.$$

Together with (D.65), this proves both claims. The construction only reduces the growth neighborhood within (D.58) and (D.60). Continuity preserves the strict signs in sufficiently nearby macroeconomic states on the same branch. ■

Proof of Lemma C.1. Log-differentiating free entry at impact, using that A^K_t is predetermined, gives

$$(\nu - 1)\frac{d\log X_{t,K}}{d\log Y_t} + \eta^K_t = \varepsilon^X_t.$$

Since $S^K_t = \zeta_K A^K_t X^\nu_{t,K}$, this yields (C.30).

For the equivalence, use $\phi = 1$ and the regular fixed-input economy $e_L = 0$ constructed in the proof of Corollary 3.1, with total research input $\bar F = 1$. The physical service suppliers in the funding economy retain $0 < \psi < \infty$. Write W_u for the research price in the comparison economy and $H_u = \bar{\omega}^S C_u / \varrho_u^d$. Given the same initial technology and shocks, set at every date

$$X_{u,K} = L_{u,K}^{S,0}, \qquad \tilde{P}_u^X = H_u, \qquad q_u = \mathsf{W}_u / H_u, \qquad P_u^X = \mathsf{W}_u. \tag{D.67}$$

Here the superscript 0 denotes the $e_L = 0$ economy. Restrict the correspondence to the strictly binding branch $\mathsf{W}_u > H_u$. Then $X_u = \bar{F} = 1$ satisfies the credit constraint, and $\tilde{P}_u^X = H_u X_u^{\psi}$ satisfies physical labor supply. The funding-inclusive free-entry condition coincides with that of the comparison economy.

Households own the lenders. Loan principal is $\tilde{P}_u^X X_u$, and net patent-sale proceeds repay principal plus the scarcity charge after the same setup payments as in the main text. Free entry implies

$$\begin{aligned} \sum_K S_u^K \mathcal{V}_u^K &= P_u^X X_u = q_u \tilde{P}_u^X X_u, \\ \tilde{P}_u^X X_u + (q_u - 1)\tilde{P}_u^X X_u &= \mathsf{W}_u \bar{F}. \end{aligned} \tag{D.68}$$

Principal cancels from the lenders' accounts, so service income plus lending rents equals the comparison economy's research income. The household budget is preserved, and the loans leave no balance at the next period boundary. At $X_u = 1$ the research-disutility term is constant; the consumption and unskilled-labor conditions remain unchanged. Research still uses labor, so the production and resource relations in (D.24) are preserved.

The identical sectoral inputs generate identical actual technology paths. Consumption and preference paths, and hence the household SDF, also agree. Thus actual operating profits, the benchmark in (C.24), and their derivatives in (D.28) coincide, including all future technology feedback. Conversely, a strictly binding funding equilibrium has $X_u = 1$ and $\tilde{P}_u^X = H_u$. Setting $L_{u,K}^{S,0} = X_{u,K}$ and $\mathsf{W}_u = P_u^X$, and combining service income and lending rents, recovers the fixed-input equilibrium. This establishes the claimed correspondence.

A sufficient condition ensuring a nonempty strictly binding branch can be obtained from the first patent payoff. Let $s_* > 0$ bound green shares from below on the maintained continuations, and define

$$\begin{aligned} \chi_{\max} &= \alpha_L + k_M + k_G, \qquad h_M = \frac{\beta k_M}{\chi_{\max}(1+\zeta_M)}, \quad h_G = \frac{\beta k_G s_*}{\chi_{\max}(1+\zeta_G)}, \\ \underline{w} &= (1-c)\left[\sum_K (\zeta_K h_K)^{1/(1-\nu)}\right]^{1-\nu}, \quad 0 < \bar{\omega}^S < \underline{w}. \end{aligned} \tag{D.69}$$

Since $X_u = 1$, $\Gamma_u^K \le 1 + \zeta_K$. The first term of (D.26) gives $A_u^K \mathcal{G}_u^K / C_u \ge h_K$ on the no-shock path. Equation (D.45) at $e_L = 0$ then yields $\mathsf{W}_u / C_u \ge \underline{w}$, and hence $q_u \ge \underline{w}/\bar{\omega}^S > 1$ uniformly. This strict bound persists for sufficiently small shocks: preference ratios and the actual/no-shock profit ratio $Z_u(\varrho_u^d)^{1/(1+\eta)}$ at fixed stocks are uniformly close to one, while total input still bounds the growth rates. The fixed-input allocation does not depend on $\bar{\omega}^S$, so this restriction is compatible with the maintained transition conditions. ■

Proof of Proposition C.1. Maintain the regular interior branch, slow-transition bounds, and positive shock persistences used for the $e_L = 0$ economy in the proof of Corollary 3.1, on the finite transition window considered there. Lemma C.1 preserves the actual technology, consumption, and benchmark paths, so the existing value-ordering proof applies without changing its feedback or remainder bounds.

For a unit innovation in $\log U_t$, write $v_K = \partial \log \mathcal{V}_t^K / \partial \log U_t$, $w = \partial \log P_t^X / \partial \log U_t$, and $d_K = \partial \log S_t^K / \partial \log U_t$. The fixed-input result gives $D_t \equiv v_G - v_M < 0$. At impact, free entry and $X_t = \bar{F}$ imply

$$d_K = \frac{\nu}{1-\nu}(v_K - w), \qquad w = n_t^G v_G + n_t^M v_M, \qquad n_t^K = \frac{X_{t,K}}{X_t}. \tag{D.70}$$

Interiority therefore gives $v_G < w < v_M$, and

$$d_G = \frac{\nu n_t^M}{1-\nu} D_t < 0, \qquad d_M = -\frac{\nu n_t^G}{1-\nu} D_t > 0. \tag{D.71}$$

In particular, $d_G < 0$ if and only if $w > v_G$. The threshold is $v_G = v_M + D_t$, so it falls when relative green net value becomes more countercyclical, holding v_M fixed. The positive impact output responses in (D.24) preserve these comparisons when elasticities are expressed with respect to output. These are the conclusions of Proposition 3.4, with P_t^X replacing W_t^S.

Finally, log-differentiating $P_t^X = q_t \tilde{P}_t^X$ yields (C.31). ■

Proof of Proposition C.2. Use the real numeraire $P_t = 1$ and maintain the baseline parameter and path restrictions, including (D.18). Monopoly pricing gives $P_t^F = \mu_F \xi_f^{-1} (A_t^F)^{1-\mu_F}$, so

$$\frac{F_t}{G_t} = \left(\frac{P_t^G}{P_t^F}\right)^{\rho}, \qquad \frac{P_t^F}{P_t^G} = \frac{\mu_F}{\xi_f \mu_G} \frac{(A_t^G)^{\mu_G - 1}}{(A_t^F)^{\mu_F - 1}}. \tag{D.72}$$

Thus a green transition requires the last ratio to increase. Write $s = s^G$ and $k_F = \alpha_E(\mu_F - 1)/\mu_F$, with $\mu_F > 1$. The resource constraint gives $C/Y = \chi(s) \equiv \alpha_L + k_M + k_G s + k_F(1-s)$. Set

$$F_M = \frac{k_M}{\chi}, \qquad F_G = \frac{k_G s}{\chi}, \qquad F_F = \frac{k_F(1-s)}{\chi}. \tag{D.73}$$

The normalized M, G value recursions and their innovation ratio in (D.19)–(D.21) are unchanged: the common skilled wage cancels, including when brown R&D uses the same labor market. Since $\alpha_L + k_M \leq \chi \leq \alpha_L + k_M + \max\{k_G, k_F\}$, the boundedness argument in Lemma D.1 still gives $\Gamma_t^M > \Gamma_t^G$. The profit ratio (D.7) therefore rises with s_t^G. This proves Proposition 3.1; the covariance proof of Proposition 3.2 then applies without change.

For Proposition 3.3, use $\phi = 1$ and extend the regular interior, small-growth domain of its proof to $K \in \{M, G, F\}$. Let $\mathbf{q} = (\log A^M, \log A^G, \log A^F)$ and retain the definitions of J_K, T_C, ω^K, x, ℓ, and g with these three coordinates and the cash flows in (D.73). The matched benchmark and the household SDF give (D.28)–(D.29) for each sector. With $n^M + n^G + n^F = 1$, the matrix and inverse in (D.30) remain valid in three dimensions; in particular, $M^{-1}\mathbf{1} = \mathbf{1}/(1 - \nu + \psi)$.

The log-state derivatives of $\log F_K$ through second order are bounded for $s \geq s_* > 0$. To bound all three valuation tails, put $L_F = \sup_{K,u} \|J_{K,u}\|_1$ and $\varepsilon = \sup_{K,u} g_{K,u}$. The first payoff bounds the denominator of each value weight, yielding

$$\omega_{u,h}^K \leq \beta^{h-1} \frac{F_K(\mathbf{q}_{u+h})}{F_K(\mathbf{q}_{u+1})} \leq \left[\beta e^{L_F \varepsilon/(1-\varepsilon)}\right]^{h-1}.$$

This bound also holds as the brown expenditure share tends to zero. Fix $\sqrt{\beta} < v < 1$ and $\beta < \beta_* < v^2$. For sufficiently small ε, these weights are bounded by β_*^{h-1}. Use $W_v = (v - \beta_*)^{-1}$ in (D.33) and (D.36), and $\beta_* e^{2vL_\ell \varepsilon} < 1$ in the derivative summability bound. The same reference and response operators are then contractions, and the second-order remainder estimates apply to all three sectors.

Define $\kappa_G = (\rho - 1)(\mu_G - 1)(1 - s)$ and $\kappa_F = (\rho - 1)(\mu_F - 1)(1 - s)$. Then $D_{\mathbf{q}} \log s = (0, \kappa_G, -\kappa_F)$ and

$$\begin{aligned} J_G - J_M + \mathbf{e}_M^\top - \mathbf{e}_G^\top &= (1, \kappa_G - 1, -\kappa_F), \\ \delta_t^F &= g_{M,t} - g_{G,t} + \kappa_{G,t} g_{G,t} - \kappa_{F,t} g_{F,t}. \end{aligned} \tag{D.74}$$

Thus δ_t^F is the first-order growth rate of relative green profits. Retain the finite-window margin $\delta_t^F \geq d_* \varepsilon > 0$ from the baseline proof. The green transition in (D.72) and the strict M, G growth ordering supply its positive first-order terms. At zeroth order all three sectors have the same duration weights, so, with $p = \rho_U$, $Q = p(1 - \beta)/(1 - \beta p)$, and B_U as in the baseline proof,

$$\ell_{K,t+h}^{(0)} = \frac{B_U Q}{1 - \nu + \psi} p^h, \qquad x_{K,t+h} = \frac{\nu B_U Q}{1 - \nu + \psi} g_K \frac{1 - p^h}{1 - p} + O(\varepsilon^2).$$

The first-order geometric value factors have difference $\beta_G - \beta_M = \beta \delta_t^F$. Hence the direct duration contribution is $-B_U \beta \delta_t^F p(1 - p)/(1 - \beta p)^2$, while (D.74) gives the state contribution $\nu B_U Q \delta_t^F / [(1 - \nu + \psi)(1 - \beta p)]$. Combining them yields

$$v_{G,t} - v_{M,t} = -\frac{B_U \beta \delta_t^F p}{(1 - \beta p)^2} \left[1 - p - \frac{\nu(1 - \beta)}{\beta(1 - \nu + \psi)}\right] + O(\varepsilon^2). \tag{D.75}$$

Under (D.31) with a strict margin, the leading term is negative and dominates the remainder for sufficiently small growth. Finally (D.42) gives the countercyclicality of $S_t^G/(S_t^G + S_t^M)$, proving Proposition 3.3. ■

Preliminaries for Propositions C.3–C.5. Write $s = s^G$, $t_c = 1 - c$, $a = \zeta^2$, and $\tau = (\rho - 1)(\mu_G - 1) > 0$. Equilibrium values are fundamental. Production and household optimality give

$$\chi(s) = \alpha_L + k_M + k_G s, \quad C = \chi(s)Y, \quad f_M(s) = \frac{1}{\chi(s)}, \quad f_G(s) = \frac{s}{\chi(s)}, \quad \pi^K = \frac{k_K C}{A^K} f_K(s),$$
$$W^S = \frac{C}{\varrho^d}\bar{\omega}^S (L^S)^\psi, \qquad \Lambda_{t,t+h} = \beta^h \frac{\varrho_{t+h}^d}{\varrho_t^d}\frac{C_t}{C_{t+h}}, \qquad H_t \equiv \frac{C_t}{C^0(A_t^G, A_t^M)} = Z_t(\varrho_t^d)^{1/(1+\eta)}. \tag{D.76}$$

Thus $\pi^{K,0} = \pi^K/H$. The original owner's expected quality coefficient is $g = (1-i)(1-e) + \lambda i = 1 - d + \delta i$, giving

$$v_t^K = \pi_t^K - \frac{W_t^S (i_t^K)^2}{A_t^K \zeta_K^2} - c i_t^K(\delta + e_t^K)\bar{F}_t^K + g_t^K F_t^K,$$
$$b_t^K = \pi_t^{K,0} - \frac{W_t^S (i_t^K)^2}{A_t^K \zeta_K^2} - c i_t^K(\delta + e_t^K)\bar{F}_t^K + g_t^K \bar{F}_t^K. \tag{D.77}$$

The incumbent maximizes $q[i(\delta + e)N - W^S i^2/(A\zeta_K^2)]$; a successful entrant obtains $\lambda q N$ if the incumbent fails. Private optimality and free entry give

$$\frac{2W_t^S i_t^K}{A_t^K \zeta_K^2} = (\delta + e_t^K)N_t^K, \qquad W_t^S = \zeta_K (L_{E,t}^K)^{-1/2}\lambda A_t^K (1 - i_t^K)N_t^K. \tag{D.78}$$

Normalize

$$y_K = \frac{a A^K N^K}{k_K W^S}, \qquad z_K = \frac{\varrho^d A^K (F^K - \bar{F}^K)}{k_K C}, \qquad \mathcal{I} = \frac{a^{\psi+1}}{\bar{\omega}^S}. \tag{D.79}$$

Solving $2i = (\delta + e)y$ and $e = \lambda(1-i)y$ gives

$$i_\delta(y) = \frac{\delta y + \lambda y^2}{2 + \lambda y^2}, \quad e_\delta(y) = \frac{\lambda y(2 - \delta y)}{2 + \lambda y^2}, \quad d_\delta = e_\delta(1 - i_\delta), \quad u_\delta = i_\delta + d_\delta,$$
$$m_\delta = e_\delta^2 + i_\delta^2, \quad j_\delta = (1 - e_\delta)y + t_c i_\delta^2, \quad \Gamma_\delta = 1 + \delta u_\delta, \quad g_\delta = 1 - d_\delta + \delta i_\delta,$$
$$\Psi = \mathcal{I}^{-1}\left[\sum_K k_K m_\delta(y_K)\right]^\psi, \qquad W^S = (C/\varrho^d)a\Psi. \tag{D.80}$$

The Bellman difference and $v - cb$ combination give

$$\begin{aligned}
\Gamma_{K,t}\Psi_t y_{K,t} &= \beta\mathbb{E}_t[f_K(s_{t+1})\mathcal{E}_{t+1} + \Psi_{t+1}j_\delta(y_{K,t+1}) + ci_{K,t+1}(\delta + e_{K,t+1})z_{K,t+1}]\,, \\
\Gamma_{K,t}z_{K,t} &= \beta\mathbb{E}_t[f_K(s_{t+1})\mathcal{D}_{t+1} + g_{K,t+1}z_{K,t+1}]\,, \\
s_{t+1} &= \frac{s_t\Gamma^\tau_{G,t}}{1 - s_t + s_t\Gamma^\tau_{G,t}}, \qquad \mathcal{E}_t = \varrho^d_t(1 - c/H_t), \quad \mathcal{D}_t = \varrho^d_t(1 - 1/H_t).
\end{aligned} \tag{D.81}$$

On the no-shock path, $z = 0$ and $\mathcal{E} = t_c$.

Proof of Proposition C.3. Consider an interior no-shock transition. Suppress δ and put $\mathcal{P}(y) = \Gamma(y)y$. On the full interior probability domain $0 < y < 2/\delta$,

$$u'(y) > 0, \qquad m'(y) > 0, \qquad 0 < j'(y) < \mathcal{P}'(y), \qquad \mathcal{P} - j = m + ci^2. \tag{D.82}$$

Indeed, $i' = [2\delta + \lambda y(4 - \delta y)]/(2 + \lambda y^2)^2 > 0$. Using i as the independent variable, set $r = 1 - i$, $\Delta = e - 2ir$, and $D_* = e^2 - 4ire + 2ir$. The research conditions imply

$$\lambda\Delta = e(1 - e), \quad \delta\Delta = 2ir - e^2, \quad D_* = (2e + \delta)\Delta > 0, \quad e \leq \sqrt{2ir} \leq 1/\sqrt{2}.$$

In particular, $1 - e = [(\lambda y - 1)^2 + 1]/(2 + \lambda y^2) > 0$. Differentiating $e(\delta + e) = 2\lambda i(1 - i)$ gives

$$\frac{du}{di} = \frac{1 - e}{D_*}[e^2 + 2r(4r - 3)e + 2r(1 - r)], \qquad \frac{dm}{di} = \frac{2}{2e + \delta}[2er + \delta\{i + 2e(1 - 2i)\}].$$

The first bracket is positive for $r \geq 3/4$. For $r < 3/4$ it equals $[e - r(3 - 4r)]^2 + r(2 - 11r + 24r^2 - 16r^3)$, whose cubic factor has minimum $(9 - \sqrt{3})/18 > 0$ on $[0, 3/4]$. The second bracket is positive for $i \leq 1/2$. For $i > 1/2$,

$$i^2 - [2e(2i - 1)]^2 \geq i(1 - 9r + 32r^2 - 32r^3) > 0,$$

since the last cubic has minimum $5(8 - \sqrt{10})/108 > 0$ on $[0, 1/2]$. Finally, for $h = (1 - e)y = e/r - 2i$,

$$\frac{dh}{di} = \frac{\Delta}{r^2 D_*}(e^2 - 4r^2 e + 2r^2) > 0.$$

If $r \leq 1/\sqrt{2}$, the last bracket is $(e - 2r^2)^2 + 2r^2(1 - 2r^2) > 0$. Otherwise it is at least $2r(1 - 2r\sqrt{2ir}) > 0$, because $8ir^3 \leq 27/32$. Hence $j_i = h_i + 2t_c i > 0$. The research conditions give $\mathcal{P} - j = m + ci^2$; differentiating proves $\mathcal{P}' > j'$.

For $B_t = \Psi_t[\mathcal{P}(y_{G,t}) - \mathcal{P}(y_{M,t})]$, the no-shock recursions imply

$$B_t = -\beta t_c \frac{1 - s_{t+1}}{\chi(s_{t+1})} + \beta\Psi_{t+1}[j(y_{G,t+1}) - j(y_{M,t+1})]. \tag{D.83}$$

If $B_t \geq 0$, then $y_{G,t+1} > y_{M,t+1}$ and $B_{t+1} > B_t/\beta$ by (D.82). Starting at $B_{t+1} > 0$, iteration diverges, contradicting the bound implied by $m < 2$, $y < 2/\delta$, and $\Gamma < \lambda$:

$$|B_t| \leq \frac{2\lambda}{\delta \mathcal{I}}[2(k_G + k_M)]^{\psi}.$$

Therefore $y_M > y_G$, so $u_M > u_G > 0$ and $\Gamma_M > \Gamma_G > 1$. The state equation gives $s_{t+1} > s_t$, and $P_t^G G_t/(P_t Y_t) = \alpha_E s_t$ proves part 1. Moreover,

$$\frac{\pi_t^G}{\pi_t^M} = \frac{k_G}{k_M} s_t \frac{A_t^M}{A_t^G}, \qquad \frac{\pi_{t+1}^G/\pi_{t+1}^M}{\pi_t^G/\pi_t^M} = \frac{s_{t+1}}{s_t}\frac{\Gamma_{M,t}}{\Gamma_{G,t}} > 1,$$

which proves part 2. ∎

Proof of Proposition C.4. Define

$$\bar{\beta} = \frac{6}{6 + (1+2\psi)(5+c)}. \tag{D.84}$$

Fix $\beta \in (\bar{\beta}, 1)$, any finite $\delta > 0$, and a compact set of initial transition states $\mathcal{T} \Subset (0,1)$. Consider $\log U_{t+h} = \epsilon p^h$, $U \in \{Z, \varrho^d\}$. Write

$$Q = 1 + 2\psi, \qquad r = \mathcal{I}^{1/Q} = \left(\frac{\zeta^{2(\psi+1)}}{\bar{\omega}^S}\right)^{1/Q}, \qquad \vartheta = \frac{1-\beta}{Q}.$$

Low-efficiency reference equilibrium. For fixed δ, define

$$u_1 = 1 + \tfrac{3}{2}\delta, \quad M_2 = \lambda^2 + \tfrac{1}{4}\delta^2, \quad \gamma = \delta u_1, \quad j_2 = -\lambda + \tfrac{1}{4}t_c\delta^2, \quad \varepsilon_1 = \frac{\lambda(1-2\delta)}{2+3\delta}. \tag{D.85}$$

The exact research conditions in (D.80) give

$$\begin{aligned} i_\delta(y) &= \tfrac{\delta}{2}y + O(y^2), \qquad e_\delta(y) = \lambda y + O(y^2), \qquad u_\delta(y) = u_1 y(1+\varepsilon_1 y) + O(y^3), \\ m_\delta(y) &= M_2 y^2 + O(y^3), \quad j_\delta(y) = y + j_2 y^2 + O(y^3), \quad \Gamma_\delta(y) = 1 + \gamma y + O(y^2). \end{aligned} \tag{D.86}$$

Take $J_* = [s_*, 1]$, where $0 < s_* < \min \mathcal{T}$. On the no-shock path, the recursion for $\Gamma_K \Psi y_K$ has forcing $\beta t_c f_K(s^+)$ and lead coefficient $\beta j_K^+/(\Gamma_K^+ y_K^+) \in (0, \beta)$, by (D.82). Thus $\Gamma_K \Psi y_K$ is bounded above and away from zero on J_*. Moreover, $m_\delta(y)/y^2$ has a positive continuous extension to $[0, 2/\delta]$, with endpoint values M_2 and $\delta^2/4$. The wage equation then gives $0 < \underline{x} \leq y_K/r \leq \overline{x} < \infty$.

Set $x_K = y_K/r$ and $n_K = \Psi y_K$. The rescaled wage equation is

$$\Psi = r^{-1}\Omega_r(x), \qquad n_K = \Omega_r(x) x_K, \qquad \Omega_r(x) = \left[\sum_K k_K \frac{m_\delta(r x_K)}{r^2}\right]^{\psi}. \tag{D.87}$$

It extends smoothly to $\Omega_0(x) = M_2^{\psi}(k_G x_G^2 + k_M x_M^2)^{\psi}$. At $r = 0$, the no-shock equilibrium is

$$n_{0,K}(s) = \frac{\beta t_c}{1-\beta} f_K(s), \qquad x_{0,G}(s) = sX(s), \qquad x_{0,M}(s) = X(s),$$
$$X(s) = \left[\frac{\beta t_c}{(1-\beta)\chi(s) M_2^{\psi}(k_M + k_G s^2)^{\psi}}\right]^{1/Q} > 0. \tag{D.88}$$

This solution is unique and smooth on J_*.

To include shocks, let $w = \log U$ and $w^+ = pw$, and use $\mathcal{E}_U(w), \mathcal{D}_U(w)$ from (D.81). Fix $p_* \in (0,1)$. For $0 \le p \le p_*$ and small $|w|$, define

$$V_U(w,p) = \beta \sum_{j\ge 0} \beta^j \mathcal{E}_U(p^{j+1}w), \qquad Z_U(w,p) = \beta \sum_{j\ge 0} \beta^j \mathcal{D}_U(p^{j+1}w),$$
$$n_{0,K}(s,w,p) = f_K(s) V_U(w,p), \qquad z_{0,K}(s,w,p) = f_K(s) Z_U(w,p). \tag{D.89}$$

Here $V_U(0,p) = \beta t_c/(1-\beta)$ and $x_{0,K}(s,w,p) = x_{0,K}(s)[V_U(w,p)/V_U(0,p)]^{1/Q}$. The series and their derivatives converge uniformly.

Policy continuation and remainder. Work on $J_* \times [-w_*, w_*] \times [0, p_*]$ in coordinates $P = (\log n, z)$. At $r = w = 0$, the current Jacobian is invertible and the preconditioned lead is βI. Indeed, $D_{\log x} \log n = I + \mathbf{1}\alpha^\top$, with $\sum_K \alpha_K = 2\psi$, so its determinant is $Q > 0$. Writing the state transition as $S_r(s, x_G)$, uniformly nearby,

$$S_r - s = O(r)(1-s), \qquad (S_r)_P = O(r)(1-s), \qquad (S_r)_s = 1 + O(r). \tag{D.90}$$

In particular, S_r maps J_* into itself.

Let $\mathcal{R}_r$ be the residual of (D.81), and R_0 the inverse current reference Jacobian. On a closed radius-a_* tube around P_0 with Lipschitz bound L, the map $\mathcal{T}_r P = P - R_0 \mathcal{R}_r(P)$ satisfies

$$\begin{aligned} \operatorname{Lip}_{C^0} \mathcal{T}_r &\le \beta + C(w_* + a_*) + Cr(1+L), \\ \operatorname{Lip}(\mathcal{T}_r P) &\le \beta L + C_0 + C(w_* + a_*)(1+L) + Cr(1+L)^2. \end{aligned} \tag{D.91}$$

Choose $L > \operatorname{Lip}(P_0)$ with $(1-\beta)L > C_0$, then w_*, a_*, r small. Since $\mathcal{R}_r(P_0) = O(r)$, the tube is invariant and contractive, with factor $q_0 < 1$, and $P_r - P_0 = O(r)$.

For derivatives, treat p as a constant state, so the full state map is (S_r, pw, p). After moving the current $O(r)$ feedback to the left, the highest future derivative coefficients satisfy

$$q_j \le [\beta + O(w_* + a_* + r)][1 + O(w_* + r)]^j + O(r) < 1, \qquad j = 1, 2.$$

These bounds give continuous derivative fixed points. The corresponding difference quotients satisfy the same equations with averaged coefficients; their errors after N iterations are bounded by

$$2L_j q_j^N + \sum_{h=0}^{N-1} q_j^h \omega_j(C_S^h |v - v'|), \qquad \omega_j(t) \to 0,$$

where C_S bounds the state-map Lipschitz constant. Taking $v' \to v$ before $N \to \infty$ proves $P_r \in C^2$. For a smooth trial policy with residual $O(r^2)$ in C^2, the policy and derivative errors obey

$$E_0 \le \frac{Cr^2}{1 - q_0}, \qquad E_j \le q_j E_j + C \sum_{k<j} E_k + Cr^2, \quad j = 1, 2,$$

and are therefore $O(r^2)$.

The probability domain is satisfied for $r\bar{x} < 2/\delta$, and the valuation kernel is $\beta g_K^+ / \Gamma_K = \beta + O(r) < 1$. All future states remain in J_* and converge to one on the no-shock path. These bounds do not require a uniform positive probability as $r \downarrow 0$. They also apply to interior fundamental continuations: the recursion for Γz gives $z = O(w_*)$, preserving the preceding bounds on y/r, while the discounted $O(r)$ one-period state changes place such continuations in the reference neighborhood.

Innovation response. Let

$$h_Z = 1, \quad h_{\varrho^d} = \frac{1}{1+\eta}, \qquad B_Z = \frac{c}{t_c}, \quad B_{\varrho^d} = 1 + \frac{c}{t_c(1+\eta)}. \tag{D.92}$$

Write $n_r = n_0 + rN_1 + O(r^2)$ and $z_r = z_0 + rZ_1 + O(r^2)$. Put $b(s) = \tau\gamma s(1-s)$ and $\mathsf{D}_U(s, w) = b(s) x_{0,G}(s, w)$, suppressing p. The first-order terms of (D.81) satisfy

$$\begin{aligned} N_{1,K}(s, w) - \beta N_{1,K}(s, pw) &= \mathsf{D}_U(s, w)\partial_s n_{0,K}(s, w) - \gamma x_{0,K}(s, w) n_{0,K}(s, w) \\ &\quad + \beta j_2 x_{0,K}(s, pw) n_{0,K}(s, pw) \\ &\quad + \frac{\beta c \delta^2}{2} x_{0,K}(s, pw) z_{0,K}(s, pw), \end{aligned} \tag{D.93}$$

$$\begin{aligned} Z_{1,K}(s, w) - \beta Z_{1,K}(s, pw) &= \mathsf{D}_U(s, w)\partial_s z_{0,K}(s, w) - \gamma x_{0,K}(s, w) z_{0,K}(s, w) \\ &\quad + \beta \left(\frac{\delta^2}{2} - \lambda \right) x_{0,K}(s, pw) z_{0,K}(s, pw). \end{aligned} \tag{D.94}$$

Their forward series have inverse bound $(1-\beta)^{-1}$. They define a smooth first-order trial policy with C^2 residual $O(r^2)$, so the preceding error estimates apply. The first term in (D.93) includes the endogenous technology response, and its last term retains the benchmark response.

At $w = 0$, write $a_U = (1-\beta) B_U p / (1 - \beta p)$. Equation (D.89) gives

$$\frac{\partial_w n_{0,K}}{n_{0,K}} = a_U, \qquad \frac{\partial_w x_{0,K}}{x_{0,K}} = \frac{a_U}{Q}, \qquad \frac{\partial_w z_{0,K}}{n_{0,K}} = \frac{(1-\beta) h_U p}{t_c(1-\beta p)}.$$

Evaluating (D.93) and its derivative yields

$$\begin{aligned}\frac{N_{1,K}}{n_{0,K}} &= \frac{bx_{0,G}\partial_s \log f_K - (\gamma - \beta j_2)x_{0,K}}{1-\beta},\\ \frac{\partial_w N_{1,K}}{n_{0,K}} &= (1-\beta)B_U p(1+Q^{-1})[bx_{0,G}\partial_s \log f_K - \gamma x_{0,K}] + O(p^2).\end{aligned} \tag{D.95}$$

The benchmark term contributes at order p^2 here. Using $\log(y_G/y_M) = \log(n_G/n_M)$ and $\partial_s \log(f_G/f_M) = 1/s$, expand

$$\log u_K = \log(ru_1) + \log x_K + r\varepsilon_1 x_K + O(r^2),$$

and subtract $a_U N_{1,K}/n_{0,K}$ when differentiating $\log n_r$. The impact response is

$$\begin{aligned}G^U(s,p,r) &\equiv \partial_\epsilon \log(u_t^G/u_t^M)\\ &= -rpB_U(1-s)X(s)C_0(s) + O(rp^2 + r^2 p),\end{aligned} \tag{D.96}$$

$$C_0(s) = \beta(\gamma - j_2) + \vartheta(\varepsilon_1 - \gamma) + (\beta - \vartheta)\tau\gamma s. \tag{D.97}$$

The remainder is uniform on $J_* \times [0, p_*]$. Indeed, at $p = 0$ all future forcing is unshocked and normalized research is independent of current w, so $G^U(s, 0, r) = 0$ exactly. The C^2 error bound above supplies the factor p in $O(r^2 p)$.

Sign and efficiency bound. Set $R = (1-\beta)/(\beta Q)$ and $a_c = (5+c)/4$. Since $\beta > \bar{\beta}$, $R < 2a_c/3 < 1$. The state term in (D.97) is positive, and

$$\begin{aligned}(2+3\delta)[\gamma - j_2 + R(\varepsilon_1 - \gamma)] &= (2+R) + (7-3R)\delta + (6+2a_c-8R)\delta^2\\ &\quad + (3a_c - \tfrac{9}{2}R)\delta^3 > 0.\end{aligned} \tag{D.98}$$

All coefficients are positive: in particular, $6 + 2a_c - 8R > 6 - (10/3)a_c > 1$. Thus $C_0(s) > 0$ for every fixed $\delta > 0$.

Let $m_* = \min_{U, s\in\mathcal{T}} B_U(1-s)X(s)C_0(s) > 0$, and bound the remainder in (D.96) by $C_* rp(p+r)$. Let $r_* > 0$ be the feasibility and convergence range established above. Choose

$$\bar{p} = \min\left\{p_*, \frac{m_*}{4(C_*+1)}\right\}, \qquad \bar{r} = \min\left\{r_*, \frac{m_*}{4(C_*+1)}\right\},$$

and define

$$\bar{\zeta} = \left[\bar{\omega}^S \bar{r}^Q\right]^{1/[2(\psi+1)]} > 0. \tag{D.99}$$

These bounds depend only on the fixed primitives and $\mathcal{T}$. For $0 < p < \bar{p}$ and $0 < \zeta < \bar{\zeta}$, $G^U \le -rpm_*/2 < 0$ uniformly on $\mathcal{T}$. The log share response is $(1 - u_t^G/(u_t^G + u_t^M))G^U < 0$. Impact output elasticities are 1 for TFP and $1/(1+\eta)$ for preference, proving countercyclicality. ■

Proof of Proposition C.5. Consider $\log U_{t+h} = \epsilon p^h$ and write $v_K = \partial_\epsilon \log N_t^K$ and $w = \partial_\epsilon \log W_t^S$. Current technology is predetermined. Thus (D.79) and (D.82) give

$$\partial_\epsilon \log u_t^K = \kappa_K(v_K - w), \qquad \kappa_K = \frac{y_K u'_\delta(y_K)}{u_\delta(y_K)} > 0.$$

This proves the green threshold $\bar{\epsilon}_U = v_G$.

Let $\mathcal{H}_U = \partial_\epsilon \log(C_t/\varrho_t^d)$, so $\mathcal{H}_Z = 1$ and $\mathcal{H}_{\varrho^d} = -\eta/(1+\eta)$. Define the labor weights and elasticities by

$$\ell_K = \frac{k_K m_\delta(y_K)}{\sum_J k_J m_\delta(y_J)}, \qquad b_K = \ell_K \frac{y_K m'_\delta(y_K)}{m_\delta(y_K)} > 0.$$

The actual skilled-labor market then gives

$$w = \frac{\mathcal{H}_U + \psi b_G v_G + \psi b_M v_M}{1 + \psi(b_G + b_M)}.$$

To establish the required value comparisons, use $n_K = \Psi y_K = \varrho^d A^K N^K/(k_K C)$ and put $\sigma_K = \partial_\epsilon \log n_K = v_K - \mathcal{H}_U$. Use $r, Q, X, \gamma, j_2, \vartheta$ and B_U from the low-efficiency proof of Proposition C.4. Its reference policy gives

$$\sigma_K = \frac{(1-\beta)B_U p}{1-\beta p} + O(rp).$$

In particular, $\sigma_M > 0$ for a sufficiently small positive efficiency bound, uniformly in sufficiently small $p > 0$.

Subtracting the two log-value responses in (D.95), including the derivative of their denominators, gives

$$D_U := v_G - v_M = -rpB_U(1-s)X(s)C_N(s) + O(rp^2 + r^2 p),$$

where

$$C_N(s) = \beta(\gamma - j_2) - \vartheta\gamma + (\beta - \vartheta)\tau\gamma s.$$

The state and benchmark terms of (D.93) are retained; the benchmark response enters the displayed remainder at order rp^2. Put $R = (1-\beta)/(\beta Q)$ and $a_c = (5+c)/4$. The maintained discount-factor condition gives $R < 2a_c/3 < 1$, so

$$\frac{C_N(s)}{\beta} = 1 + (2-R)\delta + (a_c - 3R/2)\delta^2 + (1-R)\tau\gamma s > 0.$$

On the compact set of initial transition states, the leading coefficient has a strict positive minimum. The uniform C^2 policy estimates in the preceding proof bound the remainder by $Crp(p+r)$: at $p = 0$ normalized research and net values have zero impact response.

Reducing the existing positive persistence and efficiency bounds therefore ensures $D_U < 0$ and $\sigma_M > 0$, while preserving interior probabilities and value convergence.

Consequently,

$$v_M - w = \frac{\sigma_M - \psi b_G D_U}{1 + \psi(b_G + b_M)} > 0,$$

which proves strict non-green procyclicality. Finally, $\bar{\epsilon}_U = v_G = v_M + D_U$, so the threshold decreases one-for-one as D_U falls holding v_M fixed. ■

References Appendix

Acemoglu, Daron and David Autor (2011). "Skills, tasks and technologies: Implications for employment and earnings". *Handbook of labor economics*. Vol. 4. Elsevier, pp. 1043–1171.

Aghion, Philippe, Antonin Bergeaud, Maarten De Ridder, and John Van Reenen (2026). "Lost in transition: Financial barriers to green growth".

Aghion, Philippe, Antoine Dechezleprêtre, David Hémous, Ralf Martin, and John Van Reenen (2016). "Carbon taxes, path dependency, and directed technical change: Evidence from the auto industry". *Journal of Political Economy* 124.1, pp. 1–51.

Angelucci, Stefano, F Javier Hurtado-Albir, and Alessia Volpe (2018). "Supporting global initiatives on climate change: The EPO's "Y02-Y04S" tagging scheme". *World Patent Information* 54, S85–S92.

Arora, Ashish, Sharon Belenzon, Larisa Cioaca, Lia Sheer, Hyun Moh Shin, and Dror Shvadron (2024). "DISCERN: Duke Innovation & Scientific Enterprises Research Network". *Zenodo.* 3594642.

Arora, Ashish, Sharon Belenzon, and Lia Sheer (2021). "Knowledge spillovers and corporate investment in scientific research". *American Economic Review* 111.3, pp. 871–898.

Autor, David H and David Dorn (2013). "The growth of low-skill service jobs and the polarization of the US labor market". *American economic review* 103.5, pp. 1553–1597.

Autor, David H, Lawrence F Katz, and Melissa S Kearney (2008). "Trends in US wage inequality: Revising the revisionists". *The Review of economics and statistics* 90.2, pp. 300–323.

Bauer, Michael D. and Eric T. Swanson (2023). "A reassessment of monetary policy surprises and high-frequency identification". *NBER Macroeconomics Annual* 37.1, pp. 87–155.

Bornstein, Gideon, Per Krusell, and Sergio Rebelo (2023). "A world equilibrium model of the oil market". *The Review of Economic Studies* 90.1, pp. 132–164.

Calel, Raphael and Antoine Dechezleprêtre (2016). "Environmental policy and directed technological change: evidence from the European carbon market". *Review of Economics and Statistics* 98.1, pp. 173–191.

Chow, Gregory C and An-loh Lin (1971). "Best linear unbiased interpolation, distribution, and extrapolation of time series by related series". *The review of Economics and Statistics*, pp. 372–375.

Cloyne, James, Clodomiro Ferreira, Maren Froemel, and Paolo Surico (Mar. 2023). "Monetary Policy, Corporate Finance, and Investment". *Journal of the European Economic Association*, jvad009. ISSN: 1542-4766.

Driscoll, John C. and Aart C. Kraay (1998). "Consistent covariance matrix estimation with spatially dependent panel data". *Review of Economics and Statistics* 80.4, pp. 549–560.

Engle, Robert F., Stefano Giglio, Bryan Kelly, Heebum Lee, and Johannes Stroebel (2020). "Hedging climate change news". *The Review of Financial Studies* 33.3, pp. 1184–1216.

Gilchrist, Simon and Egon Zakrajšek (2012). "Credit spreads and business cycle fluctuations". *American Economic Review* 102.4, pp. 1692–1720.

Hall, Bronwyn H., Adam B. Jaffe, and Manuel Trajtenberg (2001). *The NBER patent citation data file: Lessons, insights and methodological tools*.

Hémous, David, Morten Olsen, Carlo Zanella, and Antoine Dechezleprêtre (2025). "Induced Automation Innovation: Evidence from Firm-level Patent Data".

Jarociński, Marek and Peter Karadi (2020). "Deconstructing monetary policy surprises—the role of information shocks". *American Economic Journal: Macroeconomics* 12.2, pp. 1–43.

Kahle, Kathleen M. and René M. Stulz (2017). "Is the US public corporation in trouble?" *Journal of Economic Perspectives* 31.3, pp. 67–88.

Känzig, Diego R. (2021). "The macroeconomic effects of oil supply news: Evidence from OPEC announcements". *American Economic Review* 111.4, pp. 1092–1125.

Kogan, Leonid, Dimitris Papanikolaou, Amit Seru, and Noah Stoffman (2017). "Technological innovation, resource allocation, and growth". *The Quarterly Journal of Economics* 132.2, pp. 665–712.

Kung, Howard and Lukas Schmid (2015). "Innovation, growth, and asset prices". *The Journal of Finance* 70.3, pp. 1001–1037.

Porter, Alan L., Mark Markley, Richard Snead, and Nils C. Newman (2023). "Twenty years of US nanopatenting: Maintenance renewal scoring as an indicator of patent value". *World Patent Information* 73, p. 102178.

Romer, Paul M. (1990). "Endogenous technological change". *Journal of Political Economy* 98.5, Part 2, S71–S102.

Veefkind, Victor, Javier Hurtado-Albir, Stefano Angelucci, Konstantinos Karachalios, and Nikolaus Thumm (2012). "A new EPO classification scheme for climate change mitigation technologies". *World Patent Information* 34.2, pp. 106–111.